2020

CRISPR/CASTE: Functional Genomic Studies of the Major Evolutionary Innovations of Ants

Waring Trible

CRISPR/CASTE: FUNCTIONAL GENOMIC STUDIES OF THE MAJOR EVOLUTIONARY INNOVATIONS OF ANTS

A Thesis Presented to the Faculty of

The Rockefeller University

in Partial Fulfillment of the Requirements for

the degree of Doctor of Philosophy

by

Waring Trible

June 2020

CRISPR/CASTE: FUNCTIONAL GENOMIC STUDIES OF THE MAJOR EVOLUTIONARY INNOVATIONS OF ANTS

Waring Trible, Ph.D.
The Rockefeller University 2020

Ants are social organisms that live in groups and depend intimately on their nestmates for growth and survival. Ants have evolved a number of highly sophisticated, social phenotypes that allow them to form coherent colonies. This thesis explores two particularly derived features of ant biology: complex chemical communication and caste plasticity. To study these features, I had a particular focus on generating and characterizing germ-line mutants. I believe that the study of mutants, and applying molecular biology methods more generally, can lead to insights in ant biology that would not be possible with more traditional methods.

I first describe my efforts to develop a CRISPR protocol to make the first germ-line mutant ant lines. I conducted this work using a unique, clonal ant species, *Ooceraea biroi*, that has many properties making it favorable for laboratory genetics studies. Establishing this protocol required a multi-year optimization process to account for many of the particular features of ant biology, such as egg production and incubation, growing and maintaining lines, and optimizing experimental treatments to produce high mutagenesis rates.

I next describe the mutants I generated using these methods, null mutants of a highly conserved insect protein called *orco*. Orco, or olfactory receptor co-receptor, is required for the function of an important class of chemosensory proteins, the odorant receptors, in insects. I created *orco* mutant ants and found that they have striking deficiencies in their social behavior and fitness, including an inability to nest with other ants or follow chemical pheromone trails and severely reduced life span and fecundity. These results supported the growing consensus that odorant receptors are key chemosensory proteins for pheromone perception in ants, and provided a new window into ant social behavior and collective organization. Unexpectedly, and unlike *orco* mutants in other types of insects, I also found that *orco* mutant ants have severe neuro-anatomical deficiencies, including a loss of most antennal lobe glomeruli and sensory neurons in the antenna. This surprising result implies that *orco* may play an important role in antennal lobe morphology in ants, and could provide insights into the development and evolution of complex olfactory systems.

The following chapter is a critical literature review of the development and evolution of morphological castes, such as workers and queens, in ants. I describe a stereotyped and previously overlooked pattern of morphological variation in ants, and illustrate how this pattern may provide some early insights into the molecular mechanisms of caste plasticity. This chapter provides a falsifiable, mechanistic framework for caste development and suggests a route to start looking for the actual molecules that regulate this interesting process.

Finally, I start to realize this promise by characterizing a caste mutant in the laboratory. I discovered a spontaneous ‘winged mutant’ that belongs to one of the known clonal lineages of *O. biroi* and aberrantly expresses queen-like morphology and behavior at worker-like body sizes. These mutants bear a striking resemblance to one class of ant species with derived caste systems, the recurrently evolved workerless social parasites. They could thus provide a window into the mutations that give rise to these unique ants.

Overall, this thesis represents the first characterization of mutant lines in ants, and I hope it demonstrates how this approach can be used to generate robust conclusions about ant biology.

To the friends and family who have supported me all these years.

ACKNOWLEDGMENTS

Science is an increasingly collaborative enterprise, and this thesis may have been more collaborative than most. My usage by convention of the first person throughout this document does not imply that I conducted these experiments alone. Virtually every finding was made in collaboration with at least one other person.

Chapters 2 and 3 consist of an expanded version of a published manuscript that had eight co-authors (Trible et al. 2017). Each of these authors made essential contributions to the final published work. Daniel Kronauer advised my PhD and supervised the conception, execution, writing, and publishing of this project. Leonora Olivos-Cisneros and I worked together from the beginning to the end and collaborated on every aspect of the CRISPR project. Ben Matthews provided essential advice and assistance on CRISPR methods. Ni-Chen Chang assisted with injections, rearing, and sequencing. Peter Oxley and Ben Matthews assisted with bioinformatics and sequence analysis. Leonora Olivos-Cisneros performed brain dissections and antibody assays. Sean McKenzie performed the remaining neuroanatomical experiments and analyses, including antennal lobe data. Ni-Chen Chang and Leonora Olivos-Cisneros assisted me with behavioral experiments, and Jonathan Saragosti developed automated tracking techniques and performed behavioral analyses involving automated tracking. Beyond these co-authors, I also thank the members of the Kronauer, Vosshall, and Ruta laboratories for reagents and critical insights. I thank Ingrid Fetter-Pruneda for suggesting the Sharpie experiment, Yuko Ulrich for help with mixed-model statistics, Laura Seeholzer and Margaret Ebert, along with the Insect Genetic Technologies Research Coordination Network, for help in

developing the injection protocol, Vanessa Ruta for providing flies and the Orco antibody, Leslie Vosshall for access to laboratory equipment, Zak Frentz and Asaf Gal for help in implementing the automated behavioral tracking, as well as Cori Bargmann, Claude Desplan, and Leslie Vosshall for comments on manuscript drafts.

Chapter 4 consists of an expanded version of a published manuscript on caste evolution and development (Trible & Kronauer 2017). In addition to the essential input of my advisor and co-author, Daniel Kronauer, I received thorough input on this conceptual framework from dozens of biologists in and outside of the social insect community. If we have ever spoken on the subject, your input contributed to our mechanistic understanding of caste that is just now emerging.

Chapter 5 consists of an ongoing project to describe the unique winged mutants in the clonal raider ant. Peter Oxley originally identified these mutants. Sean McKenzie, Vikram Chandra, and Olivier Federigo assisted with genomics analyses. Vikram Chandra developed the foraging assay, and Vikram Chandra and Asaf Gal helped me to analyze the data from this assay. Gina Limon worked with me on genomics and collected the images and measurements for the morphometrics dataset.

My success in my PhD came from the extraordinary undergraduate education and mentorship I received at the University of Georgia. I am particularly grateful to Ken Ross, whose careful, patient, and rigorous approach forms the basis of how I study ant biology.

Finally, I would like to thank my advisor, Daniel Kronauer, for taking a chance on me and providing me unparalleled support these past six years. Daniel is a strong contender for the most talented biologist ever to study ants, and I simply can't wait to see what he and his collaborators will accomplish in the coming years. That he is also a kind and encouraging mentor, and that I had the privilege of being one of the first PhD students in his lab and enter into this universe of ant functional genetics – it's a stroke of luck that is impossible to describe, a bit like being the first to walk on the moon.

TABLE OF CONTENTS

LIST OF FIGURES

LIST OF TABLES

CHAPTER 1: INTRODUCTION

The work presented in this dissertation revolves around a core premise: functional genetic studies can profoundly advance our understanding of a wide range of biological phenomena. The specific questions that I sought to address relate to the unique biology of ants. Ants are highly derived eusocial insects. They obligately live in groups and have evolved a number of traits that enable them to form coherent social units called colonies.

A colony of ants cannot be accurately described as a collection of single individuals. Instead, it is a superorganism in which each ant depends on and contributes to the function of the group (Maynard Smith & Szathmary 1997; Hölldobler & Wilson 2009). An ant colony is therefore analogous to a unitary organism, like a plant or animal, whose cells cooperate to form a larger whole. Like cells, group behavior in ants is orchestrated by continuous communication between individuals, which is largely achieved via a wide range of chemicals called pheromones (Trible et al. 2017). Also similar to cells, the ants in a colony are typically divided into a germ line (the reproductive queen caste) and a soma (the non-reproductive worker caste) via an environmentally induced process known as phenotypic plasticity (Trible & Kronauer 2017).

My specific contribution to our understanding of ant biology was to conduct some early studies of pheromone communication and caste plasticity under the framework of functional genetics and molecular biology. Of all of the features of ants that one could study, pheromones and caste have a particularly high potential to produce general insights because they are directly analogous to core features of unitary organisms

(signaling and cell differentiation). Furthermore, ants exhibit some of the most elaborate examples of communication and phenotypic plasticity in the animal world and are therefore worthy of study to attain a more general understanding of these widespread phenomena.

Beyond any specific experimental result, I hope to advocate for an approach. When I started my PhD, no one had ever studied mutant ants in any significant detail. In this dissertation I introduce two: the *orco* mutants and the winged mutants. Describing mutants is not the only way to approach ant biology; it was not even the only way that I personally studied ant biology in my PhD. But it is a new way, and I have tried to illustrate how this particular approach can lead to robust, generalizable conclusions that could not have been reached from more descriptive studies or non-genetic experimental manipulations. These modest initial studies of the molecular biology of ants show extraordinary promise. It is quite clear to me that functional genetics in ants, if applied correctly, will profoundly advance our understanding of these peculiar social insects for years to come.

CHAPTER 2: GENOME EDITING IN ANTS

Mutagenesis experiments in insects

A central goal of modern evolutionary research is to identify the mechanisms underlying complex, derived traits. In the introduction, I outlined my specific focus on two central features of ant biology: pheromone communication and caste plasticity. The first ant genomes were published in 2010. Today, dozens of ant genomes have been sequenced, a few of which use '3rd generation' methods that resolve a nearly complete genome sequence assembled into chromosomes (McKenzie & Kronauer 2018).

The question this progress raises is: can we find differences between the genomes of ants and of other organisms that underlie the sophisticated derived traits that ants possess? While certain insights have been made solely from statistical associations, particularly in the areas of comparative and population genomics, the ultimate test of any genetic hypothesis is a direct functional manipulation. Functional manipulations can include transient perturbations like pharmacology or RNA interference, but one method has proven particularly valuable across a wide range of contexts: generating and characterizing germ-line mutants (Reid & O'Brochta 2016). Unlike transient manipulations, germ-line mutants are stable across generations, making it possible to conduct well-controlled, stepwise experiments with large sample sizes. Consequently, many productive fields of biological research were facilitated by the isolation of the first mutants that provide a window into the problem (e.g., Larsson et al. 2004).

In order to conduct mutagenesis experiments, a number of practical features are desirable

in an organism (Reid & O'Brochta 2016). The organism of interest should be readily reared and mated in captivity, and it should be possible to collect and mutagenize large numbers of individuals. Ideally, the organism will also have a rapid generation time. As a general rule, ants do not possess these features (Yan et al. 2014). Most ants can't be mated in captivity, reproductive individuals are hard to obtain in large numbers, and generation times are long. For all of these reasons, prior to the start of my dissertation research, mutagenesis experiments had never been conducted in ants (or, in fact, in any eusocial insect).

Three general classes of mutagenesis methods are commonly employed in animals (Reid & O'Brochta 2016). The earliest method is the mutagenesis screen: randomly introducing mutations throughout the genome, then identifying and characterizing individuals with aberrant phenotypes that arise. The second method is transgenics, using constructs such as viruses or retrotransposons to insert foreign sequences into the genome. These insertions are typically random, or are restricted to pre-defined target sites. The final and most recent method is targeted mutagenesis. Targeted mutagenesis relies on the use of programmable site-specific nucleases: enzymes that create DNA breaks at specific positions in the genome. These DNA breaks can be used to create a number of useful site-specific mutations, including: A) loss-of-function mutations in protein-coding genes, B) large deletions, and C) insertions of short or long sequences. All mutagenesis methods have their own strengths and weaknesses; an ideal genetic model organism is one in which many approaches can be applied interchangeably.

My primary goal for my PhD was to make and characterize germ-line mutants in ants. As a first step, I focused on establishing a particularly promising method for targeted mutagenesis: CRISPR. This system was originally discovered as part of an adaptive immune system in bacteria, and has been optimized for use in genome editing (Reid & O'Brochta 2016). While CRISPR is not the only method for targeted mutagenesis, its robustness, efficiency, and ease of use have made it an integral feature of molecular biology research in recent years. CRISPR has proven particularly valuable for conducting mutagenesis experiments outside of the traditional genetic model organisms (Wright et al. 2016).

CRISPR experiments require a minimum of two components: the Cas9 endonuclease and a short single stranded RNA called a guideRNA (gRNA). The gRNA binds and activates the Cas9 enzyme, targeting it to cut DNA at a site complementary to a specific 20bp region found in the gRNA sequence. The regions that Cas9 can target are loosely constrained: they require the presence of a short 'NGG' sequence adjacent to the binding site of the gRNA, known as the Promoter Adjacent Motif (PAM). gRNAs can thus be designed to induce a targeted DNA break at any site in the genome that is flanked by a 'GG' or 'CC' sequence. Cas9 and gRNA can be injected without additional reagents, usually in order to induce small insertions or deletions, and can also be co-injected with DNA constructs to induce site-specific insertions.

In insects, CRISPR experiments are typically conducted by microinjecting embryos during early development; ideally embryos are so young that they possess just one or a

few nuclei at the time of injection (Reid & O'Brochta 2016). These injected individuals, or G0s, are genetic mosaics, possessing both wild-type and mutant cells. If their germ cells or progenitors are mutant, the G0s will produce non-mosaic mutant offspring, which represents the successful end-point of a mutagenesis experiment (Figure 2.1).

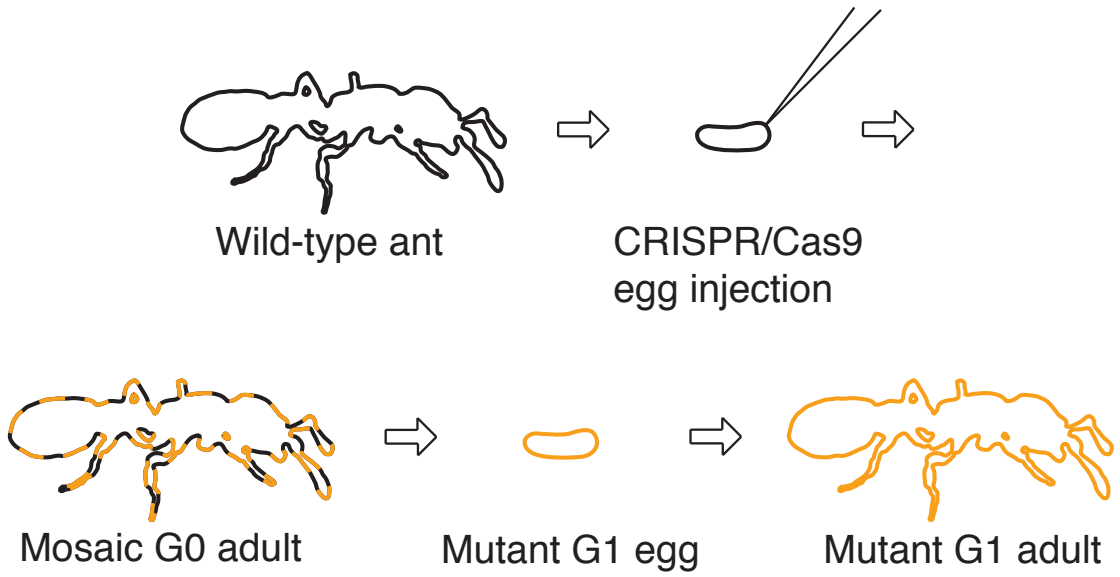

Figure 2.1: Schematic for creating mutants in the clonal raider ant. Injected eggs develop into G0 adults that are genetic mosaics of wild-type and mutant cells. These adults lay G1 eggs, some of which are germ-line mutants that can be propagated as clonal mutant lines.

Certain aspects of this protocol, like obtaining and validating reagents, screening for mutations, and microinjecting embryos, are relatively standard across insects. Other aspects, like collecting embryos, incubating injected eggs, and rearing and maintaining lines, require species-specific methods. In order to establish a CRISPR protocol in an ant, I underwent a multi-year troubleshooting project. I established initial methods for each step, and then gradually improved my efficiency (i.e., mutagenesis rate, survival rate, and sample size) until it was possible to generate CRISPR mutants. In the following section, I present a detailed overview of the CRISPR methods I developed for the clonal raider ant, with an eye toward highlighting relevant considerations for researchers hoping to develop CRISPR methods in other ant species.

Choice of experimental organism

I took advantage of the unique biology of the clonal raider ant, *Ooceraea biroi*, to generate the first mutant lines in ants (Trible et al. 2017). This species is a promising genetic model system because, unlike most other ant species, *O. biroi* reproduces via parthenogenesis, so stable germ-line modifications are obtained from the clonal progeny of injected individuals without laboratory crosses (Oxley et al. 2014). *O. biroi* also has a generation time of approximately 2 months, which is among the shortest known for any ant species (Oxley et al. 2014). Finally *O. biroi* has evolutionarily lost the morphological queen caste, with colonies instead composed of reproductively active workers. This means that, unlike other species, all eggs develop into adults that are capable of laying eggs and propagating mutant lines (Figure 2.1). Here I develop a CRISPR/Cas9 protocol in *O. biroi* and optimize this method to produce null mutants of protein-coding genes.

Obtaining reagents

The first step of a CRISPR experiment is obtaining reagents to inject, Cas9 and gRNA. I recommend Cas9 in protein form, which can be purchased from PNAbio, and synthetic gRNAs purchased from Synthego. When creating my own reagents, I have also had success synthesizing gRNAs and/or Cas9 mRNA in the laboratory using an in-vitro transcription reaction (see e.g. Kistler et al. 2015). The majority of my initial troubleshooting experiments were conducted to target the gene *orco* (see Chapter 3). Orco, or odorant receptor co-receptor, is required for the function of all insect odorant receptor genes, and *orco* mutants are commonly used to test for a role of odorant receptors in a wide range of insect behaviors (DeGennaro et al. 2013; Li et al. 2016; Koutroumpa et al. 2016; Butterwick et al. 2018).

Confirmation of gene identity

When conducting a candidate gene study (i.e., following results from *Drosophila*), it is important to target the correct locus in the genome. For single-copy orthologs, such as *orco*, identifying reciprocal best hits can evince this. Candidate *orco* orthologs for eight insect species were detected as reciprocal best hits using phmmer (Eddy 1998) with *D. melanogaster orco* (flybase id: FBgn0037324) as the initial query sequence. To confirm orthology, homologs ±50% the length of *orco* were aligned with MAFFT (Katoh & Standley 2013) using default parameters. This alignment was then used to construct a bootstrapped phylogeny with RAxML (Stamatakis 2006), providing unambiguous

support for a single copy ortholog of *orco* in *O. biroi* (Figure 2.2). I recommend this general procedure for all candidate genes that are targeted using CRISPR.

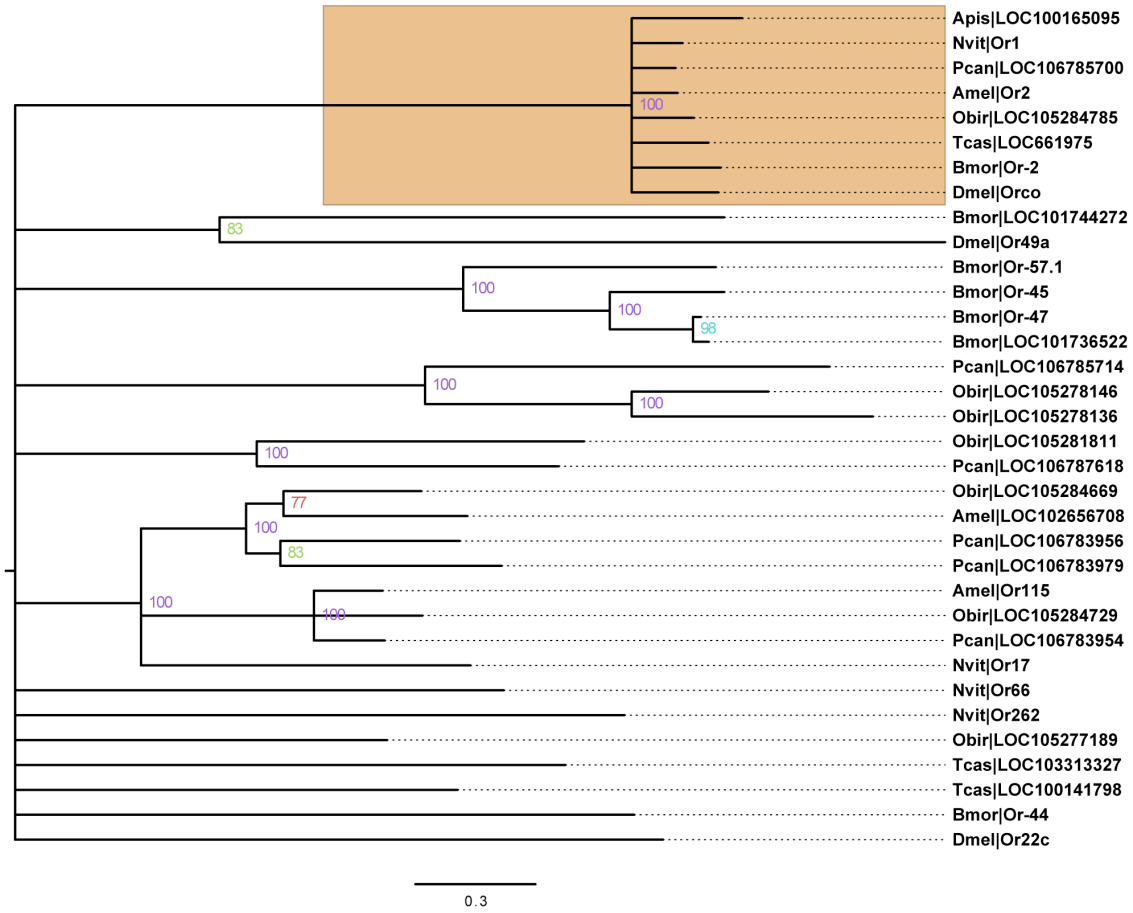

Figure 2.2: Phylogeny of *orco* and other odorant receptor genes. *orco* orthologs in orange. *O. biroi orco* is included in a clade with the *orco* genes from other studied insect species (100% bootstrap support). All nodes with less than 75% bootstrap support have been collapsed for clarity. All other bootstrap values are shown at the respective node. Species are indicated by a four letter code: Apis – *Acyrthosiphon pisum*; Nvit – *Nasonia vitripennis*; Pcan – *Papilio canadensis*; Amel – *Apis mellifera*; Obir – *Ooceraea biroi*; Tcas – *Tribolium castaneum*; Bmor – *Bombyx mori*; Dmel – *Drosophila melanogaster*. NCBI gene symbols are shown on the right. The scale bar indicates an average of 0.3 substitutions per site.

gRNA design

The script cris.py, part of the genomepy package (commit #94cc628), available at https://github.com/oxpeter/genomepy, can be used to identify target sites. For *orco*, the genomic sequence was searched on both strands for the CRISPR guide RNA (gRNA) recognition sequence 5' - N20NGG - 3' using BLASTN (Altschul et al. 1990) and checked for off-target hits using CRISPRseek (Zhu et al. 2014). I recommend picking gRNAs that minimize off-target cutting. In the case of *orco* I detected no off-target sites with 2 or fewer mismatches and only one site with 3 mismatches for my *orco* gRNA, which is expected to lead to low or no off-target cutting (Fu et al. 2013). As a further control for off-target effects, I recommend conducting experiments using multiple independent mutant lines (see Chapter 7: Methods).

CRISPR reagent preparation

Activity of Cas9 and gRNA was validated using in-vitro digestion of PCR amplicons containing the gRNA recognition site with Cas9 and buffer from New England Biolabs. This validation ensures that the reagents are not inactive, but will not provide sufficient resolution to check the efficiency of gRNAs. Instead, multiple gRNAs should be tested *in vivo* for any particular experiment to identify the most efficient candidate (see *Testing multiple experimental treatments*). The appropriate injection concentration of these reagents will depend on both the species and the efficiency of the reagents (particularly the gRNA). Immediately prior to injection, Cas9 and gRNA were mixed in water to produce a solution of the desired concentration, then spun at top speed in a standard micro centrifuge for 10 minutes. Successful experiments in *O. biroi* have ranged from 100 ng/µL Cas9 and 10 ng/µL gRNA to 400 ng/µL Cas9 and 200 ng/µL gRNA.

Egg collection

Egg collection is an essential component of microinjection-based CRISPR methods and may require substantial optimization for any focal species. *O. biroi* eggs were collected from egg-laying units consisting of 70 adults without larvae or pupae. Eggs were collected and placed on double-sided tape with the ventral side up on a glass slide. Eggs were injected into the anterior end, which is where the nuclei are found in early development (Oxley et al. 2014). Slides were prepared with up to 80 eggs for injection and ~25 control eggs to validate incubation conditions.

I observed that the presence of eggs in *O. biroi* colonies inhibits the production of new eggs and employed this observation for efficient egg collection (Figure 2.3). Egg-laying units were left with eggs for 7 days to inhibit worker egg-laying. On day 0 eggs were removed to release inhibition, and on day 2 eggs were removed again to further prevent inhibition. This led workers to synchronously activate their ovaries, and on days 5, 6, and 7 eggs were collected for injection. Following day 7, eggs were not collected from these colonies for 7 days, causing workers to become inhibited, and the protocol was then repeated.

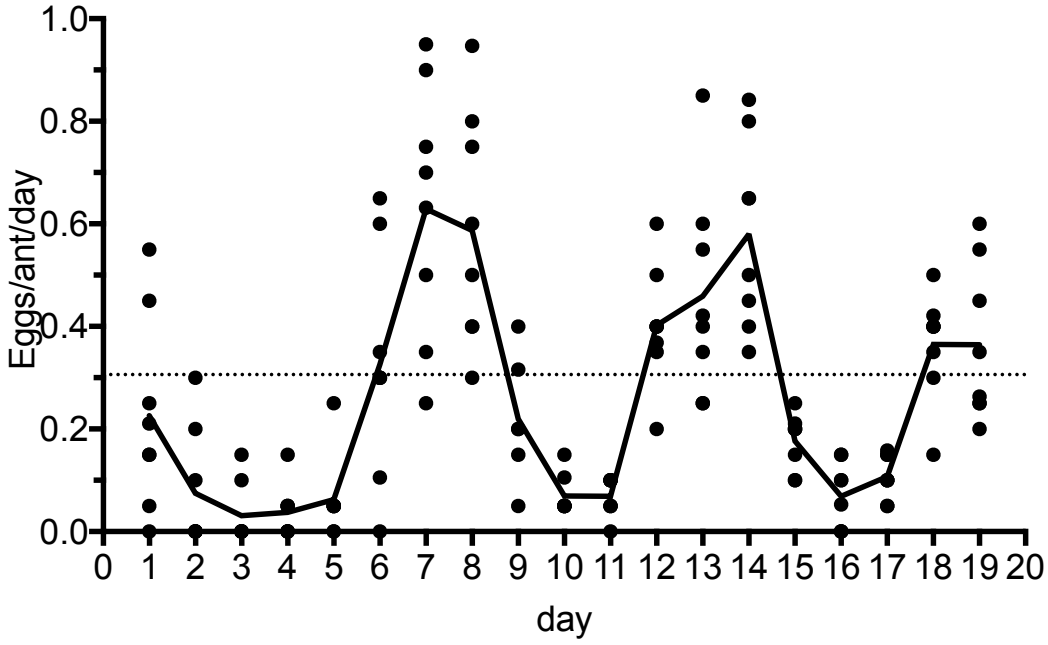

Figure 2.3: Egg laying cycles in wild-type ants. Colonies were left with eggs for 7 days prior to the start of the experiment, causing the ants to become inhibited. To release this inhibition, eggs were removed on day 0, and then all eggs were removed and counted every day from day 1-20. Colonies underwent ~7 day cycles of high and low egg production.

Multiple independent clonal lineages of *O. biroi* (termed Lines A, B, C, D) have been collected in its invasive range (Kronauer et al. 2012). I exploited this natural genetic variation to differentiate injected eggs from those produced by chaperones (see below), and also to increase the fecundity of egg-laying units. Teseo et al. 2014 found that rearing Line B workers with Line A adults leads to an increase in body size and fecundity. To maximize egg yields, I used wild-type Line B ants reared by Line A chaperones for egg production when possible. These two methodological changes allowed me to greatly boost my efficiency in collecting eggs from *O. biroi* colonies (~8 to >40 eggs/hour of effort), illustrating the importance of optimizing egg collection methods for one's focal species.

Eggs were collected from colonies under a stereoscope using insect pinning needles. On a typical injection day, eggs were removed from colonies from 10-11 am, and those eggs were used as uninjected incubation controls or fostered into rearing units. Eggs were collected for injections from 2-3 pm and 6-7 pm and injected from 3-4 pm and 7-8 pm, respectively. Therefore, all injected eggs were less than 5 hours old, when *O. biroi* eggs are in a syncytial stage of development with <100 nuclei (Oxley et al. 2014). Typical egg-laying units produced 2-5 eggs per day, and I collected from up to 60 egg-laying units, injecting 100-300 eggs per day.

Egg injection

Injection needles were prepared as in previous studies (Lobo et al., 2006). Injections were performed using an Eppendorf Femtojet with a Narishige micromanipulator. The

Femtojet was typically set to Pi 1800 hPa and Pc 500 hPa. Needles were broken by gently touching the needle against a capillary submerged in halocarbon oil. Alternatively, I generated sharper needles by setting the Femtojet to maximum pressure (6000 hPa) and lightly touching the capillary against fibers on the tape. My published *orco* data result from a combination of both methods (Trible et al. 2017).

The anterior end of *O. biroi* eggs is slightly wider than the posterior end, and the ventral surface is concave while the dorsal surface is convex (Figure 2.1). To inject, eggs were placed on double-sided 3M tape (Model S-10079 from Uline) on a glass slide, with the anterior end forward and the ventral side upward. Eggs were injected into the anterior end, where nuclei are located in early *O. biroi* embryos (Oxley et al. 2014). The ventral side was placed upward, so that larvae hatched with the mouth facing away from the tape, which facilitated successfully recovering larvae from the tape. To inject, eggs were individually submerged in 1-2 μL drops of water. Eggs were gently pierced with the needle and injected for 1-2 seconds. During successful injections, little or no cytoplasm is discharged from the egg when the needle is removed. Preliminary trials showed that injection under liquid was necessary to remove the needle without rupturing the chorion, and that water led to higher survival than Ringer, PBS, or halocarbon oil. Especially when training new personnel for injections, it is helpful to record videos of injection sessions to verify that hatching larvae had been successfully injected.

I have conducted injections using a range of batches of reagents and variable Cas9 and gRNA concentrations. Trials across multiple genes suggest that hatch rates vary inversely

with cut-rates, independent of the toxicity of the reagents or mechanical damage of injections (see also *Testing multiple experimental treatments*). For instance, in one *orco* injection round, eggs were injected with either low (1800 hPa) or high (6000 hPa) pressure, with sharper needles and lower injection volumes used in injections with high pressure. 46 of 2535 eggs (1.8%) hatched after injections with low pressure, and 58 of 756 eggs (7.6%) hatched after injections with high pressure. 25 of the 42 G0s were Illumina sequenced (see Chapter 7), and I observed an average of at least 27% cut-rates at the predicted cut site resulted from low pressure injections (n = 17) relative to 22% from high pressure injections (n = 8). *orco*$^{wt/-}$ and *orco*$^{-/-}$ G1s were recovered from G0s injected with each method.

Egg incubation

I developed a standardized incubation procedure to maximize the hatch rate of injected eggs. Following injections, slides with eggs were incubated in air-tight plastic boxes (0.9L SpaceCube boxes from ClickClack). Incubation boxes were prepared with a plaster of Paris floor (85 g plaster of Paris mixed with 50 mL distilled water). The plaster was dried completely after casting, and water was then added to determine the saturation volume. The plaster was then dried completely once again, after which 20% of the saturation volume of distilled water is added. This procedure produces suitable egg incubation conditions for 2 weeks, after which the plaster was discarded. Incubating eggs should be checked daily, and any water that condenses on the eggs removed with Kimwipes™ tissue. Fungus can sometimes grow on injection slides. Growth can be controlled by spacing the eggs at least ~2 mm apart and mechanically breaking up fungal

hyphae and destroying overgrown eggs under 100% ethanol using insect pinning needles. This egg-incubation protocol robustly yielded ~60% hatch rates of un-injected control eggs, which is similar to hatch rates of eggs in laboratory colonies.

To synchronize hatching of larvae from injected eggs, eggs injected on days 5, 6, and 7 were incubated at different temperatures. Preliminary trials showed that eggs incubated at 25 °C hatch after 9-10 days, while eggs incubated at 30 °C hatch after 7-8 days. I therefore incubated eggs injected on days 5 and 7 at 25 °C and 30 °C, respectively, while eggs injected on day 6 were incubated at 25 °C for the first 5 days and then at 30 °C until hatching. This protocol resulted in most larvae hatching on days 14 and 15. Once hatching had commenced, larvae were manually removed from the egg membrane with an insect pinning needle, taking care to prevent them from becoming stuck to the double-sided tape. Eggs that were expected to hatch overnight could be surrounded with a sheet of Parafilm® (stretched to be as thin as possible) to prevent the larvae from falling onto the tape.

Larval rearing

To rear G0 larvae, uninjected control eggs slightly older than the eggs injected on day 5 were placed with ~20 adult Line A workers in a Petri dish with a plaster of Paris floor and maintained at 25 °C. These eggs hatched slightly earlier than the injected eggs, priming the workers to rear larvae derived from injected eggs. When the larvae hatched from injected eggs, control larvae were replaced with experimental (injected) larvae. Preliminary trials showed that highest survival was obtained with 7 to 40 larvae per unit.

Control (i.e., not injected) larvae were used to supplement rearing units if insufficient experimental larvae were available. The G0 adults reported in my *orco* results therefore include an unknown, likely <10%, fraction of adults derived from control larvae. Survival of larvae under these conditions was approximately 50%.

Testing multiple experimental treatments

Successfully creating a CRISPR mutant line requires bringing together all of the above methods. Here I have presented my most efficient current methods for each individual step. Most of these methods will not vary based on any particular gene that is being targeted with CRISPR, and could even be adapted for other types of mutagenesis experiments (e.g., random mutagenesis or injections of transgenic constructs). A few aspects of this protocol will need to be customized to conduct a successful experiment, however, so it is useful to describe the typical workflow of executing a successful CRISPR project.

I recommend designing and ordering 3-4 synthetic gRNAs from Synthego for every gene one wishes to target; typically I will test the first two gRNAs for initial screening (Figure 2.4). Inject each gRNA (with Cas9) into <5hr embryos, and then incubate these eggs to hatching. I recommend an initial concentration of 100ng/uL gRNA and 400ng/uL Cas9. Eggs that survive and hatch into larvae should be frozen and Sanger sequenced using a custom-designed PCR assay, as described above. A subset of the 'dead eggs' that did not hatch into larvae should also be sequenced. A minimum of 5 larvae and 10-20 dead egg sequences are required to obtain robust results. Batch effects in hatch rates are commonly

observed across different days of injection within the same experimental treatment, requiring injection of ~400 eggs over multiple days to accurately estimate hatch rates of any given experimental treatment. Hatch rates for successful CRISPR experiments are typically 0.5-5%; I have never observed efficient mutagenesis in treatments with hatch rates higher than 5% (although, due to batch effects, certain successful injection days may have hatch rates this high).

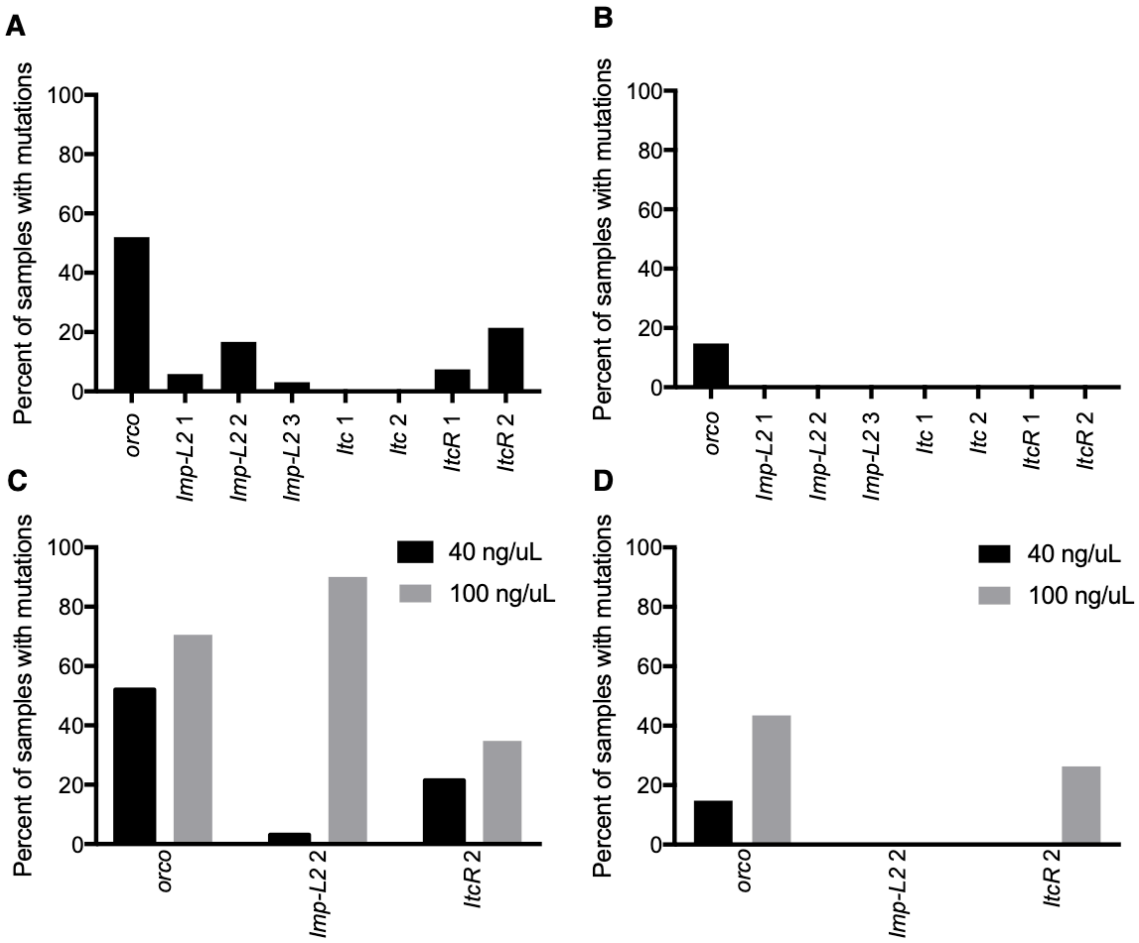

Figure 2.4: Test of 8 gRNAs across 4 genes. My initial CRISPR troubleshooting was conducted using the *orco* gRNA (see Chapter 3). (A) Percent of eggs with mutations for 8 gRNAs. 6/8 gRNAs showed mutagenesis in eggs, with the highest rates observed for *orco*. (B) Percent of larvae with mutations for all 8 gRNAs. At 40ng/uL gRNA, mutant larvae were only observed with *orco*. (C) Percent of eggs with mutations at 40ng/uL and 100ng/uL for 3 gRNAs. In all cases, mutagenesis rates were higher at 100ng/uL gRNA. (D) Percent of larvae with mutations at 40ng/uL and 100ng/uL for 3 gRNAs. A high fraction of mutant larvae were recovered at 100ng/uL for *orco* and *ItcR* gRNAs.

By injecting this minimal sample size for every gRNA, it will be possible to determine whether the mutagenesis rate (primarily estimated from dead eggs, but also from a limited number of larvae) and larval hatch rate are sufficient to generate mutant lines (Figure 2.4). To maximize the chance of recovering germ-line G1 mutants, I recommend injecting enough eggs to recover a cohort of 20-40 G0 adults, with detectable mutagenesis in ~20% or more of the G0 larvae. I have always observed a higher mutagenesis rate in dead eggs than larvae, often substantially so. Dead eggs can provide a qualitative test of whether a particular treatment is mutagenic, but a treatment can only be considered successful if it generates a high fraction of mutant larvae.

My original CRISPR troubleshooting was conducted using the *orco* gRNA. This gRNA was highly mutagenic, and I was able to generate germ-line mutants injecting at 10-40ng/uL of gRNA. In contrast, for 7 gRNAs targeting 3 other genes, I found that a higher concentration of 100ng/uL was required to obtain efficient mutagenesis. In the case of *ItcR*, this increased concentration was suitable to obtain a high fraction of mutant larvae and thus potentially generate mutant lines. In the case of *Imp-L2*, I never observed mutant larvae, despite a very large number of injections and very high rates of mutagenesis in eggs (additional experimental treatments not shown). I thus interpret these results as indicating that *Imp-L2* is essential for embryonic development in *O. biroi*.

CHAPTER 3: *ORCO* MUTAGENESIS

Introduction

Ants live in complex societies and display sophisticated social behavior, including reproductive division of labor between queens and workers, behavioral division of labor between nurses and foragers, the formation of adaptive foraging networks, nestmate vs. non-nestmate discrimination, and collective nest construction (Morgan 2009; Richard & Hunt 2013; Grüter & Keller 2016; Leonhardt et al. 2016). All of these behaviors are largely mediated via chemical communication using a wide range of pheromones. In *Drosophila*, pheromone receptors have been identified that belong to multiple insect chemosensory receptor families, including odorant receptors (ORs), gustatory receptors (GRs), ionotropic receptors (IRs), and pickpocket channels (PPKs) (Kohl et al., 2015). Ants have numbers of GRs, IRs, and PPKs that are typical for insects, while their OR repertoire is highly expanded (C. R. Smith et al. 2011; C. D. Smith et al. 2011; Zhou et al. 2012; Oxley et al. 2014; McKenzie et al. 2016) (Table 3.1, Figure 3.3.1A). This raises the possibility that the expansion of ORs specifically, rather than chemoreceptors in general, may underlie the evolution of complex chemical communication in ants. Ants also have exceedingly large numbers of glomeruli in their antennal lobes, which likely mirror their expanded OR gene repertoire (Zube et al. 2008; McKenzie et al. 2016; McKenzie & Kronauer 2018) (Table 3.1, Figure 3.1A). Insect ORs function as chemosensory receptors by dimerizing with the highly-conserved co-receptor protein Orco to form ligand-gated ion channels (Larsson et al. 2004; Jones et al. 2005; Sato et al. 2008; Butterwick et al. 2018). *orco* null mutants in fruit flies, locusts, mosquitoes, and moths therefore lose OR function and show impaired responses to odorants such as food

volatiles and sex pheromones (Asahina et al. 2008; DeGennaro et al. 2013; Koutroumpa et al. 2016; Li et al. 2016; Yang et al. 2016). Thus, *orco* constitutes a prime candidate to test the hypothesis that the expanded OR repertoire of ants is required for chemical communication.

Table 3.1: Numbers of ORs and antennal lobe glomeruli in select insects (Figure 3.1A).

Common name	Scientific name	OR number	Antennal lobe glomerulus number
Dampwood termite	*Zootermopsis nevadensis*	63 (Terrapon et al., 2014)	70-74 (Terrapon et al., 2014)
Pea aphid	*Acyrthosiphon pisum*	62 (Smadja et al., 2009)	25-40 (Kollmann et al., 2011)
Vinegar fly	*Drosophila melanogaster*	60 (Robertson et al., 2003)	42 (Laissue and Vosshall, 2008; Laissue et al., 1999)
Red flour beetle	*Tribolium castaneum*	259 (Engsontia et al., 2008)	90 (Dippel et al., 2016)
Jewel wasp	*Nasonia vitripennis*	225 (Robertson et al., 2010)	Not published
Honey bee	*Apis mellifera*	163 (Robertson et al., 2010)	156-166 (Flanagan and Mercer, 1989)
Jerdon's jumping ant	*Harpegnathos saltator*	347 (Zhou et al., 2012)	275 (Yan et al., 2017)
Clonal raider ant	*Ooceraea biroi*	503 (McKenzie & Kronauer, 2018)	493-509 (McKenzie et al., 2016)
Florida carpenter ant	*Camponotus floridanus*	352 (Zhou et al., 2012)	434-464 (Zube et al., 2008)
Big headed leafcutter ant	*Atta cephalotes*	376 (Engsontia et al., 2015)	349 (Kelber et al., 2009)

The receptor families involved in pheromone perception in ants have not been functionally characterized, in part because the complex life cycle of ants has hindered the development of functional genetic tools (Schulte et al. 2014; Grüter & Keller 2016; Kohno et al. 2016; Reid & O'Brochta 2016). Indeed, prior to this study no mutant lines in ants had been generated (e.g., using transgenesis, random mutagenesis, or targeted mutagenesis). Most ant species reproduce sexually, so generating homozygous mutant lines requires multiple generations of crosses, which is challenging given that the generation times of ants tend to be many months (Yan et al. 2014). Furthermore, performing such crosses raises methodological concerns, as inbreeding individuals to generate homozygous mutants also has the potential to homozygose off-target mutations (Fu et al. 2013). In other model organisms this issue can be addressed by using multiple generations of outcrossing, but this is not feasible in species with long generation times such as ants (Fu et al. 2013; Kistler et al. 2015). Thus, most ant species pose major challenges to the generation of mutant lines that can be used to generate reliable scientific results. As described in Chapter 2, in this study I took advantage of the unique biology of the clonal raider ant to generate *orco* mutant ants and characterize the role of ORs in ant social behavior.

To reduce the potential for off-target mutagenesis, I designed a gRNA that has a unique sequence relative to the rest of the genome (see Chapter 2, Chapter 7) and characterized multiple, independently generated lines of heterozygous and homozygous *orco* mutants. I found that *orco* mutant ants, as expected, lacked Orco antibody staining and possessed deficiencies in general olfactory behaviors. These ants also had deficiencies in social

behavior, including an inability to nest with other ants or follow pheromone trails, and exhibited reduced fitness. In contrast with previously studied insects, I also found that *orco* mutant ants possessed striking neuro-anatomical phenotypes, including a loss of olfactory sensory neurons (OSNs) in the antennae and a striking reduction in the number of glomeruli in the antennal lobes. Collectively, these results illustrate the crucial significance of *orco* and ORs in ant biology.

Generation of orco mutant ants

I confirmed the identity of *orco* in the *O. biroi* genome (see Chapter 2) and designed and synthesized a guide RNA (gRNA) to target *orco* (Figure 3.1B). To produce *orco* mutants, I injected Cas9 protein and gRNA into 3,291 eggs less than 5h of age and produced 42 G0 adults, some of which displayed mutations in at least 97% of PCR amplicons of the *orco* target site (Figure 3.1C, Chapter 7). G0 mutations in the germline can be inherited by G1s to produce stable modifications to the genome (Reid & O'Brochta 2016). Given that *O. biroi* reproduces through parthenogenesis (Oxley et al. 2014), stable mutant lines can be clonally propagated from individual mutant G1s and subsequent generations. *orco* loss-of-function mutant lines were thus derived from G1 eggs with independent frameshift mutations in both *orco* alleles. I recovered a diverse set of *orco* mutant lines, including two $orco^{wt/-}$ lines with one frameshift allele and five $orco^{-/-}$ lines with two frameshift alleles (Figure 3.1D). The phenotypes reported below were consistent across the two $orco^{wt/-}$ lines and across the five $orco^{-/-}$ lines, respectively.

Figure 3.1: Number of OR genes and *orco* mutagenesis. (A) Phylogeny with numbers of ORs for ants (green) and other insects (black), showing ant OR expansion (Table 3.1). (B) Position of predicted CRISPR/Cas9 cut site in Orco protein model (red circle). Frameshift mutations at this position truncate the wild-type protein between the third and fourth transmembrane domains, and the resultant mutant protein is unlikely to form functional ion channels. (C) Proportion of Illumina sequencing reads of orco amplicons with insertions or deletions (indels) relative to gRNA sequence in G0s, showing mutation rates of at least 97% in some individuals. Red circle indicates predicted CRISPR/Cas9 cut site. Protospacer adjacent motif (PAM) in bold. (D) Wild-type orco sequence compared to sequences for the two $orco^{wt/-}$ and the five $orco^{-/-}$ mutant lines. Deletions are shown in red and insertions in green. $orco^{-/-}$ ants have two frameshift alleles and are therefore expected to be complete loss-of-function orco mutants. Each of these lines arose independently; *n* indicates the number of ants of each line (G1s and subsequent generations) used across all experiments in this study (see Table S3 in Trible et al. 2017 for a description of the lines used in each specific experiment; it is too lengthy to reproduce here). PAM in bold.

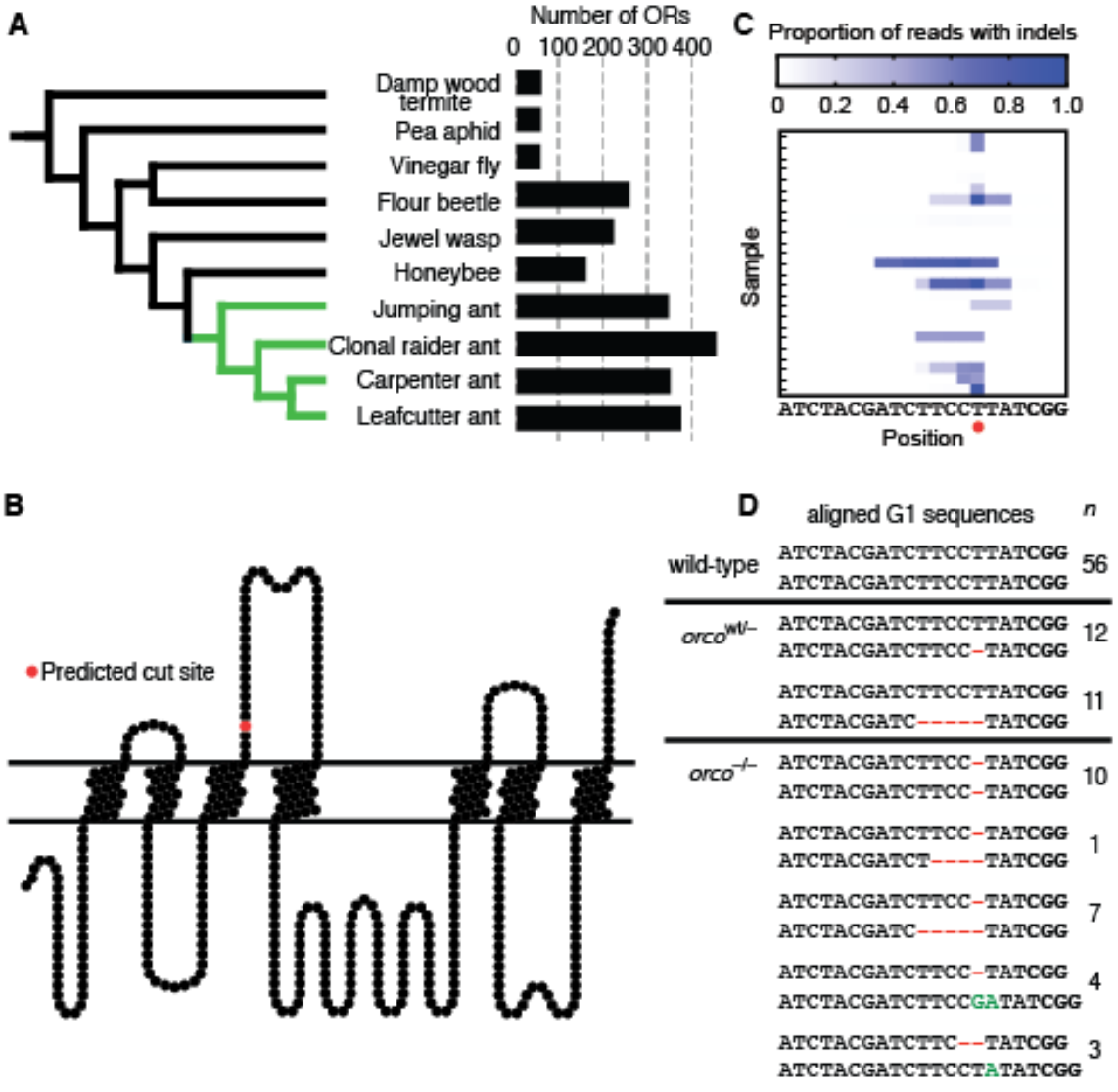
A
Number of ORs
0 100 200 300 400
Damp wood termite
Pea aphid
Vinegar fly
Flour beetle
Jewel wasp
Honeybee
Jumping ant
Clonal raider ant
Carpenter ant
Leafcutter ant
C
Proportion of reads with indels
0 0.2 0.4 0.6 0.8 1.0
Sample
ATCTACGATCTTCCTTATCGG
Position
B
Predicted cut site
D
aligned G1 sequences
n
wild-type
ATCTACGATCTTCCTTATCGG
ATCTACGATCTTCCTTATCGG
56
orco wt/–
ATCTACGATCTTCCTTATCGG
ATCTACGATCTTCC–TATCGG
12
ATCTACGATCTTCCTTATCGG
ATCTACGATC-----TATCGG
11
orco –/–
ATCTACGATCTTCC–TATCGG
ATCTACGATCTTCC–TATCGG
10
ATCTACGATCTTCC–TATCGG
ATCTACGATCT----TATCGG
1
ATCTACGATCTTCC–TATCGG
ATCTACGATC-----TATCGG
7
ATCTACGATCTTCC–TATCGG
ATCTACGATCTTCCGATATCGG
4
ATCTACGATCTTC--TATCGG
ATCTACGATCTTCCTATATCGG
3

Antennal morphology

To test whether *orco* frameshift mutations cause a loss of the full-length Orco protein and/or change the distribution of olfactory sensory neurons (OSNs), I immunostained *O. biroi* wild-type and *orco* mutant antennal sections with an Orco antibody and counterstained the cell nuclei with DAPI. Wild-type and $orco^{wt/-}$ *O. biroi* antennae contained a dense region of Orco-positive OSNs in the center of the antennal club, as indicated by DAPI and Orco staining (Figure 3.2A, B). As predicted, antennae of $orco^{-/-}$ ants lack Orco staining, indicating that the full-length Orco protein is absent (Figure 3.2C). Surprisingly, the majority of OSNs in the *O. biroi* antenna are also absent in *orco* mutants, as indicated by a reduction in DAPI signal (Figure 3.2C). This result suggests that the *orco*-positive OSNs in the *O. biroi* antenna are absent in *orco* mutants, but that the smaller number of other types of sensory neurons may remain present. This contrasts with *D. melanogaster*, in which the antennal OSNs that express *orco* in wild-types are still present in *orco* mutant adults (Chiang et al. 2009).

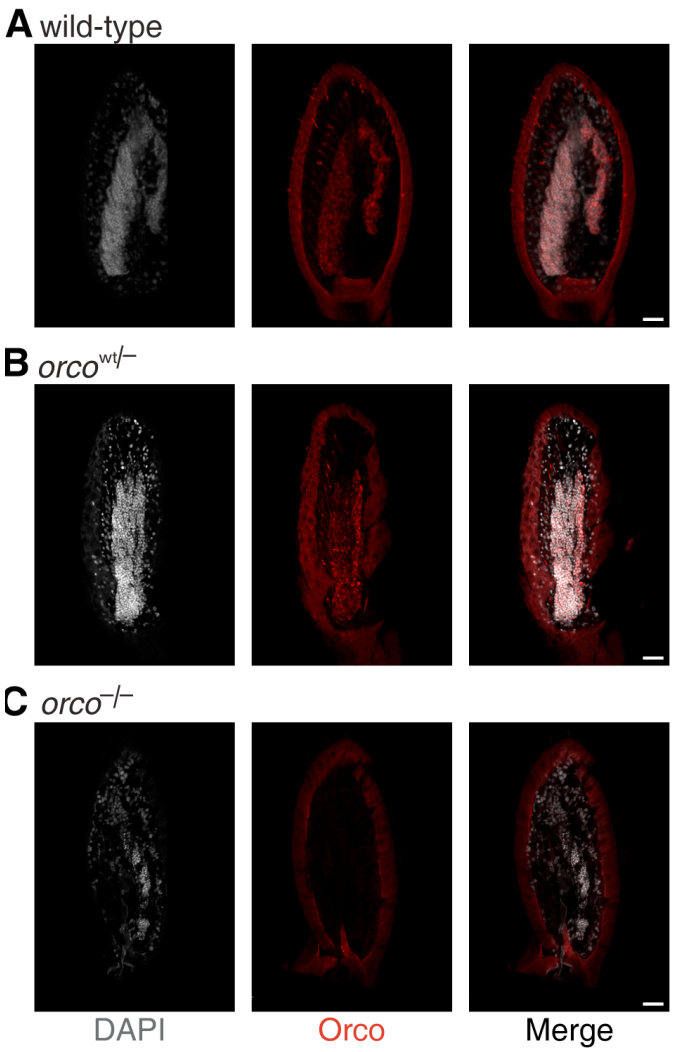

Figure 3.2: Loss of Orco expression and OSNs in *orco*$^{-/-}$ ants. (A) and (B) Antennal section of wild-type *and orco*$^{wt/-}$ *O. biroi* showing DAPI counterstain (gray), Orco immunostain (red), and the merged image (black). Wild-type *and orco*$^{wt/-}$ ants possess a dense region of Orco-positive OSNs in the center of the antenna. (C) Antennal section of *orco*$^{-/-}$ ant. *orco*$^{-/-}$ ants lack Orco staining, indicating that the full-length Orco protein is absent. *orco*$^{-/-}$ ants also lack the dense region of cells in the center of the antenna, indicating that most or all of the OSNs that would express orco in wild-types are absent in *orco*$^{-/-}$ ants. Scale bars are 20 μm.

Antennal lobe morphology

In *D. melanogaster*, all antennal lobe glomeruli that have been examined remain present in *orco* mutants, implying that OR function is not required for gross antennal lobe morphology (Larsson et al. 2004; Chiang et al. 2009). These results contrast strongly with mice, where olfactory receptor function and neuronal activity are essential for the formation and maintenance of the analogous brain region, the olfactory bulb (Yu et al. 2004). However, *D. melanogaster* has only 60 ORs and a similar number of glomeruli, while mice possess over one thousand olfactory receptors and glomeruli. This striking difference suggests that complex olfactory systems must rely on receptor function for their development and/or maintenance. Ants have highly expanded numbers of ORs and antennal lobe glomeruli (Zube et al. 2008; Zhou et al. 2012; Oxley et al. 2014; McKenzie et al. 2016; McKenzie & Kronauer 2018) (Table 3.1), raising the possibility that the development and/or maintenance of ant antennal lobes may require additional mechanisms to exceed the complexity found in other insects.

To address whether OR function might be required for the structure of the ant antennal lobe, I imaged brains using confocal microscopy, measured antennal lobe volumes and the number of glomeruli, and reconstructed antennal lobes in wild-type and *orco* mutant adults in *O. biroi* and *D. melanogaster*. I found that the antennal lobes of $orco^{-/-}$ ants measured only one third of the volume of wild-type and $orco^{wt/-}$ antennal lobes, and approximately 82% of the glomeruli were lost (Figure 3.3A,B). However, all six glomeruli in the T7 cluster of the ant antennal lobe, which is believed to be innervated by olfactory sensory neurons that do not express ORs (Nakanishi et al. 2010), were still

present in *orco*$^{-/-}$ individuals. No differences were observed in the volume of the protocerebrum, mushroom bodies, or central complex relative to wild-type ants ($p = 0.45$, 0.17, and 0.20, respectively; t-test). In contrast, I detected no significant difference in antennal lobe volumes and only minor potential differences in glomerulus numbers between wild-type and *orco*$^{-/-}$ flies (Figure 3.3C,D). To test whether antennal lobes degenerate as a function of age in *orco*$^{-/-}$ flies, I imaged antennal lobes of additional wild-type and *orco*$^{-/-}$ flies aged for 30 days, showing that antennal lobe glomeruli were not reduced (Figure 3.3C). These results demonstrate that development and/or maintenance of antennal lobes in ants, but not flies, are indeed dependent on Orco function.

Figure 3.3: Reduced antennal lobes in *orco*$^{-/-}$ ants. (A) *O. biroi*: dorsal (n-ventral) 3D projections of *orco*$^{-/-}$ and wild-type ants. Antennal lobes indicated by dashed lines. *orco*$^{-/-}$ antennal lobe was highly reduced relative to the wild-type. Two *orco*$^{-/-}$ ants had 90 and 91 glomeruli relative to 493 and 509 glomeruli for two wild-type ants (one of the wild-type reconstructions has been published previously [McKenzie et al. 2016]); small differences between replicates within treatments might reflect reconstruction errors or actual biological variation. (B) Antennal lobe volumes for wild-type (n = 5), *orco*$^{wt/-}$ (n = 5), and *orco*$^{-/-}$ (n = 4) ants (*orco*$^{wt/-}$ and *orco*$^{-/-}$ were age-matched at 4 months old). *orco*$^{-/-}$ ants, but not *orco*$^{wt/-}$ ants, had significantly smaller antennal lobes than wild-types. (C) *D. melanogaster*: anterior (n-ventral) 3D projections for wild-type and *orco*$^{-/-}$ brains from 1-month-old flies. Antennal lobes indicated by dashed lines. *orco*$^{-/-}$ antennal lobe was similar to wild-type. Two *orco*$^{-/-}$ flies had 43 and 44 glomeruli, and two wild-type flies each had 46 glomeruli. These glomerulus numbers were higher than has been previously reported, which is likely due to differences in sample preparation and imaging techniques. Slight differences in glomerulus numbers between replicates may be due to reconstruction errors, or may reflect modest antennal lobe phenotypes in *orco* mutant flies. (D) Antennal lobe volumes for wild-type (n = 5) and *orco*$^{-/-}$ (n = 5) flies. Volumes of wild-type and *orco*$^{-/-}$ antennal lobes were not significantly different ($p = 0.20$, t test). Scale bars, 20 μm. NS, not significant. Genotypic classes marked by different letters are significantly different ($p < 0.05$) after ANOVA followed by Tukey's test (B).

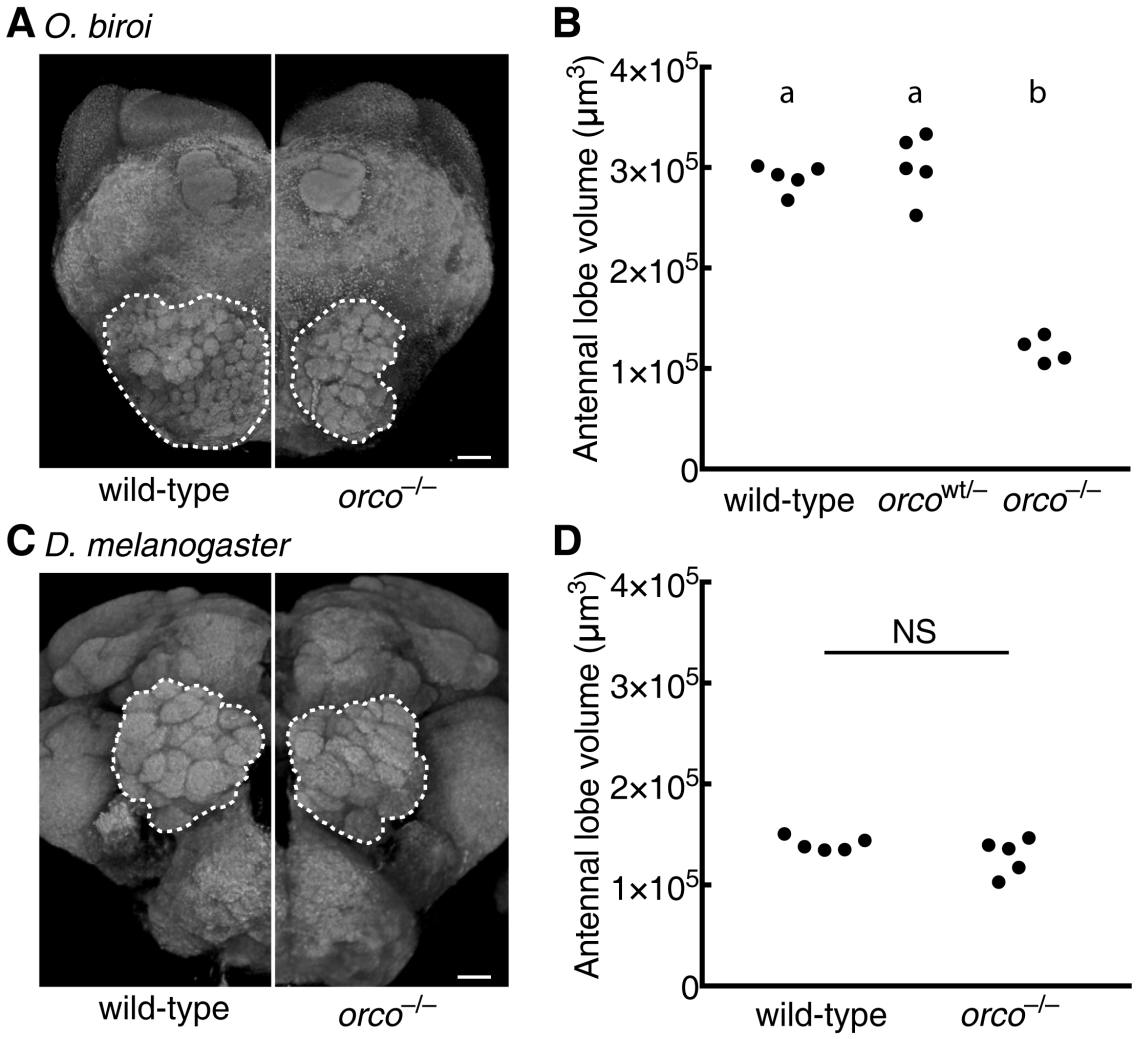
A O. biroi
wild-type
orco–/–
B
Antennal lobe volume (µm3)
4×10^5
3×10^5
2×10^5
1×10^5
0
a
a
b
wild-type
orcowt/–
orco–/–
C D. melanogaster
wild-type
orco–/–
D
Antennal lobe volume (µm3)
4×10^5
3×10^5
2×10^5
1×10^5
0
NS
wild-type
orco–/–

Behavioral phenotypes

Based on the general observation that ants are often repelled by the smell of permanent markers, I developed a simple assay to test whether *orco* mutants have compromised chemosensory abilities. I found that wild-type and *orco*$^{wt/-}$ *O. biroi* are strongly repelled by lines drawn with Sharpie^{TM} permanent marker, and rarely contact or cross Sharpie lines (Figure 3.4A-C). Given that *O. biroi* is blind and that the ants are often repelled before touching the Sharpie lines, it was clear that this behavior is mediated via olfaction, rather than visual or tactile cues. *orco*$^{-/-}$ *O. biroi* were significantly less repelled by Sharpie (Figure 3.4A-C), implying that *orco* is required to perceive the odorants that cause Sharpie lines to be repulsive. These results suggested that *orco* mutant ants possess general olfactory deficiencies, similar to *orco* mutants in other types of insects (Asahina et al. 2008; DeGennaro et al. 2013; Koutroumpa et al. 2016; Li et al. 2016; Yang et al. 2016).

Pheromone trails are a major feature of chemical communication in many ants, and are important for coordinating collective behaviors (Zube et al. 2008; Morgan 2009). In many doryline ants, including *O. biroi*, disturbance of colonies leads to robust trail formation, likely for the purpose of nest relocation (Schneirla 1971 p. 94; Gotwald 1995 p. 99; Hölldobler 1982). To test whether *orco* influences the ability of *O. biroi* to follow pheromone trails, I set up 5 experimental colonies composed of 12-14 identically-reared G1s with wild-type, *orco*$^{wt/-}$, and *orco*$^{-/-}$ genotypes, and individually tagged each ant with color dots (Figure 3.4D). I recorded videos of each colony and used a novel custom-built automated behavioral tracking system employing painted color tags (rather than paper

barcodes (Mersch et al. 2013)) to individually identify the ants and quantify their behavior (Figure 3.4D, see Chapter 7). I disturbed each colony at the beginning of each video, causing the ants to form conspicuous trails. During the ensuing period of high activity, I created a 2-D histogram, or density map, of movement for each ant, and measured the Pearson correlation coefficient of this density map with the density map of the other ants in the colony, reasoning that density maps would be more highly correlated when ants were following pheromone trails (Figure 3.4E,F). To provide a null expectation, I also compared the density maps of individual ants to a randomized density map of other ants in the colony (Figure 3.4E,F). I found that individual ants had density maps with significantly higher correlations to the density maps of the rest of the ants in the colony than with the randomized density maps in wild-type, but not *orco*$^{-/-}$ ants (Figure 3.4F; average correlation coefficients were 0.31 versus 0.04 in wild-type and 0.07 versus 0.02 in *orco*$^{-/-}$, respectively). These findings imply that trail following behavior is reduced or absent in *orco*$^{-/-}$ ants, likely because they are unable to perceive chemical pheromone trails.

Nesting behavior, and the formation of aggregations more generally, is a ubiquitous feature of social insect biology (Depickère et al. 2004). Immediately upon eclosion, I noticed that some G1s did not nest with other ants, but instead showed a wandering phenotype (Figure 3.4G). In a set of 16 G1 colonies, I used this wandering phenotype to identify colonies containing *orco*$^{-/-}$ ants with 100% accuracy ($p < 0.001$, Fisher exact test, see Chapter 7). To more precisely measure nesting behavior in *orco* mutants, I recorded and analyzed 24 hr videos of each experimental colony. I found that wild-type and

orco$^{wt/-}$ ants aggregated into tight clusters and exhibited little movement outside the cluster, while *orco*$^{-/-}$ ants frequently exited the cluster and wandered around the dish (Figure 3.4H). Overall, *orco*$^{-/-}$ ants spent a significantly larger fraction of time without contact with other ants when compared to wild-type and *orco*$^{wt/-}$ ants (Figure 3.4I). These findings demonstrated that typical nesting behavior is compromised in *orco*$^{-/-}$ ants. This observation is consistent with the idea that *orco* mutants are unable to perceive odorants, such as aggregation pheromones (Bell et al. 1972; Depickère et al. 2004; Li et al. 2016), which might be involved in nesting behavior.

Figure 3.4: Deficient olfactory and social behavior in *orco*$^{-/-}$ ants. (A) Example trajectories of wild-type and *orco*$^{-/-}$ ants in Sharpie assay. (B) Line crossing events for wild-type (n = 9), *orco*$^{wt/-}$ (n = 10), and *orco*$^{-/-}$ (n = 8) ants in Sharpie assays, with ants from (A) highlighted. Wild-type and *orco*$^{wt/-}$ ants crossed Sharpie lines (red) less frequently than printed lines (gray), but *orco*$^{-/-}$ ants crossed both lines at approximately equal frequencies. (C) Repulsion indices for ants in Sharpie assays. Repulsion index was calculated as proportion of printed line crosses. *orco*$^{-/-}$ ants, but not *orco*$^{wt/-}$ ants, were significantly less repelled than wild-types. (D) Example colony used for trail pheromone analysis. The same colony, containing a mixture of wild-type, *orco*$^{wt/-}$, and *orco*$^{-/-}$ ants, is shown twice, with a wild-type or *orco*$^{-/-}$ focal ant highlighted. (E) Example trail pheromone analysis. Trajectories, during which ants were moving and edges were excluded, were used to create 2D histograms, or density maps, for each ant in the colony. These density maps were compared to the actual and randomized density maps for all other ants in the colony. The wild-type density map was more strongly correlated with the actual colony density map than with the randomized colony density map, while the *orco*$^{-/-}$ density map was poorly correlated with both colony density maps. (F) Pearson correlation coefficients for individual ant density maps with the actual or randomized density map of the other ants in the colony. Pearson correlation coefficients for wild-type ants (n = 28), but not for *orco*$^{-/-}$ ants (n = 9), were significantly higher in actual than randomized density maps (sample sizes were too small to test *orco*$^{wt/-}$). (G) Example colony showing an individual outside of the nest. (H) Distances traveled in 24 hr videos by ants in experimental colonies. *orco*$^{-/-}$ ants (n = 10), but not wild-type (n = 40) or *orco*$^{wt/-}$ (n = 8) ants, exhibited a wandering phenotype. (I) Time without contacting other

ants in 24 hr videos. *orco*$^{-/-}$ ants spend more time without contact than wild-type or *orco*$^{wt/-}$ ants. ***$p < 0.001$; NS, not significant. Genotypic classes marked by different letters are significantly different ($p < 0.05$) after ANOVA followed by Tukey's test (C), or from log-likelihood ratio tests on generalized linear mixed models followed by Tukey's tests with colony as a random variable and actual/randomized maps (F) or genotypic class (H and I) as fixed variables.

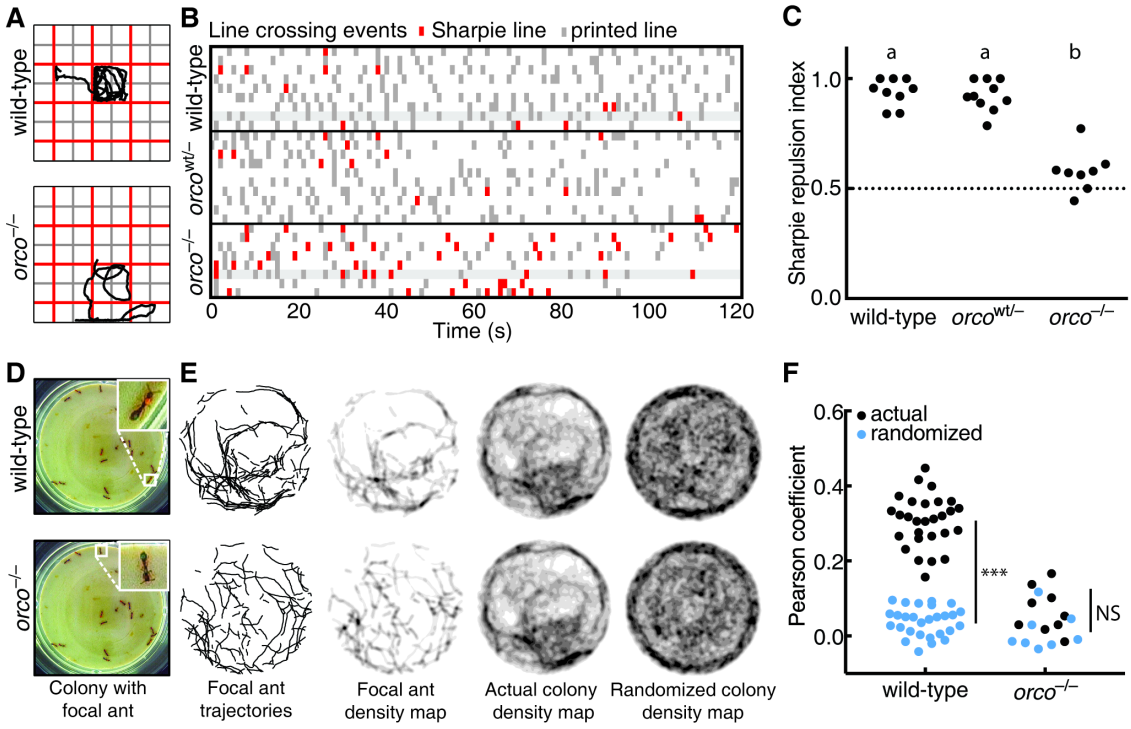
A
wild-type
orco−/−
B
Line crossing events
Sharpie line
printed line
wild-type
orcowt/−
orco−/−
0
20
40
60
80
100
120
Time (s)
C
Sharpie repulsion index
1.0
0.5
0.0
a
a
b
wild-type
orcowt/−
orco−/−
D
wild-type
orco−/−
Colony with focal ant
E
Focal ant trajectories
Focal ant density map
Actual colony density map
Randomized colony density map
F
actual
randomized
Pearson coefficient
0.6
0.4
0.2
0.0
***
NS
wild-type
orco−/−
G
H
Distance traveled (m)
200
150
100
50
0
a
a
b
wild-type
orcowt/−
orco−/−
I
Time outside nest (hrs)
24
18
12
6
0
a
a
b
wild-type
orcowt/−
orco−/−

Fitness of orco mutants

Finally, I investigated whether *orco* mutations influence fitness by measuring egg-laying and survival rates of wild-type and *orco* mutant ants. I found that $orco^{-/-}$ ants laid significantly fewer eggs than wild-type and $orco^{wt/-}$ ants over a two week period (Figure 3.5A), and $orco^{-/-}$ ants exhibited significantly higher mortality than wild-types over a 34 day period (Figure 3.5B). These results contrast with *orco* mutant *Drosophila* and mosquitoes, in which no fitness effects are observed under typical laboratory rearing conditions (Asahina et al. 2008; DeGennaro et al. 2013). This suggests that the *orco* mutant phenotype has serious consequences for ant fitness. It is possible that these fitness effects result because $orco^{-/-}$ ants are unable to integrate into the colony, as wandering behavior and reduced fitness are also seen in wild-type ants that are kept in social isolation (Koto et al. 2015).

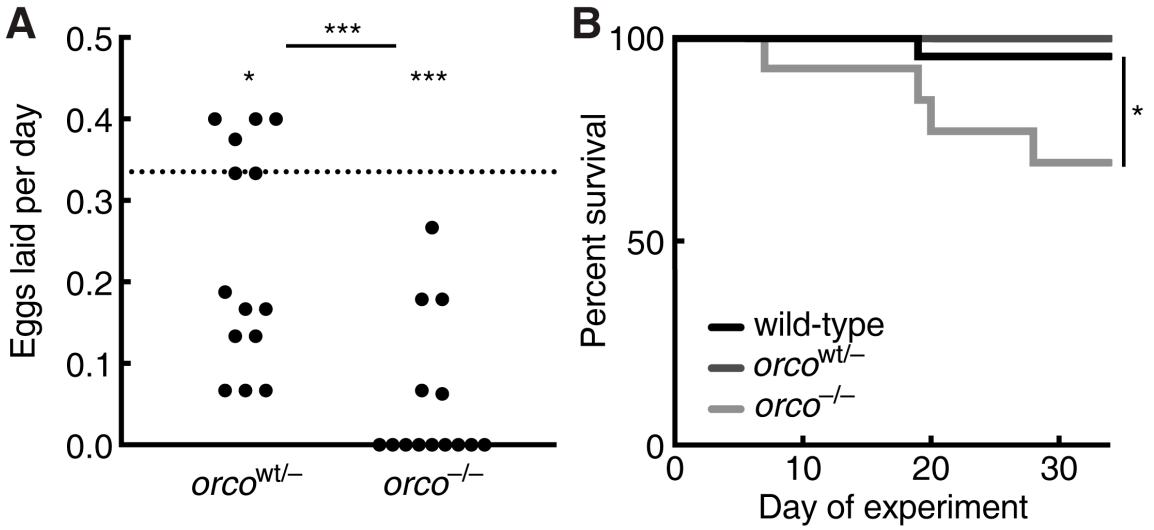

Figure 3.5: Reduced fitness in *orco*$^{-/-}$ ants. (A) Eggs laid per day over a two week period by *orco*$^{wt/-}$ (n = 12) and *orco*$^{-/-}$ (n = 14) ants relative to wild-type average (dotted line). *orco*$^{-/-}$ ants laid significantly fewer eggs than *orco*$^{wt/-}$ ants. Both *orco*$^{wt/-}$ and *orco*$^{-/-}$ ants laid significantly fewer eggs than the wild-type average of 0.34 eggs per day. Wild-type data are given as an average, rather than individual values, because most ants in each colony were wild-type and it was therefore not possible to obtain individual egg-laying rates for wild-type ants (see Chapter 7). (B) Survival of identically-reared and age-matched wild-type (n = 42), *orco*$^{wt/-}$ (n = 7), and *orco*$^{-/-}$ (n = 13) ants over a 34-day period. Survival of *orco*$^{-/-}$ ants was significantly lower than that of wild-type ants. Survival of *orco*$^{wt/-}$ ants was not statistically tested due to small sample size, but no trend toward reduced survival was observed. *$p < 0.05$; ***$p < 0.001$; NS, not significant. p values from an unpaired two-way Wilcoxon test (comparison of *orco*$^{wt/-}$ and *orco*$^{-/-}$ egg-laying rates) and one-way Wilcoxon tests (comparisons of *orco*$^{wt/-}$ and *orco*$^{-/-}$ egg laying rates to wild-type) using the mean egg-laying rate of wild-type ants in this experiment (A) or from a Fisher exact test (B).

While I observed many striking deficiencies in *orco*$^{-/-}$ ants, it is important to note that these ants were viable, fed, laid eggs, and likely still exhibited some typical social behaviors. For example, I observed *orco*$^{-/-}$ ants groom eggs, touch other ants with their antennae, and elicit trail and alarm responses. Thus, *orco* mutants could provide an important resource to study the role of ORs in ant biology in the future.

Discussion

I have demonstrated that *orco* is crucial for many aspects of ant biology, including individual responses to repulsive odorants and pheromones, and fitness. Surprisingly, I also found striking neuro-anatomical phenotypes in *orco* mutant ants at the level of the antennae and antennal lobes. In *D. melanogaster*, *orco* mutants possess normal numbers of OSNs, and ablation of *orco*-expressing neurons in adults does not cause the loss of antennal lobe glomeruli (Berdnik et al. 2006). However, experiments in *D. melanogaster*, as well as honeybees and moths, indicate that OSNs are likely required for the formation of the antennal lobe glomeruli (Gascuel & Masson 1991; Malun et al. 1994; Jhaveri & Rodrigues 2002). Thus, it is likely that the development, but not maintenance, of insect antennal lobe glomeruli is dependent on the presence of OSNs. Unlike in *D. melanogaster*, I observed that *orco* mutant ants lack the majority of OSNs and antennal lobe glomeruli. I therefore hypothesize that the antennal lobe phenotype in *orco* mutant ants results because the OSNs that typically express Orco either fail to develop or die early in development, preventing the formation of OR glomeruli.

orco mutant *O. biroi* possess about 90 antennal lobe glomeruli, which is more than the

total of non-OR chemosensory receptors that have been identified in the genome (Oxley et al. 2014; McKenzie & Kronauer 2018). Interestingly, half of the remaining glomeruli appear to be in the T6 cluster, which is believed to be composed entirely of OR glomeruli (McKenzie et al. 2016). Therefore, it is likely that some OR glomeruli are still present in *orco* mutant ants. I propose that the initial formation of OR glomeruli in *O. biroi* is independent of *orco* function, similar to *D. melanogaster*, but the subsequent expansion to large numbers of glomeruli is *orco* dependent (possibly due to OSN innervation and/or OR function). If this model is correct, then this *orco*-dependent stage of glomerulus expansion could represent an evolutionary change in the development of ants relative to flies that is related to the evolution of expanded OR repertoires. Inspired by my initial findings, colleagues decided to also examine brains of a second ant species in which they had generated an *orco* mutant, and they found an antennal lobe phenotype similar to what I had observed in *O. biroi* (Yan et al. 2017). These results further indicate that the role of *orco* in neuro-anatomy is likely conserved throughout the ants.

It is tempting to describe these striking neuro-anatomical phenotypes as activity-dependent neuroplasticity, but I believe that this would not be warranted based on the present data. It is possible that OR-mediated neuronal activity is required for the development or maintenance of OR glomeruli, and that environmental influences on neuronal activity (such as sensory deprivation) could therefore lead to the same loss of OR glomeruli that I observed in *orco* mutant ants. On the other hand, it is also possible that these phenotypes are unrelated to plasticity if the loss of OR glomeruli is not activity dependent. For example, *orco* could play a role in antennal lobe development mediated

by transcriptional regulation, the survival of OSNs, or response to signaling molecules. I have demonstrated that *orco* (and therefore likely OR function) is essential for typical adult neuro-anatomy, but future experiments will be required to test whether these phenotypes arise due to its canonical role in neuronal activity, or if *orco* in ants may possess additional biochemical functions.

While the neuro-anatomical phenotypes I observed in these *orco* mutants are largely unprecedented, the behavioral phenotypes are consistent with a generally reduced olfactory capacity, as has been seen in *orco* mutants of other types of insects. These phenotypes therefore likely result from peripheral sensory deficiencies affecting communication, rather than from more specific effects on social cognition. Chemosensation is arguably the primary sensory modality in ants, particularly in a blind species such as *O. biroi*, so behavioral and fitness phenotypes in *orco* mutant ants may be generally expected to be more obvious than in insects that rely more heavily on other senses (Asahina et al. 2008; DeGennaro et al. 2013; Koutroumpa et al. 2016; Li et al. 2016; Yang et al. 2016).

More than half of the data presented here were collected using G1 ants. G1 adults in *O. biroi* can be obtained just four months after performing injections, which is much quicker than any other social insect model system (Yan et al. 2014). Thus, the clonal raider ant provides a unique opportunity to rapidly generate and phenotype mutant lines in a social insect. While all data in the present study were collected from germ-line mutants (G1s and subsequent generations), I also found very high somatic cut-rates among the G0 ants

(Figure 3.1C). Multiple G0s displayed nearly 100% mutation rates, and exhibited wandering phenotypes similar to germ-line mutants in subsequent generations (Figure 3.1C, Chapter 7). Thus, my results show that CRISPR/Cas9 can have very high efficiency in social insects and may be useful for conducting experiments in G0s even in the large number of species where it is not feasible to maintain stable mutant lines. Recent studies in honeybees have echoed this general conclusion (Roth et al. 2019).

Major transitions in evolution require the coordinated action of individuals to operate as a functional, higher-level unit (Maynard Smith & Szathmary 1997). During the transition from solitary to eusocial living in ants, this coordination was largely achieved via pheromones, and ants accordingly possess highly expanded antennal lobes and OR repertoires. My results illustrate the functional significance of these striking changes, and imply that the expansion of ORs may have been an important component of the evolution of eusocial behavior.

CHAPTER 4: A THEORY OF CASTE EVOLUTION AND DEVELOPMENT

Following my proof-of-concept with *orco*, I wanted to eventually use functional genomics to study a long-standing mystery in ant biology: the development and evolution of morphological castes (such as workers, soldiers and queens). Before conducting laboratory experiments, I needed some kind of conceptual framework to organize the prior literature and outline which aspects of this phenomenon remain poorly understood. I conducted an extensive literature review, trying to combine the historical literature of caste in ants with more recent advances in functional biology and evo-devo from other types of organisms. In this chapter, I present an overview of the model I proposed. The major conclusion of this research is that, with respect to certain features, ant castes have surprisingly simple patterns of phenotypic variation. Castes fall into a relatively small number of categories in terms of their morphology and behavior, and a simple developmental model with a few degrees of freedom is capable of producing this variation. Chapter 4 organizes the core features of caste development in ants, and my empirical efforts to identify the mechanisms producing these features are described in Chapter 5.

The mystery of caste in ants

Many insect species, such as locusts and dung beetles, display morphological polyphenisms (Simpson et al. 2011; Hartfelder & Emlen 2012). Perhaps the most elaborate polyphenisms are observed in ants, in which female individuals can develop into a wide range of morphological castes, including workers, soldiers, ergatoid queens, and queens (Figure 4.1; Molet et al. 2012). Development into alternative castes is caused

by diverse factors in different ant species, ranging from strictly environmental to genetic (Brian 1979; Wilson & Hölldobler 1990; Anderson et al. 2008; Schwander et al. 2010). Castes have been gained and lost repeatedly across the ant phylogeny, and often exhibit striking convergent and parallel evolution, exemplified by multiple independent origins of soldiers or independent losses of workers in socially parasitic species (Oster & Wilson 1978; Bourke & Franks 1991; Molet et al. 2012; Peeters 2012). Caste in ants has attracted the attention of many biologists, as it touches on subjects including epigenetics, developmental plasticity, developmental constraints, and sympatric speciation (Bourke & Franks 1991; West-Eberhard 2003; Bonasio 2012; Rajakumar et al. 2012; Rabeling et al. 2014). Despite many years of investigation, however, the mechanisms underlying both caste development and evolution remain poorly understood.

Figure 4.1: Caste systems in ants. (A) *Syscia augustae* has a caste system similar to the ancestral condition in ants, displaying workers (right) and winged queens (left) with modest differences in size and morphology. Note that queen ants shed their wings after founding colonies, but retain a highly segmented thorax and wing scars indicative of wing development. (B) *Eciton burchellii* has a derived caste system, displaying workers (top), subsoldiers (middle right), soldiers (middle left) and wingless ergatoid queens (bottom). (C) Cartoon schematic of the most common types of caste systems in ants. While no systematic ancestral state reconstruction has been conducted, these four classes of modified caste systems have evolved many times from the ancestral system many times throughout the ants. These are the five most common classes of caste systems, but many other combinations of workers, soldiers, ergatoid queens, and winged queens can be found in extant species. Images: Daniel Kronauer. Cartoons modified from Keller et al. 2014.

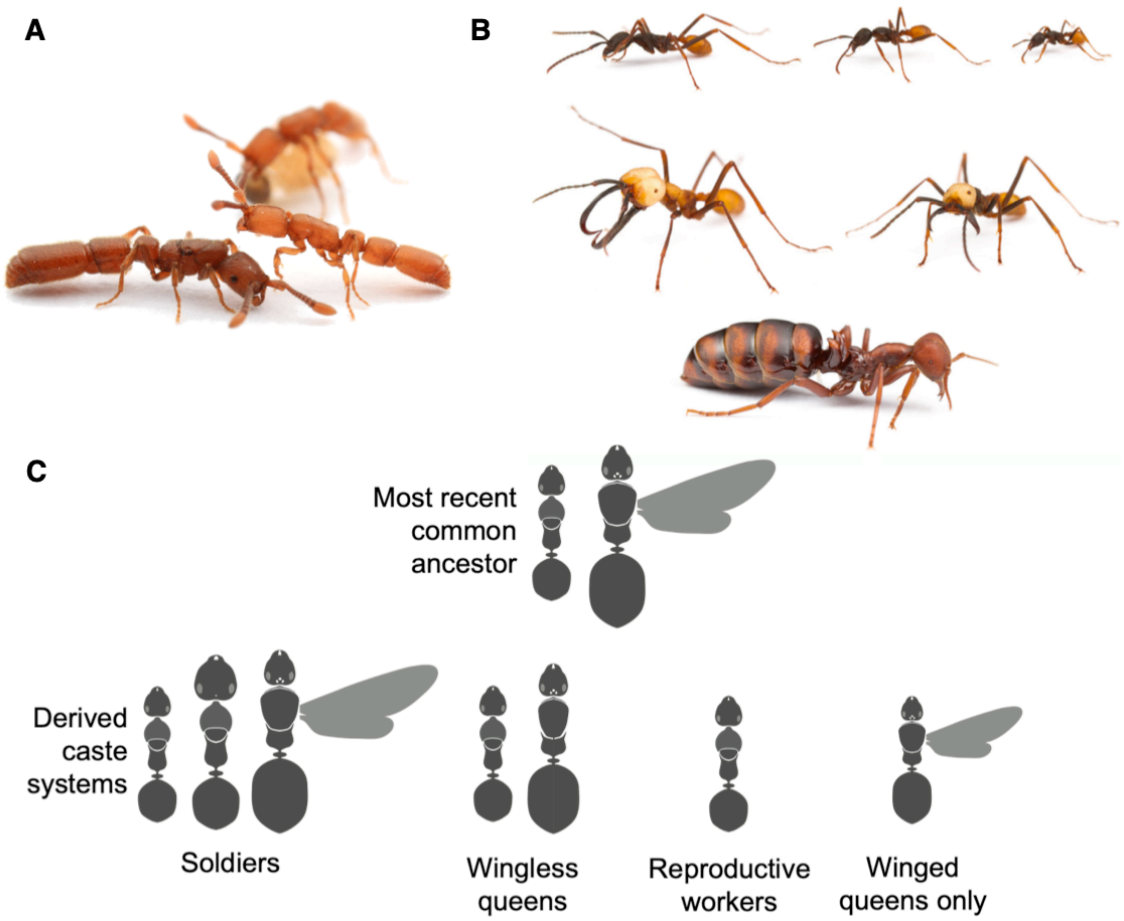
A
B
C
Most recent common ancestor
Derived caste systems
Soldiers
Wingless queens
Reproductive workers
Winged queens only

The ant fossil record contains multiple extinct lineages of early ants with winged queens and wingless workers, so it is likely that the most recent common ancestor of modern ants also possessed these two castes (Barden and Grimaldi, 2016) (Figure 4.1A). Many researchers have discussed how various groups of ants depart from this ancestral system, for example via the loss of the worker or queen caste, or the evolution of novel castes from workers, queens, or intercastes (worker-queen intermediates) (Wilson 1953; Oster & Wilson 1978; Bourke & Franks 1991; Wheeler 1991; Nonacs & Tobin 1992; Urbani & Passera 1996; Ward 1997; Urbani 1998; Molet et al. 2012; Peeters 2012; Rajakumar et al. 2012) (Figure 4.1B, C). Theories of caste development have also been proposed, describing how alternative caste morphology can arise from differential growth of imaginal discs, and how alternative caste development can be induced by genetic rather than environmental factors (Wilson 1953; Wheeler 1991; Anderson et al. 2008; Schwander et al. 2010; Rajakumar et al. 2012; Rajakumar et al. 2018). These theories provide partial explanations of development and evolution in certain types of caste systems, but a coherent synthesis is still lacking.

Here I attempt to unify the literature on ant caste development and evolution with a single theoretical framework, drawing on recent advances in evolutionary developmental biology (Carroll et al. 2001; West-Eberhard 2003; Hartfelder & Emlen 2012; Bopp et al. 2014; Wagner 2014; Londe et al. 2015; Xu et al. 2015). Ants possess a developmental spectrum of phenotypes, which I term the caste reaction norm, under which increasing body size is associated with increasingly queen-like morphological traits (Figure 4.2). Here I define body "size" as pupal mass, but it may also be estimated by adult dry mass

or body length. Measurements of body size should exclude developmentally irrelevant factors that might affect mass or volume measurements, such as gut contents or developing eggs inside ovaries (Brian 1974; Honěk 1993). In many species, the size distribution is bimodal, with one mode of fully worker-like individuals and a second mode of fully queen-like individuals (Wilson 1953; Wheeler 1991; Fjerdingstad & Crozier 2006). Species gain or lose castes over evolutionary time either by modifying this size distribution or by modifying the relationship of tissue growth and size (Figure 4.3). I hope that this review will clarify our understanding of caste development and evolution, and provide a framework for discovering the mechanisms that generate morphological diversity in ants as well as other types of insects.

Figure 4.2: The caste reaction norm. (A) Schematic representation of the progression of size, caste and phenotypic state in ants. Size is estimated by body mass and/or length. Phenotypic state is estimated by either the number or the presence/absence of ovarioles, eyes/ocelli and wings, and/or by measurements of abdomen, head and thorax width (Brian 1955; Brian 1956; Tsuji et al. 1991; Tsuji & Dobata 2011; Okada et al. 2013). (B) Same as (A), but with the bimodal size distribution found in species possessing workers and queens. Caste determination mechanisms produce the size distribution (green), while caste differentiation mechanisms produce the caste reaction norm (black).

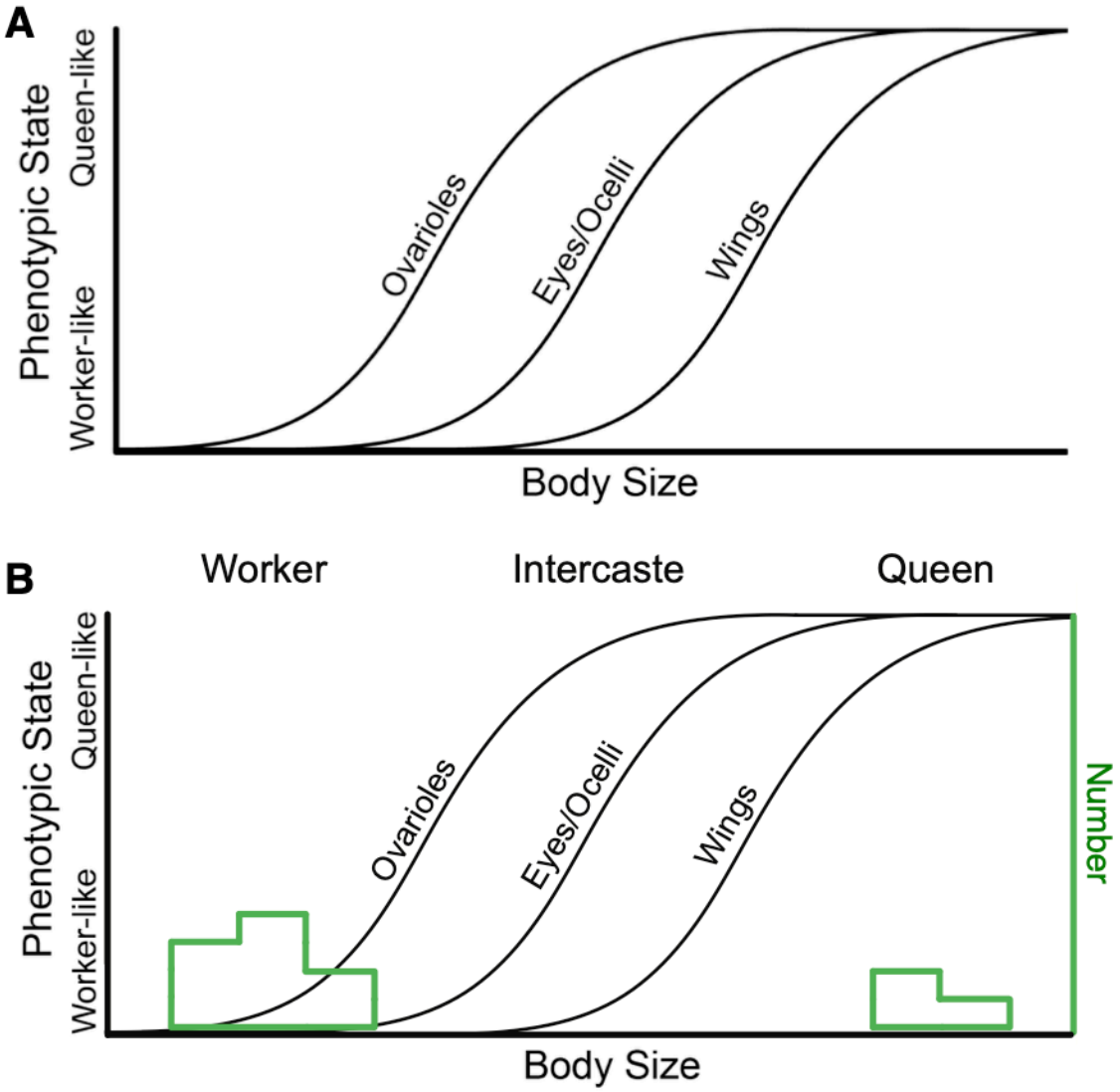
A
Phenotypic State
Queen-like
Worker-like
Ovarioles
Eyes/Ocelli
Wings
Body Size
B
Worker
Intercaste
Queen
Phenotypic State
Queen-like
Worker-like
Ovarioles
Eyes/Ocelli
Wings
Number
Body Size

The caste reaction norm

The definition of castes has been a contentious subject (Wilson 1953; Boven 1970; Peeters & Crozier 1988; Urbani 1998). Here I define castes as any sets of adult female ants within a species that can be morphologically distinguished (Peeters & Crozier 1988). Following Molet et al. 2012, I primarily classify castes into four categories: workers, soldiers, ergatoid queens, and queens (Figure 4.1C). Workers and queens differ by a suite of caste-associated traits (Molet et al. 2012). Workers are universally wingless and have reduced or absent eyes, ocelli, and reproductive systems. Queens typically possess wings, large eyes and ocelli, and a well-developed reproductive system with a spermatheca (a sperm storage organ) and a large number of ovarioles. Ergatoid queens lack wings but have a well-developed reproductive system (Peeters 1991). Soldiers are typically defined by allometry, with a large head size relative to body size, and they also lack wings (Wilson 1953). These categories are useful for general discussion, but caste morphology is often continuous and will not always fit into a given classification system with discrete categories.

To my knowledge, the queen caste within an ant species is the largest and most massive, on average (see comparison from 10 subfamilies in Peeters and Ito 2015). In many species, each caste occupies a fairly discrete mode in the size distribution, and intercastes, individuals intermediate in size between castes, are rare or absent. However, some species exhibit a continuous range of sizes from workers to queens (Molet et al. 2012; Londe et al. 2015). Figure 4.2A summarizes the most detailed available data on size and phenotype for ant workers, intercastes, and queens (based on studies of *Myrmica rubra*,

Mystrium rogeri, *Pristomyrmex punctatus*, *Technomyrmex albipes*, and *Temnothorax nylanderi*) (Brian 1955; Brian 1956; Tsuji et al. 1991; Tsuji & Dobata 2011; Okada et al. 2013). Note that Figure 4.2A does not depict a developmental series, but a series of adult phenotypes at varying sizes. Comprehensive data are only available for a few species, but the general patterns is observed in many additional species and I am not aware of any exceptions (see also Tulloch 1930; Hall & Smith 1953; Bolton 1986; Heinze & Buschinger 1989; Ohkawara et al. 1993; Ito et al. 1994; Miyazaki et al. 2005). Intercastes possess a combination of worker- and queen-like features, illustrating that discrete workers and queens simply constitute extreme outcomes along a developmental continuum (Londe et al. 2015).

These data show that phenotypes progress from worker- to queen-like states as individuals become larger. Rather than changing abruptly at a single size threshold, each caste-associated trait has its own function of size and phenotypic status (Londe et al. 2015). For example, *M. rubra* intercastes can have worker-like eyes and wing morphology, but a queen-like reproductive system (Brian 1955). As intercastes progress from slightly larger than workers to slightly smaller than queens, they first begin to develop a more queen-like reproductive system, then queen-like eyes and ocelli, and finally wings (Figure 4.2A). This is a hierarchical progression: within a species, individuals with queen-like ovarioles may have otherwise worker-like features, but individuals with queen-like wings also have queen-like eyes, ocelli, and ovarioles. While it is likely that this hierarchy possesses some flexibility, this flexibility is constrained such that, within a single genetic background, smaller individuals on average never

possess more queen-like traits than larger individuals. Put differently, caste in ants appears to be one dimensional: size and multiple morphological traits all change in parallel.

The definitions of 'caste determination' and 'caste differentiation' are not consistent in the ant literature, which has contributed to confusion in the understanding of caste development. Here I borrow from the sex development literature to provide definitions that are explicitly tied to biological processes. The available data reveal that caste-associated traits vary in association with overall size: larvae that pupate at greater mass become adults with more queen-like traits. In light of this evidence, caste determination can be defined as the complex integration of many mechanisms that influence the size of larvae at pupation (Figure 4.2B). The size distribution therefore is the outcome of caste determination across all of the larvae in a colony (Wilson 1953; Wheeler 1991). This does not necessarily imply that size necessarily causes variation in tissue growth, just that size and tissue growth are highly correlated and vary in tandem via a single joint mechanism (caste determination).

Caste differentiation, on the other hand, is the developmental mechanism producing the caste reaction norm (Figure 4.2B). It is specifically the process by which tissues in developing larvae and pupae differentiate in a worker- or queen-like manner in association with size (Miyazaki et al. 2010). Under normal conditions, the caste differentiation mechanisms within a genetic background appear to be fixed, resulting in a single coherent reaction norm of size and multiple morphological traits (along which

adults are positioned by caste determination mechanisms). It is clear that these caste differentiation mechanisms can vary between species or even genotypes, however (see following sections). The caste differentiation mechanisms can thus be conceptualized as the core derived feature of caste plasticity in ants; they produce a characteristic reaction norm of size and morphology in response to variation in environmental conditions.

Caste determination and differentiation position individuals within the phenotypic space of Figure 4.2B. Caste determination mechanisms position individuals along the reaction norm (i.e., along the x-axis; depicted in green), while caste differentiation mechanisms produce the structure of the reaction norm itself (i.e., along the y-axis; depicted in black). In this space, certain combinations of phenotypes are possible (such as worker-like eyes, ocelli, and wings combined with a queen-like reproductive system), but other combinations of phenotypes are not (such as queen-like eyes, ocelli, and wings, combined with a worker-like reproductive system) (Figure 4.2; Londe et al. 2015). This simplistic model has two sets of mechanisms that can vary independently, and is highly predictive. Many prior theories of caste development and evolution can be re-framed as outcomes of this model, and the model also makes a number of new predictions. To my knowledge, the predictions of this caste reaction norm model are not violated in any ant species.

In this review, I will discuss how my model encompasses the available data on caste development, and how it can help explain caste evolution. In Sections 3 and 4, I show how caste determination and differentiation interact to produce worker and queen castes

in a variety of ant species. In Section 5, I show how caste evolution could occur by modifying the caste determination and differentiation mechanisms to alter the phenotypes realized within a given species. For simplicity, I will focus on the ancestral worker and queen caste system in Sections 3 and 4, and limit my discussion of derived caste systems (including those with soldiers and ergatoid queens) to Section 5.

Determining adult size

Because larger size is associated with more queen-like phenotypes, understanding the mechanisms of caste determination requires understanding the mechanisms that affect size in ants. Intriguingly, many previously described caste determination mechanisms also affect size in other insects. In holometabolous insects, growth occurs during the larval stage and adult size is dictated by the size at pupation (Nijhout and Callier, 2015). Consequently, high nutrition during larval growth in ants can induce queen development, and starvation can prevent it (Brian 1956; Brian 1979). However, high nutrition during larval growth does not necessarily result in large adult size, as variation in developmental timing (which can result from genetic and other factors) can cause individuals under poor nutritional conditions to prolong development and attain large size, or individuals under rich nutritional conditions to truncate development and attain small size (Brian 1956; Brian 1974).

Two endocrine hormones, juvenile hormone (JH) and ecdysone, are important regulators of developmental timing in insects. Pupation (and the cessation of larval growth) is triggered by ecdysone, and the action of ecdysone is inhibited by JH (Hiruma & Kaneko

2013). Thus, larvae treated with JH or JH analogs exhibit prolonged growth and larger size, as long as necessary nutrition is present. JH removal and/or ecdysone treatment leads to premature pupation and smaller adult size (Hiruma & Kaneko 2013). This endocrine regulation of insect size has been demonstrated in Coleoptera and Lepidoptera, and is also supported by experiments in ants. JH treatment in *Harpegnathos saltator* and *M. rubra*, for example, prolongs larval development, allowing for increased feeding (Brian 1974; Penick et al. 2012). This in turn translates to larger size at pupation and queen development (Brian 1974; Penick et al. 2012). In *M. rubra*, it has been further shown that ecdysone treatment has little effect while JH is present, but leads to premature pupation later in development after JH has been cleared (Brian 1974). This demonstrates that nutrition and the endocrine system are important regulators of size and caste in ants.

Many factors, including genotype, maternal effects, wounding, temperature, and rearing environment can influence nutrition and/or the endocrine system, affecting size and caste development. In *M. rubra*, larvae do not have the potential for queen development under normal conditions (Brian 1979). However, larvae that are forced to diapause just before pupation reorganize their endocrine organs and delay pupation after growth is resumed (Brian 1979). If sufficient nutrition is available, these totipotent larvae attain large size and develop into queens (Brian 1956). Many factors can prevent totipotent larvae from developing into queens, including sub-optimal rearing temperature, aggression from workers, parasite infection, and small colony size (presumably leading to inefficient rearing) (Brian 1953; Brian 1973; Brian 1973; Brian 1974; Brian 1979). These factors lead to reduced size and appear to prevent queen development, inducing worker or

intercaste development (Brian 1955; Brian 1956).

A variety of studies corroborate the generality of Brian's findings from *M. rubra*. For example, worker aggression (triggered by a hydrocarbon 'princess pheromone' Penick & Liebig 2017) can prevent queen development in *H. saltator*, and sub-optimal rearing temperature prevents queen development in *Plagiolepis pygmaea* and *Pheidole pallidula* (Brian 1979; Penick & Liebig 2012). Large colony size (which is associated with high worker: larva ratios and therefore may be associated with higher nutrition) is a necessary condition for queen production in a wide variety of ant species (e.g., Brian 1979; Tschinkel 2006; Schwander et al. 2008; Aron et al. 2011).

The queen can also control caste development. The presence of reproductive queens is known to inhibit the production of new queens in a number of ant species (Brian 1979). Maternal factors deposited into eggs, such as vitellogenin, ecdysone, and JH, can affect size and bias larvae toward worker or queen development. In *P. pallidula*, overwintered queens produce eggs with a potential for queen development, possibly due to increased JH in the eggs (Suzzoni & Passera 1979). In *Pogonomyrmex rugosus*, queens must be both mature and overwintered to lay eggs with a potential for queen development, possibly due to differences in ecdysone or vitellogenin levels (Schwander et al. 2008; Libbrecht et al. 2013).

In species with genetic caste determination, some genotypes are biased toward worker or queen development, and in extreme cases only have the potential to develop into one

caste (Anderson et al. 2008; Schwander et al. 2010). Based on current evidence, it is likely that, as the name implies, these genotypes typically influence caste by biasing the caste determination mechanisms, and could be viewed analogously to the maternal effects described in the previous paragraph. For example, *P. rugosus* larvae with queen-biased genotypes only become queens if sufficient nutrition is available. Under conditions of low nutrition they die or, rarely, become workers or intercastes, rather than becoming worker-sized queens (as would be expected in the hypothetical case of 'genetic caste differentiation') (Anderson et al. 2008). A similar phenomenon may occur in *Cataglyphis* with genetic caste determination. In small colonies, these queen-biased genotypes develop into workers or die, but in large colonies they develop into queens (presumably due to improved nutrition) (Aron et al. 2011; Kuhn et al. 2018). Conversely, worker-biased genotypes that are treated with juvenile hormone can develop into queens (Kuhn et al. 2018). Caste-biasing genotypes may therefore influence caste by restricting the size range, with worker-biased genotypes producing individuals whose growth is stunted, and queen-biased genotypes producing individuals that are starvation intolerant (and therefore either attain large size or die). Both types of genotypic effects on size have been observed in *Drosophila melanogaster* (Kramer et al. 2008; Zhang et al. 2009).

Some of the caste determination mechanisms described above, such as maternal effects and genetic caste determination, arise before an egg is even laid, while others, such as differences in hormone titers, can arise at the very end of larval development (Brian 1974; Anderson et al. 2008; Schwander et al. 2010). Caste determination is the process that determines the ultimate size of a larva, and therefore could operate at any time

between the formation of the embryo and the pre-pupal stage (after which adult size is fixed). In many cases, multiple caste determination mechanisms will interact throughout development to produce a larva's ultimate size.

Generating the size distribution

The colony-wide outcome of caste determination is the size distribution of adults. The size distribution has been employed to describe worker polymorphism, but queens are rarely included in these studies (Wilson 1953; Wheeler 1991; Huang & Wheeler 2011). However, it is clear that workers and queens are typically dimorphic and queens are larger, so it follows that the size distribution is typically bimodal, with one mode for workers and one for queens, and little or no intermediates (Fjerdingstad & Crozier 2006; Molet et al. 2012; Peeters & Ito 2015). Given that the extent of queen-worker dimorphism has independently increased in multiple ant lineages, it is possible that highly non-normal size distributions have also evolved multiple times and may be produced by different mechanisms (Fjerdingstad & Crozier 2006; Keller et al. 2014). The size distribution arises from interactions between larval and worker traits (Linksvayer & Wade 2005; Linksvayer 2007; Teseo et al. 2014). Thus the evolution of non-normal size distributions is a product of both the intrinsic development of larvae and extrinsic influences on these larvae (e.g., high nutrition of some larvae but not others), often resulting from worker behavior (Linksvayer & Wade 2005; Linksvayer 2007; Teseo et al. 2014).

In honeybees, which have evolved worker and queen castes similar to ants, larvae are

reared individually in small or large wax cells. Larvae that are placed in large cells receive higher nutrition, resulting in a discrete queen caste. If larvae are reared outside of the colony, a full range of intermediates between workers and queens is observed (Linksvayer et al. 2011; Leimar et al. 2012). Such spatial segregation has not yet been found in ants, but temporal segregation is known to produce caste dimorphism: many species rear queens from cohorts of larvae that receive high nutrition. In the army ant *Eciton burchellii* (Figure 4.1B), queens are produced together with males in special sexual broods that contain only ~1% of the larvae of worker broods, so queen development could result from increased nutrition of female larvae in these cohorts (Schneirla, 1971). In many other species queens are produced at the time of year when resources are most abundant (e.g., Hart & Tschinkel 2011; Murdock & Tschinkel 2015).

Non-normal size frequency distributions may also arise when discrete events reprogram larval development. Often called developmental switches, it is important to note that these switches (see Linksvayer et al. 2011; Leimar et al. 2012) are of size (caste determination), not phenotype (caste differentiation). In *M. rubra*, overwintered larvae have prolonged development, allowing them to attain larger size (Brian 1956). In *P. rugosus*, only the first eggs laid by overwintered queens have the potential for queen development (Libbrecht et al. 2013). Overwintering is a discrete event, ubiquitous in temperate regions, so it may have been co-opted multiple times by natural selection to produce non-normal size frequency distributions in ants.

A second promising way to reprogram development is to modulate Dyar's rule (Dyar &

Rhinebeck 1890; O'Neal & Markin 1975; Wheeler 1990). Dyar's rule states that larval growth occurs at a constant ratio between instars, i.e., the head width of larvae at the end of an instar is 1.4x the head width at the end of the previous instar (Dyar & Rhinebeck 1890; O'Neal & Markin 1975). This leads to exponential growth between instars, allowing larvae with small differences in absolute size at the end of the 1st instar to develop into larvae with large differences in absolute size at the end of the final instar (ants possess 3-5 instars) (Wheeler & Wheeler 1976). Dyar's rule may amplify non-normal size distributions in some ant species. In the fire ant *Solenopsis invicta*, 1st instar larvae from incipient colonies are substantially smaller than 1st instar larvae from mature colonies, and give rise to tiny minim workers rather than regular workers or queens (O'Neal & Markin 1975), suggesting that maternal effects are amplified via Dyar's rule. Furthermore, within cohorts the size of worker larvae at the end of the 3rd instar is correlated with size at the end of the 4th instar (O'Neal & Markin 1975; Wheeler 1990). This within-cohort size variation could be due to any mechanism that produces size variation early in development. Thus, maternal effects (including queen age and overwintering), as well as early larval nutrition, may produce modest size variation in early development that, through Dyar's rule, eventually leads to great variation in size at the time of pupation (O'Neal & Markin 1975).

Caste differentiation

As seen in Section 3, caste determination encompasses a wide range of mechanisms that produce joint variation in overall size and caste morphology, positioning individuals along the caste reaction norm. Caste differentiation mechanisms produce the caste

reaction norm itself. The simplest mechanistic interpretation of my model is that caste determination mechanisms affect overall size and that some factor(s) associated with size are responsible for producing variation in tissue differentiation. Whether or not size is causally upstream of tissue differentiation, it is clear that tissues in ants do develop in a more queen-like manner in larger individuals, and I define the mechanisms that cause this association as the caste differentiation mechanisms.

To my knowledge, castes are always different in size on average, but in many species castes overlap in size slightly (Brian 1955; Brian 1956; Brian 1979; Peeters 1991; Tsuji et al. 1991; Urbani 1998). I propose that caste determination mechanisms cause correlated variation in size and some unknown caste differentiation factors, which in turn produces variation in tissue growth. An imperfect association of size and caste differentiation factors will produce some size overlap between castes. Such dissociation may result from an imperfect match of size and caste differentiation factors, or from differences in the time when factors affect size and tissue growth.

If the association of size and phenotype can be experimentally uncoupled, it may be possible to implicate the role of specific molecules in caste differentiation. In stag beetles, large males have disproportionately large mandibles. Analogously with ants, JH treatment of small male stag beetle larvae causes them to attain large size with large mandible growth (Gotoh et al. 2011; Gotoh et al. 2014). However, if small male stag beetle pupae are treated with JH, this results in an increase in mandible length without affecting overall body size (Gotoh et al. 2011; Gotoh et al. 2014). Thus, it seems that in

stag beetles, JH retains its typical effect on overall size during larval development, but during pupal development, it also acts at the tissue level to influence mandible growth without affecting size. JH has been shown in ants to induce queen development and is correlated with an increase in size (Brian 1974; Penick et al. 2012). In *H. saltator*, JH-treated larvae that are wounded develop into workers, rather than worker-sized queens, raising the possibility that JH primarily affects size (Penick & Liebig 2012). However, in most studies the size of JH-induced castes has not been reported, so it is possible that JH may also affect growth of specific tissues directly, as in stag beetles (Gotoh et al. 2014). In general, the association of size and caste in ants has not been sufficiently appreciated, and none of the caste determination factors in Section 3 have been tested for an effect on caste differentiation (i.e., a capacity to produce size-independent morphological variation).

In developing insect larvae, cell primordia of adult tissues are sequestered in imaginal discs, which differentiate into adult tissues at the late larval/prepupal stage of development. Caste associated phenotypes (including variation in ovarioles, spermatheca, head morphology, brain, ocelli, eyes, and wings) result from variation in development of these imaginal discs (Wilson 1953; Brian 1979; Miyazaki et al. 2010). The suite of queen-like phenotypes is similar to the ancestral state of holometabolous insects, with fully developed adult tissues, while the suite of worker-like phenotypes results primarily from reduced growth of caste-associated tissues. This type of growth variation is well known from a variety of insect species. Ovariole number varies with body size ancestrally in insects, and in *D. melanogaster* this is mediated by the insulin/insulin-like

signaling pathway (IIS) (Honěk 1993; Honegger et al. 2008; Tu & Tatar 2003; Green & Extavour 2014). IIS may also be responsible for the reduction in eye size and wing size observed in small *D. melanogaster* individuals (Tang et al. 2011). More extreme variation in tissue growth has been observed in other insects, where it is associated with IIS, but also JH, ecdysone, and even the hedgehog signaling pathway (Lobbia et al. 2003; Hartfelder & Emlen 2012; Gotoh et al. 2014; Niitsu et al. 2014; Xu et al. 2015; Kijimoto & Moczek 2016; see also the excellent discussion in Zinna et al. 2016). Any or all of these factors (and others yet to be discovered) are candidate caste differentiation factors in ants.

Caste differentiation factors can influence tissue growth at different times in development (Miyazaki et al. 2010). This effect is clearly seen in the wingless castes in the genus *Pheidole*, in which most species possess workers, soldiers, and queens, but some species also have a super-soldier caste that is intermediate in size between soldiers and queens (Huang & Wheeler 2011). In super-soldiers all four wing discs are present at the time of pupation, in soldiers only two wing discs are present, and in workers no wing discs are present (Abouheif & Wray 2002; Rajakumar et al. 2012). Fitting with this variation in wing disc development, aberrant expression of the gene network underlying wing development in wingless castes occurs at more downstream parts of the pathway in larger castes (Abouheif & Wray 2002; Rajakumar et al. 2012; Favé et al. 2015). It was proposed that selection or drift has caused wing development to arrest via different mechanisms in different wingless castes (Abouheif and Wray, 2002; Favé et al., 2015). I propose a more parsimonious and mechanistic model: the same caste differentiation factors lead to the

developmental arrest of the wing disc loss in different wingless castes, but levels of these factors vary in individuals of different sizes, changing the specific timing and pattern of wing degeneration that is observed.

Caste evolution

The last common ancestor of extant ants likely possessed morphologically distinct worker and queen castes, but many species have subsequently gained or lost castes (Molet et al. 2012; Keller et al. 2014; Barden & Grimaldi 2016). Additionally, the degree of queen-worker dimorphism has increased in some lineages of ants (Keller et al. 2014). In Section 2, I presented a phenotypic space that permits some combinations of worker-like and queen-like phenotypes but not others (Figure 4.2). The novel castes that have evolved in a wide range of ant species can always be placed in the phenotypic space presented in Figure 4.2 (Molet et al. 2012). Soldiers and ergatoid queens are phenotypically intermediate between workers and queens and, within a species, are never larger than queens or smaller than workers on average (Wilson 1953; Peeters 1991; Molet et al. 2012). Ergatoid queens possess queen-like ovarioles, but can otherwise range from worker- to queen-like in caste associated features (Molet et al. 2012). Soldiers similarly range from worker- to queen-like, but do not necessarily possess ovarioles and may thus be more worker-like than ergatoid queens (Wilson & Hölldobler 1990; Bolton & Ficken 1994; Molet et al. 2012). In other cases, soldiers are very queen-like, with well-developed eyes, ovarioles, and even wing discs (Figure 4.2; Abouheif & Wray 2002; Molet et al. 2012; Peeters et al. 2013). I propose that positions within the phenotypic space can be

modified via caste determination, by changing the size distribution, and via caste differentiation, by changing the association of tissue growth and size (Figure 4.3).

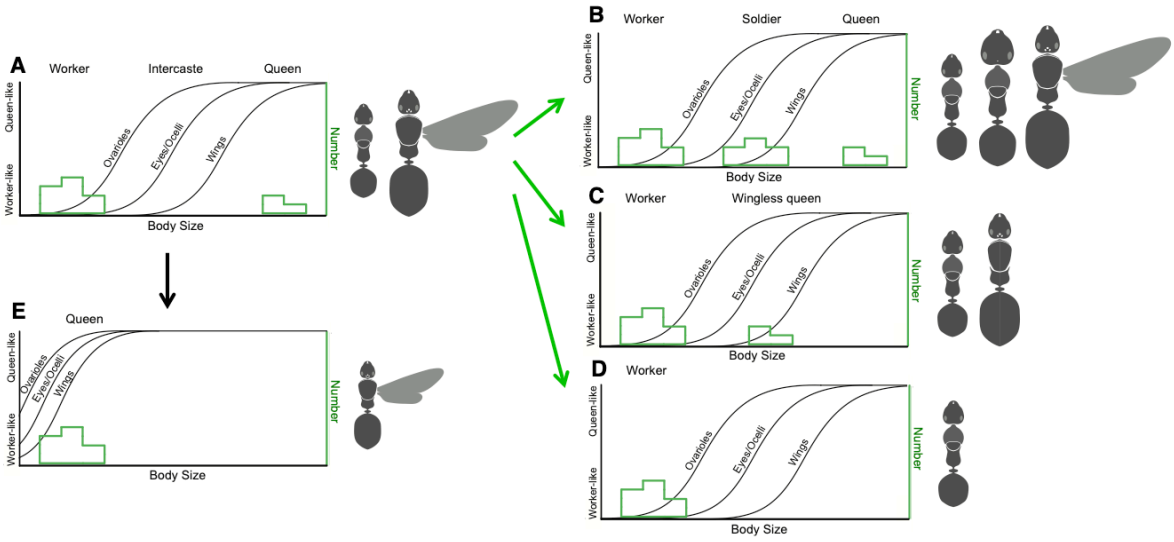

Figure 4.3: Caste evolution. The ancestral system (A) can be modified to produce (B) soldiers, (C) wingless queens, and (D) worker-only caste systems by modifying the size distribution (green). (E) Queen-only caste systems (workerless social parasites) can be produced by shifting the caste reaction norm (black); these species may lack the larger size mode corresponding to the ancestral queen caste. Not shown: the caste reaction norm can also vary in slope (which can change the absolute size differences between castes), or intercept (which can change the absolute size of castes).

Caste evolution via caste determination

As with caste development, most of the attention on caste evolution has centered on caste determination. Castes can be gained via changes to the caste determination mechanisms that cause adults to occupy new positions in the phenotypic space (Figure 4.3B,C). In a phylogenetic analysis, clades with a greater size difference between workers and queens were more likely to possess additional castes, supporting the notion that novel castes can evolve from worker-queen intermediates (Fjerdingstad & Crozier 2006; Molet et al. 2012). These novel castes can arise in either a continuous or discontinuous manner. Wilson (1953) proposed a theory of continuous caste gain, arguing that discrete soldier castes evolve by expanding the size range of the worker caste and subsequently losing worker-soldier intermediates (Wilson 1953; Oster & Wilson 1978). Molet et al. 2012 and Rajakumar et al. 2012 proposed theories of discontinuous caste gain, arguing that aberrantly produced intercastes possess novel phenotypes that, if useful, can be retained and subsequently fine-tuned by natural selection (this idea has a long history - see also Haskins & Whelden 1965). Some empirical evidence supports these theories. In *Pristomyrmex punctatus*, a 'cheater' lineage possesses both larger body size and more queen-like morphological traits than wild-types (Tsuji & Dobata 2011). Another example is found in the super-soldier castes of some *Pheidole* species. Rajakumar et al. 2012 demonstrated that intercastes resembling super-soldiers can be induced in *Pheidole* species lacking super-soldiers by treating soldier-destined larvae with JH. They proposed that this JH sensitivity in *Pheidole* represents an ancestral developmental potential to produce super-soldiers (see also Favé et al. 2015). I agree with this conclusion, but further assert that this ancestral developmental potential is not restricted to *Pheidole* JH

sensitivity and super-soldiers: all ants possess an ancestral developmental potential to produce a wide range of caste morphologies, according to the phenotypic space in Figure 4.2. The caste reaction norm can produce a range of caste morphologies that can arise initially via changes to the size distribution, and then be subsequently fine-tuned by natural selection.

Such an ancestral potential to produce novel castes is not solely a late-larval sensitivity to JH. Indeed, Rajakumar et al 2018 showed that worker-soldier intercastes can be produced by an alternative developmental mechanism, ablation of the wing disc from soldier-destined larvae. Novel castes can emerge from any caste determination or differentiation mechanism that causes individuals to occupy a new position in the phenotypic space. For example, if size variation in *Pheidole* can be amplified according to Dyar's rule, changes in maternal factors could theoretically result in the same super-soldier phenotype as an increase in late larval JH. Due to the complex feedback between the endocrine system and size, it is even possible that super-soldiers arise from variation in late larval JH, but that maternal effects (or any other caste determination factors) are in fact the mechanism that causes this variation. More detailed phylogenetic analysis is required to determine whether the evolution of novel castes tends to occur in a continuous or discontinuous sequence, but it is clear that novel castes can evolve simply when species occupy new regions of the phenotypic space (Wilson 1953; Oster & Wilson 1978; Molet et al. 2012; Rajakumar et al. 2012; Rajakumar et al. 2018).

Modified caste determination mechanisms can also lead to caste loss (Figure 4.3D). In

many species lacking winged queens (or lacking queens entirely), the maximum size simply seems to have been reduced (Peeters 2012). The genetic caste determination systems of *H. sublaevis* and *Leptothorax species a* provide an elegant example of caste loss, in which a single dominant allele causes the replacement of winged queens with smaller ergatoid queens (Buschinger & Winter 1978; Heinze & Buschinger 1989). A similar phenomenon most likely occurred in *Monomorium emersoni* populations inhabiting mountaintops in Arizona. In these populations, winged queens have been repeatedly replaced with apparently smaller ergatoid queens over a ~10,000 year period (Favé et al. 2015). Unfortunately, however, direct size measurements were not reported in this study; I hope to encourage future researchers to do so.

Caste evolution via caste differentiation

Caste systems evolve via changes to caste differentiation when the association between size and phenotype is modified (Figure 4.3E). The role of caste differentiation in caste evolution has received relatively little attention, but in theory castes can be gained or lost via changes to caste differentiation in ways analogous to caste determination. For example, it is possible that the worker caste could be lost by shifting the reaction norm so that worker-sized individuals develop queen-like morphology. Such a process may very possibly underlie the recurrent origin of workerless social parasites in ants (see below, and Chapter 5).

If the association of tissue growth and size is modified, this will affect the caste system of a species without necessarily changing the size distribution. In *Pheidole*, the threshold

size for soldier development is labile, both within and between species (Yang et al. 2004; McGlynn et al. 2012). In populations of *P. morrisi* with a higher threshold size for soldier development, the worker size range expands to encompass larger workers, leading to the development of more workers relative to soldiers (Yang et al. 2004). In a comparison of 26 Neotropical *Pheidole* species, species with larger workers also had larger and fewer soldiers (McGlynn et al. 2012). Therefore, caste size, frequency, and morphology evolve in *Pheidole* via changes to caste differentiation.

Modifications to caste differentiation may also include changes in the magnitude of phenotypic variation across the size range of a species. For example, in some species both workers and queens possess eyes, while in others queens possess eyes and workers are completely eyeless (Figure 4.1) (Wilson & Hölldobler 1990; Bolton & Ficken 1994). In still others both workers and queens are eyeless (Wilson & Hölldobler 1990; Bolton & Ficken 1994). Similar variation is seen in ovariole number, ranging from modest to massive differences between workers and queens (Peeters & Ito 2015). This may result from changes in the degree of size variation between workers and queens, or from changes in the slope of the functions of tissue growth and size. If the slope for a given trait is flat, small amounts of phenotypic variation will be observed over a given increment of size. If the slope is steep, on the other hand, large amounts of phenotypic variation will be observed over a given increment of size (Emlen and Nijhout, 2000).

Finally, caste differentiation can theoretically change if the interaction of tissues during development is modified. Queens are larger than other castes in overall size, but smaller

castes can still be larger than queens in certain body dimensions. Soldiers often possess heads or mandibles larger than those of both queens and workers (Figure 4.1) (Wilson 1953; Jaffé et al. 2007; Molet et al. 2014). In dung beetles, artificial selection for increased horn size also leads to a reduction in eye size, indicating that developing tissues may compete for resources (Emlen 1996; Nijhout & Emlen 1998). Queens invest large amounts of energy in traits such as wing and ovariole growth, so it is possible that individuals just below the size threshold for queen-like trait development have more resources available for growth of other organs. This may occur in *M. rogeri*, where the largest intercastes (which lack wings) have longer legs than the smallest queens (which bear wings) (Londe et al. 2015). Such competition may also explain the overgrowth of the head or mandibles in soldiers relative to queens: the total growth must be a positive function of size, but the growth of a single tissue could be greater in smaller individuals. Developing tissues have many potential interactions, particularly in the context of the dramatic morphological divergence between workers and queens. In addition to the caste-associated traits discussed here, any morphological or even behavioral trait may exhibit size-associated variation and evolve according to my model.

Caste determination and differentiation often change together

In many cases, caste evolution occurs via changes to both caste determination and caste differentiation. In *Mystrium oberthueri*, the reproductive caste has shifted from queens to small intermorphs (Molet et al. 2007). The loss of the queen caste is due to caste determination: the large individuals that develop into queens in the closely related *M. rogeri* are absent in *M. oberthueri* (Molet et al. 2007). In addition, changes to caste

differentiation allowed the gain of a novel caste: the size range of workers is restricted in *M. oberthueri* relative to *M. rogeri*, such that individuals that would develop into small workers in *M. rogeri* instead develop into morphologically distinct intermorphs in *M. oberthueri* (Figure 4.3B) (Molet et al. 2007). Note that, while these intermorphs form a reproductive caste smaller than the worker caste, they do not appear to be more queen-like than workers in terms of caste-associated morphology (i.e., ovariole number, eyes/ocelli, and wings). This result illustrates the important fact that worker-like vs. queen-like morphology is not necessarily associated with reproductive activity during the adult stage. For example, many soldier ants possess elevated ovariole numbers but never lay eggs, and in many ant species the primary egg-layer in the colony is not necessarily the largest individual (Gotoh et al. 2005; Peeters et al. 2013).

A particularly dramatic form of caste evolution is the recurrent origin of inquiline social parasites. Queens in social parasites have repeatedly evolved reduced size, producing the smallest ant queens (Bourke & Franks 1991; Nonacs & Tobin 1992; Aron et al. 1999). Social parasites often also have a worker caste that is reduced in size or absent. For example, *Plagiolepis xene* is a workerless social parasite closely related to the non-parasitic *Plagiolepis pygmaea*. The large individuals that become queens in *P. pygmaea* are absent in *P. xene*, and smaller individuals that, based on their size, would develop into workers in *P. pygmaea* instead develop into queens in *P. xene* (Aron et al. 1999). It has been proposed that the loss of the worker caste results from selection lowering the threshold size for queen development (Nonacs & Tobin 1992; Aron et al. 1999; Linksvayer et al. 2013); in other words, shifting the caste reaction norm to the left (Figure

4.3E).

In *Myrmoxenus*, queens of most species obligately found colonies parasitically, but the worker caste is retained to conduct slave raids (Heinze et al. 2015). *Myrmoxenus* queens are reduced in size relative to queens in closely related non-parasitic species, demonstrating that parasitic colony foundation is associated with reduction in queen size even when workers are present (Heinze & Foitzik 2009). *Myrmoxenus alderzi* is a workerless species closely-related to *Myrmoxenus ravouxi*, and it shows an additional reduction in queen size (phylogeny from Heinze et al. 2015; queen measures from Douwes et al. 1988). The parasitic lifestyle of these queens may select for an initial reduction in body size, but this appears to be constrained by the presence of the worker caste, allowing a further reduction in size after the worker caste is lost. This sequence of caste evolution occurs via changes to caste differentiation, shifting the reaction norm to induce queen-like morphology in smaller individuals, and caste determination, losing the large individuals that developed into queens in the ancestral species. Caste evolution in this case reduced the degree of queen-worker dimorphism; in other lineages, queen-worker dimorphism has increased.

Conclusions

The developmental data reviewed in Sections 2-4 closely fit with the evolutionary data reviewed in Section 5, implying that caste determination and differentiation position individuals within the phenotypic space described in Figure 4.2, and caste evolution occurs via modifications to the caste determination and caste differentiation mechanisms

(Figure 4.3) (Wilson 1953; Oster & Wilson 1978; Molet et al. 2012; Rajakumar et al. 2012; Favé et al. 2015). This theory constitutes an hourglass model, in which a large number of evolutionarily labile caste determination mechanisms influence a conserved set of caste differentiation mechanisms, which then produce diverse and evolutionarily labile caste morphologies (Figure 4.4) (Akhshabi & Dovrolis 2011; Bopp et al. 2014; Wagner 2014; Friedlander et al. 2015). This is reminiscent of sex development in insects, in which sex determination and sex morphology are highly variable, but sex differentiation results from conserved roles of the genes *doublesex* and *transformer* (Figure 4.4) (Akhshabi & Dovrolis 2011; Bopp et al. 2014; Wagner 2014; Friedlander et al. 2015). Caste development and sex development share many similarities, with variation in environmental (e.g. temperature and nutrition) or genetic (e.g. sex chromosomes and genetic caste determination) factors leading to development of alternative phenotypic states (Brian 1979; Anderson et al. 2008; Schwander et al. 2010; Bopp et al. 2014; Klein et al. 2016). However, caste development seems to be more frequently mediated by environmental factors, whereas sex development is more frequently mediated by genetic factors (as might be expected to exclude "cheater" genotypes).

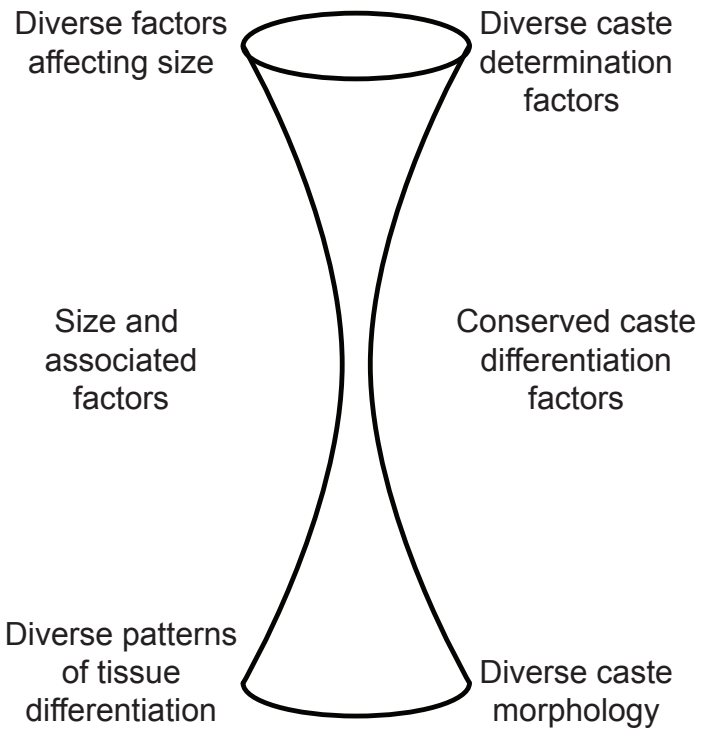

Figure 4.4: Hourglass model of caste development. A diverse and evolutionarily labile set of factors affect size, leading to size variation among individuals (caste determination). Conserved factors then affect tissue differentiation in response to size (caste differentiation). As a result, diverse and evolutionarily labile adult morphologies emerge. These patterns can be described using general (left) or specialized (right) terminology. While much is known about caste determination factors and caste morphology, caste differentiation factors, which are the master regulators of caste in ants, have been largely overlooked.

Polyphenisms have evolved in many types of insects, some of which appear to be size-based (e.g. in hymenopterans, dung beetles, and stag beetles), while others are independent of size (e.g. in aphids, butterflies, locusts, and planthoppers) (Simpson et al. 2011; Hartfelder & Emlen 2012). I propose that caste plasticity in ants is size-based, such that, within a genetic background, differences in morphology are always associated with differences in size, on average, and caste-associated traits undergo more queen-like development in larger individuals. The evidence I present in Figure 4.2 comes from species in three subfamilies that span the ant phylogeny, and I have reviewed evidence from many additional taxa, so it is likely that the patterns I have described here are general and ancestral in ants (Figure 4.2).

Wheeler (1991) and Urbani (1998) proposed that ant castes do not necessarily differ in size. It has been argued that microgynes such as those in *Aphaenogaster tenneseensis* and the *Formica microgyna* species group are sometimes the same size or smaller than the worker caste (Wilson 1953). I am not aware of any published mass measurements, and it is possible that these queens are simply more compact than workers without being less massive. If these queens are truly less massive than workers, there are two possible explanations. The first is that this is a system of 'genetic caste differentiation', which would not violate the mechanistic model I have proposed. Alternatively, it is possible that these castes are truly plastic, and that caste development in these ants does not follow the typical association with overall size. If this is the case, it could represent a secondary change to the mechanisms of caste development that I have proposed. Finally, if it could be shown that the association of size and phenotype that I propose here is not a general

pattern in ants, my model would be falsified.

It is worth mentioning some additional consequences of a size-based polyphenism in ants. First, ovariole number varies with size ancestrally in insects, so once other queen-like traits (e.g. eye and wing development) became reduced in small individuals, ovariole number became reduced as well (Honěk 1993). Therefore, the polyphenism in flight apparatus was necessarily associated with some degree of reproductive division of labor in the early stages of ant evolution, which may have facilitated the transition to eusociality. Second, as has been noted by other authors, size-based caste determination can be built into simple models that produce the elegant patterns of sociogenesis, sexual maturity, and seasonal reproduction observed in many species (Tschinkel 2006). Let us assume that increased worker number causes colonies to produce larger larvae (possibly due to improving nutritional conditions of larvae and/or queens), and those larvae above a threshold size develop into queens. Small colonies therefore produce small larvae that exclusively develop into workers. These workers contribute to colony function by nursing, foraging, etc., which allows the colony to produce both more and larger workers, which then contribute to further colony growth. This positive feedback cycle is broken when larvae become large enough to develop into queens. At this point worker and queen production reach an equilibrium; any deviation in the production of workers or queens causes corresponding changes in future worker or queen production that bring the colony back to the appropriate level (Tschinkel 2006). If larval size is also associated with additional factors like queen age or season, this simple model can produce many of the complex life cycles observed throughout the ants. Intriguingly, if larval size were not

correlated with worker number, this could cause colonies to collapse by continuing to produce new queens even if worker numbers decline. Such a hypothetical scenario might be quite similar to what occurs in socially parasitic lineages, in which some individuals become genetically determined to develop into queens at a lower body size threshold (Nonacs & Tobin 1992; Aron et al. 1999; Linksvayer et al. 2013).

Finally, I would like to discuss the concept of allometry. Wilson (1953), Wheeler (1991), and others have argued that castes in ants can be defined as sets of individuals that differ in their allometric coefficients (i.e., changing slope in the regression of two trait measures). Allometry is a useful descriptive tool for ant castes, but it should be recognized that it will not always be the most accurate descriptor of evolutionarily-relevant caste variation. The association of body size and caste-associated phenotypes is non-linear, so it follows that individuals differing in size will often differ in allometry as well, regardless of whether these different groups do not have unique functional roles in the colony (Figure 4.2) (Londe et al. 2015). Conversely, individuals in other regions of the phenotypic space may differ greatly in size and their functional roles in the colony, but not in allometry (Figure 4.2 (Londe et al. 2015). Allometric variation indicates that differently-sized individuals vary in caste differentiation (i.e., their position on the caste reaction norm). Another useful description of a caste system is the size distribution itself; individuals occupying distinct size modes could justifiably be defined as distinct castes (Figure 4.3). In some species, trying to define castes as discrete entities may not be useful, and it may be more useful to instead consider all of the morphologies within a species as a continuum.

The theory presented here provides a framework for interpreting data about caste development and evolution in ants and potentially other social insects, and I hope that it will facilitate a unified research program moving forward. In particular, I hope to highlight the critical importance of including measurements of size in any study of caste development and evolution, which is necessary to decide whether a given factor affects caste determination or differentiation. Central attributes of caste determination and differentiation remain poorly understood. We know a host of caste determination factors that affect size, but the combination of larval and worker traits that give rise to non-normal size distributions in the vast majority of ant species remain mysterious. Caste differentiation is even less well explored. It is clear that variation in caste-associated traits is associated with size and results from variation in imaginal disc development, but how this variation arises and how it evolves remains unclear. These two issues are critical features of ant biology, and further inquiry is poised to yield far-reaching insights in the years to come.

CHAPTER 5: THE WINGED MUTANTS

Caste differentiation and workerless social parasites

The morphological castes of ants, such as workers, soldiers, and queens, represent one of the most extreme examples of phenotypic plasticity in nature (Trible & Kronauer 2017). Caste morphology is highly variable across the ants and is intimately associated with the ecology and natural history of any particular species. Consequently, many biologists have sought to understand the mechanism and patterns of caste evolution in ants. As I discussed in Chapter 4, the published literature regarding caste development and evolution has focused primarily on caste determination: joint variation in morphology and overall body size. In contrast, virtually nothing is known about the mechanisms of caste differentiation.

The socially parasitic inquiline ants are particularly divergent with respect to caste morphology and ecology (Bourke & Franks 1991; Nonacs & Tobin 1992). Inquilines obligately live inside the colonies of other ant species. In some inquilines, called workerless social parasites, female adults develop exclusively into morphological queens and the worker caste is absent. These queens are never found living in isolation, but instead survive by parasitizing colonies of other ants (usually close phylogenetic relatives) (Buschinger 2009). In principle, there are two mechanistic routes from the ancestral worker/queen caste system to a workerless social parasite: A) Altering caste determination by deleting the small mode of individuals that ancestrally developed into workers, and B) altering caste differentiation by shifting the caste reaction norm to induce queen-like morphology at worker-like size (Figure 5.1).

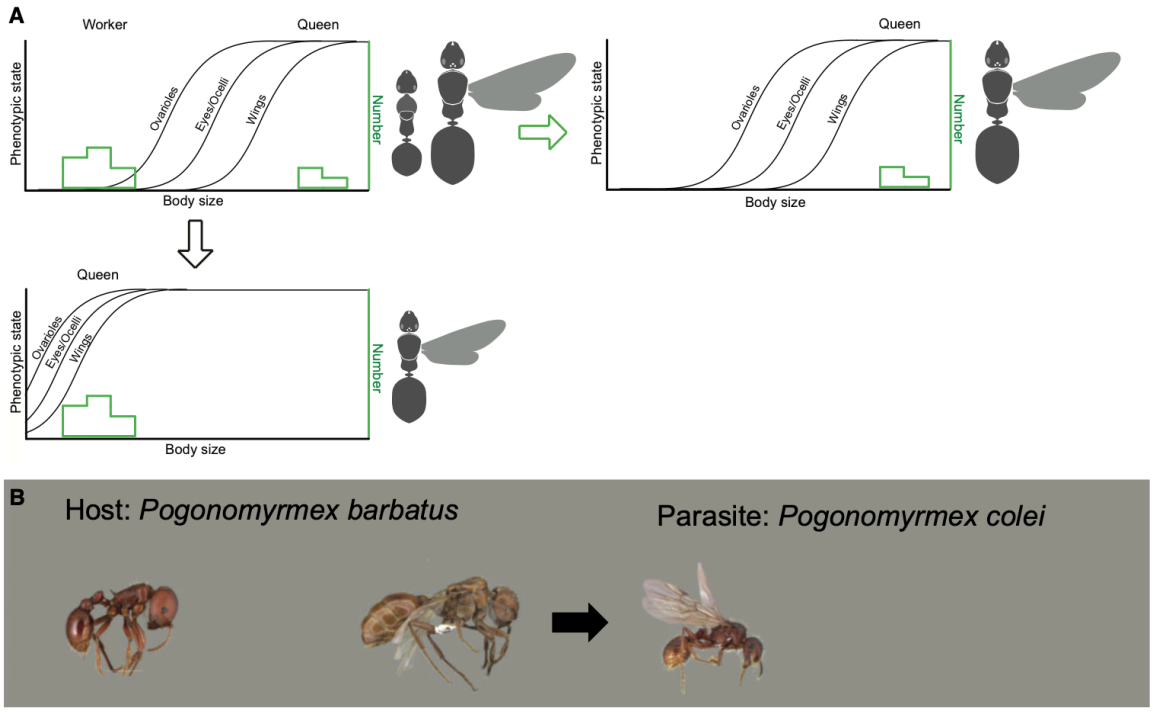

Figure 5.1: The two mechanisms that can produce workerless social parasites from an ancestral queen/worker caste system. (A) Caste reaction norm overview. Workerless social parasites can evolve by changes to caste determination (green arrow) or caste differentiation (black arrow). (B) Real-world example of a host-parasite system in *Pogonomyrmex*. In this case, the workerless inquiline social parasite *Pogonomyrmex colei* (right) appears to have evolved via the caste differentiation route, inducing queen-like morphological traits at worker-like body size. A worker (far left) and queen (center left) of the closely related host species *Pogonomyrmex barbatus* are shown for comparison. Images: Antweb.org, Smith et al. 2015.

Both queen-sized and worker-sized workerless social parasites occur in nature (e.g., Rabeling et al. 2015; Rabeling et al. 2019). Worker-sized (differentiation-mediated) parasites are more common, potentially because worker-sized parasite larvae require less nutrition to develop and are readily disguised among the host larvae (Figure 5.1B) (Nonacs & Tobin 1992). In fact, small body size is one component of the inquiline syndrome, a suite of phenotypic traits that have evolved many times in parallel in workerless social parasites (Wilson 1984; Rabeling et al. 2015; Rabeling et al. 2019). Nothing is known about the mutations or evolutionary trajectory that produces this distinctive phenotypic syndrome, and workerless social parasites provide a unique opportunity to study the evolution of social parasitism and the mechanisms of caste differentiation more generally.

In some cases, workerless social parasites are genetically distinct from their hosts and can be confidently defined as distinct species. In other cases, workerless social parasites are nested within the phylogeny of their host species, rendering the host paraphyletic. Given that workerless social parasites are found exclusively inside their host colonies, this phylogenetic pattern has led to the conclusion that certain workerless social parasites arose via intraspecific social cheaters that eventually underwent sympatric speciation (Buschinger 1990; Savolainen & Vepsalainen 2003; Rabeling et al. 2014; Leppänen et al. 2016). This sympatric speciation model requires strong disruptive selection to differentiate an incipient parasite, or cheater, from its host lineage. In order for this disruptive selection to be realized, adaptive genetic variants producing parasite

phenotypes must not be dissociated via gene flow with the host population, a requirement that is ameliorated if these loci are highly pleiotropic (Rosenweig 1978; Ward 1996).

To escape extinction, any parasite must strike a fine balance. It must exploit its host enough to reproduce, but not so much that it kills the host population on which it depends for survival. The sympatric origin of a workerless social parasite is thus further constrained by the requirement that it must coexist with its ancestral host species without going extinct or driving its host extinct. In nature, workerless social parasites are typically found at very low frequencies at the colony and population level (Buschinger 1990; Savolainen & Vepsalainen 2003; Rabeling et al. 2014; Leppänen et al. 2016). These low frequencies may benefit the parasites by limiting their negative impacts on their hosts, just as many derived parasites and pathogens have evolved reduced virulence relative to recent 'spillover' outbreaks (Cressler et al. 2016).

In a perfect world, it would be possible to directly observe the nascence of workerless social parasites in order to understand their unique mode of evolution. Unfortunately, these parasites are rare and short-lived in nature and are difficult to maintain in captivity, so researchers have been unable to attain a detailed understanding of their behavior, development, or evolution. Here I report the serendipitous discovery of a phenotypically-divergent 'winged mutant' strain of the clonal raider ant, *Ooceraea biroi* (Figure 5.2A).

Wild-type colonies of *O. biroi* are composed of worker ants that reproduce asexually via thelytokous parthenogenesis. Parthenogenesis in this species arises because haploid

meiotic nuclei fuse to restore heterozygosity (automixis with central fusion) (Oxley et al. 2014). Morphological queens, or winged females of any kind, have never been reported in *O. biroi*, despite extensive collections in its invasive and native range. The winged mutants constitutively possess wings and other queen-like morphological features, even at worker-like body sizes. These mutants exhibit a number of traits, including a highly pleiotropic morphological syndrome, dependence on wild-types for survival, and a potential for long-term coexistence that could provide an unprecedented window into the mechanisms of caste differentiation and the evolution of social parasitism in ants.

Results

Winged mutant ancestry

The winged mutants were originally discovered in the Line A colony C1, after which I removed them from the colony and bred them for a series of genetic, morphometric, behavioral, and fitness analyses.

To test whether the winged mutant phenotype is a genetic trait, I obtained larvae from pure colonies of winged mutant or Line A wild-type adults, then cross-fostered these larvae to be reared by winged mutant or wild-type adult chaperones. All wild-type larvae reared by wild-type or winged mutant chaperones developed into wild-type adults, while all winged mutant larvae reared by wild-type chaperones developed into winged mutant adults (Table 5.1). These experiments demonstrate that the winged mutant phenotype results from the egg, not the rearing environment, and that the winged mutants are 100% penetrant (within the sample size of this experiment). Indeed, I have been rearing winged

mutants for four years (~20 generations), and my observations collectively imply that this is a fully penetrant genetic trait.

Table 5.1: Cross-fostering and penetrance experiments.

Trial	Chaperone genotype	Larvae genotype	Wild-types produced	Winged mutants produced
1	WT	WT	3	0
2	WT	WT	4	0
3	WT	WT	13	0
4	WT	WT	14	0
5	WT	WT	9	0
6	WT	WT	13	0
7	WT	WT	15	0
8	WT	WT	8	0
9	WT	WT	15	0
10	WT	WT	10	0
11	WT	WT	3	0
13	WT	WT	13	0
14	WT	WT	15	0
15	WT	WT	14	0
16	WT	WM	0	7
17	WT	WM	0	13
18	WT	WM	0	9
19	WT	WM	0	8
20	WT	WM	0	6
21	WT	WM	0	10
22	WT	WM	0	10
23	WT	WM	0	3
24	WT	WM	0	12
25	WT	WM	0	1
26	WT	WM	0	1
27	WT	WM	0	17
28	WM	WT	13	0
29	WM	WT	17	0
30	WM	WT	13	0
31	WM	WT	14	0
32	WM	WT	14	0
33	WM	WT	13	0
34	WM	WT	15	0
35	WM	WT	7	0
36	WM	WT	7	0
37	WM	WT	12	0
38	WM	WT	6	0
39	WM	WT	11	0
40	WM	WT	10	0

O. biroi is a clonal species, and four clonal lines, Lines A, B, C, and D, have been identified from its invasive range (Kronauer et al. 2012). These clonal lines are distinct genome-wide, including at the mitochondrial barcode, *cytochrome oxidase 1* (*CO1*), and many microsatellite loci (Kronauer et al. 2012). To test whether the winged mutants belong to any known clonal line, I sequenced mitochondrial *CO1* and six microsatellite loci from winged mutants and wild-types (Table 5.2). The winged mutants were originally identified within a Line A colony, and were identical to Line A wild-types in *CO1* sequence and all six microsatellites. These data demonstrate that the winged mutants belong to Line A, and that the winged mutants are parthenogenetic (like wild-type *O. biroi*) (Table 5.2).

Table 5.2: Winged mutants are Line A *O. biroi*. Fragment size for 6 microsatellite loci in Lines A, B, C, D, and winged mutants. Each multi-locus genotype is reported individually (Kronauer et al. 2012; Kronauer et al. 2013). Winged mutants are also identical to Line A in mitochondrial *CO1* sequence (n = 17 individuals).

Clonal Line	Colonies	Individuals	DK371	ES177	D8Z0W	D8M16	D4XW2	ER4IH
Line A	19	27	192/192	219/219	231/231	180/188	214/220	227/227
Line A	4	5	192/192	219/219	231/231	180/188	220/220	227/227
Line B	31	31	192/192	216/219	231/233	180/182	217/220	227/230
Line B	9	9	192/192	219/219	231/233	180/182	217/220	227/230
Line B	3	3	192/192	216/216	231/233	180/182	217/220	227/230
Line B	2	2	192/192	216/219	231/231	180/182	220/220	227/230
Line B	1	1	192/192	216/216	231/233	180/182	217/220	227/227
Line B	1	1	186/192	219/221	229/231	176/180	214/220	227/230
Line B	1	1	186/192	219/221	229/231	176/180	214/220	227/227
Line C	8	8	186/192	213/213	229/231	176/199	214/214	236/236
Line D	1	1	186/186	213/213	231/231	176/197	214/220	227/236
Line D	1	1	192/192	219/219	231/231	176/197	214/220	227/236
Winged mutant	1	6	192/192	219/219	231/231	180/188	214/220	227/227
Winged mutant	1	1	192/192	219/219	231/231	180/188	214/214	227/227

Within Line A, independently collected wild colonies differ slightly in genome-wide data due to the accumulation of mutations in the course of clonal reproduction (Kronauer et al. 2012; Kronauer et al. 2013; Oxley et al. 2014). To resolve the specific colony origin of the winged mutants, I used Illumina to resequence two winged mutant and two Line A wild-type genomes (Figure 5.2B). One wild-type genome was derived from C1 and the other came from the Line A colony C16, the colony most closely related to C1 based on extensive microsatellite genotyping (Kronauer et al. 2012, Kronauer et al. 2013, and data therein). I aligned these data to a haploid long-read reference genome (McKenzie & Kronauer 2018), and used VariantCaller and a custom Python script to identify polymorphic loci in this dataset. Finally, I concatenated these data into a synthetic sequence, and used this sequence to build a phylogeny of winged mutants and wild-types using MEGA and RAxML. This phylogeny demonstrated that the two winged mutant genomes were monophyletic and were much more closely related to C1 wild-types than C16 wild-types.

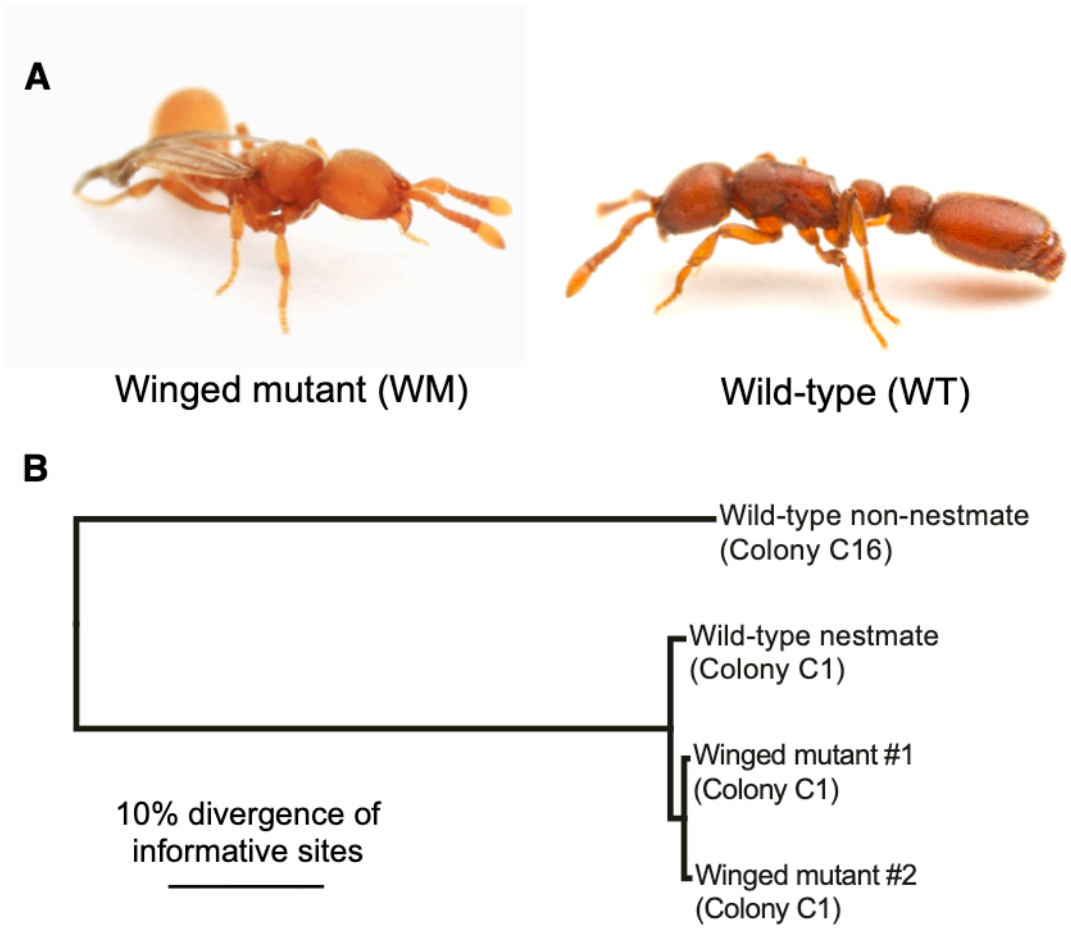

Figure 5.2: Winged mutant phylogenetics. (A) Photograph of winged mutant and wild-type ants. (B) Phylogeny of winged mutants and wild-types using whole-genome data. Winged mutants are monophyletic and more closely related to wild-types from their Line A C1 host colony than to wild-types from the most closely-related known Line A colony, C16. This phylogeny was constructed from a random set of 1,946 loci that vary in at least one of the four genome libraries. Images: Daniel Kronauer.

Taken together, these genetic data indicate that the winged mutants are derived from Line A wild-types, and most likely arose as a mutant lineage within Colony C1. The winged mutants may have arisen in the lab, or may have existed within Colony C1 when it was originally collected in the wild.

Morphology

I next described the morphological syndrome of the winged mutants. I dissected and imaged a set of winged mutants and Line A wild-types, and measured 13 linear morphometric dimensions plus the ovariole number (see Chapter 7), then subjected this dataset to a principal component analysis (PCA) using Python (Figure 5.3).

The first two principal components explained 50% of the variation in this dataset. Of these, only PC1 possessed a significant linear association with body length (Figure 5.3A). Winged mutants and wild-types were fully overlapping in total body length and PC1 values, indicating that the winged mutant phenotype is independent of overall size. Even though genotype was not coded into this analysis, winged mutants and wild-types were distinguished by their PC2 values, confirming that the winged mutants are morphologically distinct from wild-types (Figure 5.3B).

Manually inspecting individual dimensions in this morphometric dataset reveals that the winged mutants have a greater number of ovarioles than wild types and longer thoraces, indicative of wing development (Figure 5.3C, D). Interestingly, the winged mutants also have reduced head length and petiole width, both of which have been observed in some

socially parasitic ants (Kennedy & Dennis 1937; Elmes 1976; Rabeling et al. 2015) (Figure 5.3E, F).

Figure 5.3: Wild-type and winged mutant morphometrics. (A) PC1 has a strong association with body length (linear regression $R^2 = 0.79$, $p < 0.001$). (B) PC2 is not significantly associated with PC1 (linear regression $R^2 = 0$, $p = 1$). PC2 does, however, cleanly separate winged mutants from wild-types ($p < 0.001$). (C) Winged mutants possess more ovarioles than wild-types ($p < 0.001$). (D) Winged mutants possess longer thoraces than wild-types ($p < 0.001$). (E) Relative head length is reduced in winged mutants ($p < 0.001$). (F) Relative petiole width is reduced in winged mutants ($p < 0.001$). All statistics performed using Prism 7. p-values obtained from linear regression (A), t test of raw data (B, C, D), or t test of residuals from the best fit line (E, F).

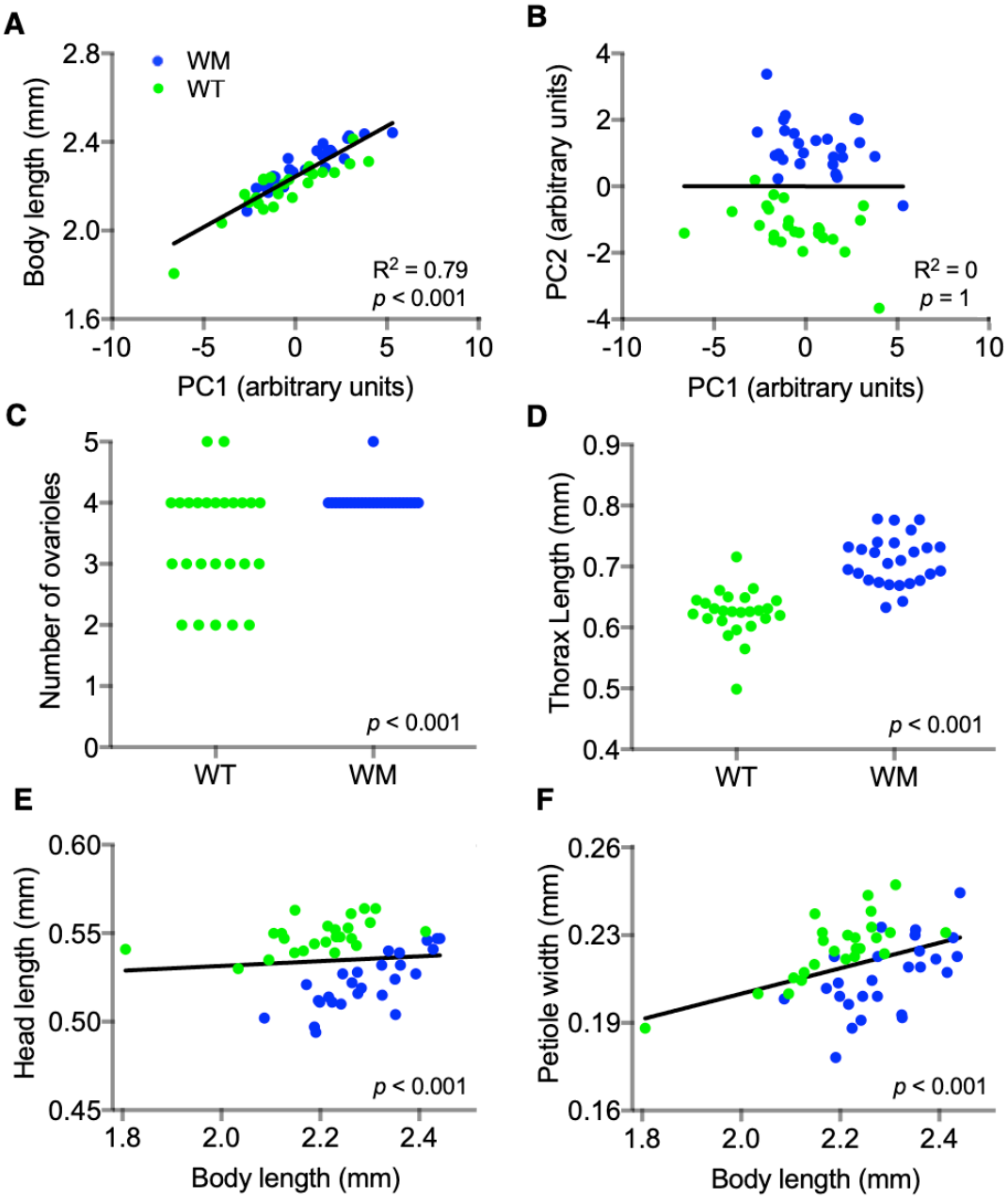
A
WM
WT
Body length (mm)
PC1 (arbitrary units)
R² = 0.79
p < 0.001
B
PC2 (arbitrary units)
PC1 (arbitrary units)
R² = 0
p = 1
C
Number of ovarioles
p < 0.001
WT
WM
D
Thorax Length (mm)
p < 0.001
WT
WM
E
Head length (mm)
p < 0.001
Body length (mm)
F
Petiole width (mm)
p < 0.001
Body length (mm)

Taken together, these morphometric results demonstrate that the winged mutants constitute a caste differentiation, rather than a caste determination, mutant, leading to the induction of queen-like morphology at worker-like body size. This morphological syndrome resembles that of the workerless social parasites in other species, and is distinct from previous experimental studies of caste development, which consist invariably of perturbations that affect caste morphology and overall size in tandem (caste determination) (Trible & Kronauer 2017).

Social behavior and fitness

My genetic and morphological data illustrate that the winged mutants are derived from wild-type ants and display a suite of queen-like morphological traits. In this sense, the winged mutants resemble a number of workerless social parasites and cheaters that are nested phylogenetically within their hosts and are biased toward queen-like morphology. I therefore wished to describe the social behavior of the winged mutants to understand whether they integrate themselves into wild-type colonies in a parasite-like manner. Specifically, I sought to test whether the winged mutants possess four features that are characteristic of social parasites and cheaters in ants:

1) Reproductive advantage over wild-types
2) Reliance on wild-types for survival
3) Queen-like behavior
4) Persistence without extinction, often at low frequency

I used six experiments to address these questions. In the first set of experiments, I measured the relative fitness of winged mutants and wild-types across distinct stages of their life cycle. I divided the life cycle into five segments: adult egg-laying rate, survival from egg to pupa, survival from pupa to adult, adult larval nursing efficiency, and adult foraging behavior. Finally, I conducted a long-term evolution experiment in which I established colonies with a mixture of winged mutants and wild-types and grew them under naturalistic conditions for one year. All ants used in these fitness experiments were either winged mutants or Line A C1 wild-types, and were generated using a standardized cross-fostering procedure that allowed me to precisely match them in rearing environment and age (see Chapter 7).

To measure the egg-laying rate of the winged mutants, I established pure colonies of winged mutant and wild-type adults with no brood and collected eggs from these colonies 2 times per week. Consistent with their increase in ovariole number (Figure 5.3A), I found that the winged mutants had a two-fold increase in egg-laying rate compared to wild types (Figure 5.4A).

To measure egg to pupa survival, I cross-fostered winged mutant and wild-type eggs into standardized units to be reared by wild-type adults. Winged mutants and wild-types did not differ significantly in egg to pupa survival when reared in pure cultures. Interestingly, however, in units established with 50% winged mutant and 50% wild-type eggs, the winged mutants pupated at approximately half of the rate of wild-types (Figure 5.4B). These experiments indicate that winged mutant larvae do not have lower intrinsic

viability compared to wild-types, but do have a competitive disadvantage when grown in mixed conditions.

During rearing experiments, I observed that many winged mutants died during the process of eclosion, possibly because they were unable to disentangle the pupal skin from their bulky wings. To measure this mortality, I established colonies with wild-type adults rearing variable proportions of winged mutant and wild-type pupae. When fewer than 10% of pupae were winged mutants, winged mutants and wild-types did not differ significantly in survival (in both cases, virtually all individuals survived eclosion). When the majority of pupae were winged mutants, however, survival was substantially reduced (Figure 5.4C). These experiments indicate a negative frequency-dependent effect on survival of metamorphosis in winged mutants: higher frequency leads to lower survival. I speculate that this frequency-dependent effect may arise because high frequencies of winged mutant pupae may require more aid in eclosing than can be provided by the adults in the colony.

Finally, I measured the ability of winged mutant and wild-type adults to rear brood from the larval to adult stage under standardized conditions (20 age-matched adults with 16 first-instar larvae). I tested three experimental treatments: wild-type adults with wild-type larvae, winged mutant adults with wild-type larvae, and wild-type adults with winged mutant larvae. I recorded the day that the majority of brood underwent four developmental transitions: hatching, final larval molt, pre-pupation, pupation, and eclosion. I also recorded the net survival from the larval to adult stage. Winged mutant

larvae did not differ from wild-types in their intrinsic development time or survival in these experiments (Figure 5.4D). Furthermore, winged mutant adults did not differ from wild-types in their ability to rear larvae (Figure 5.4D).

Figure 5.4: Four components of winged mutant fitness. (A) Winged mutants laid eggs at a higher rate than wild-types ($p < 0.001$) across multiple egg collection rounds from five replicate colonies. Winged mutants: 0.43 ± 0.03 eggs/ant/day, n = 62 collections. Wild-types: 0.19 ± 0.018 eggs/ant/day, n = 62 collections. (B) Winged mutants did not differ from wild-types in egg to pupa survival when reared under pure conditions, but when reared in 50:50 mixed colonies winged mutants had significantly lower survival than wild-types ($p < 0.01$). (C) Winged mutants did not differ from wild-types in eclosion survival at low proportions of winged mutant pupae, but had significantly reduced survival as the frequency increased ($p < 0.001$). (D) In small arenas with food added directly to the nest, winged mutant adults did not differ from wild-types in larval rearing efficiency in development time ($p > 0.05$). No differences were observed in percentage of larvae surviving to becomes callows ($p > 0.05$) (not shown; WTxWT: 80.8 ± 20.7 %, WTxWM: 61.5 ± 14.5 %, WMxWT: 72.7 ± 18.1 %). P-values derived from a t test (A), (B), (C), or ANOVA (D). Confidence intervals are standard error of the mean.

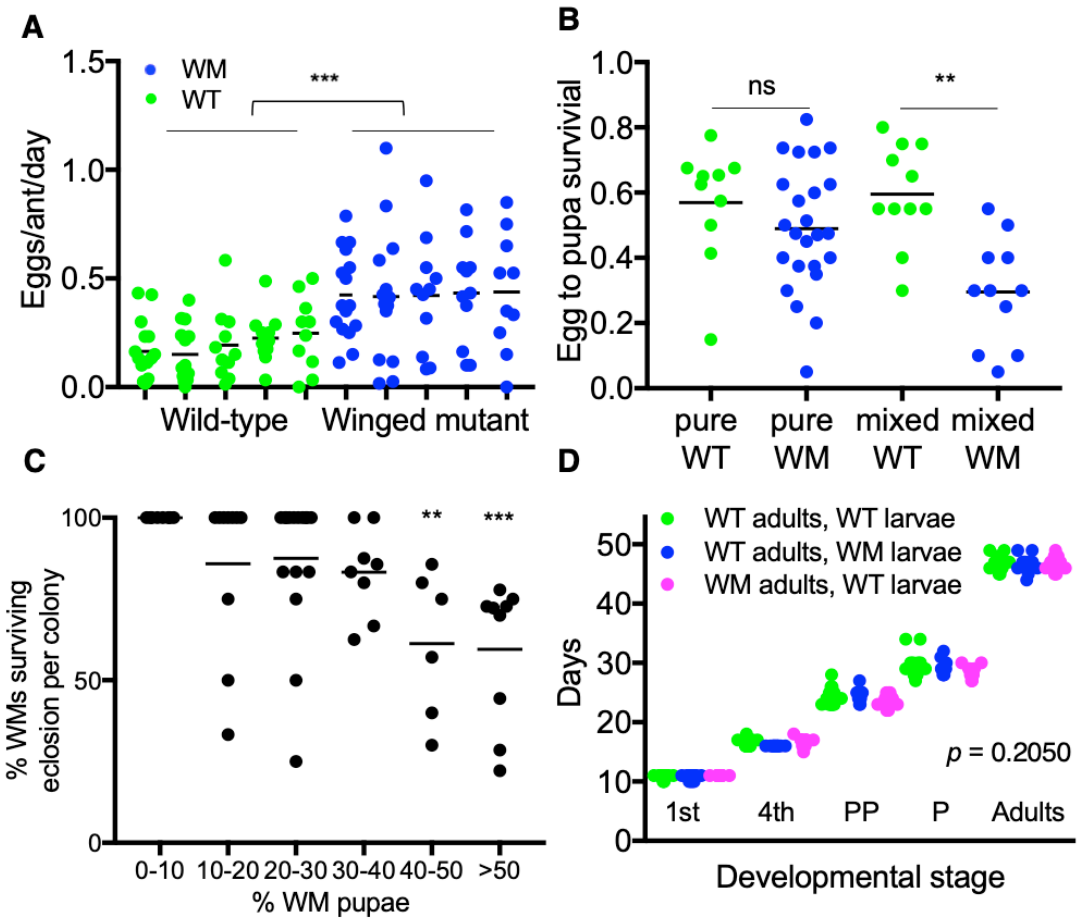
A
WM
WT
***
Eggs/ant/day
1.5
1.0
0.5
0.0
Wild-type
Winged mutant
B
ns
**
Egg to pupa survivial
1.0
0.8
0.6
0.4
0.2
0.0
pure WT
pure WM
mixed WT
mixed WM
C
**
***
% WMs surviving eclosion per colony
100
50
0
0-10
10-20
20-30
30-40
40-50
>50
% WM pupae
D
WT adults, WT larvae
WT adults, WM larvae
WM adults, WT larvae
Days
50
40
30
20
10
0
p = 0.2050
1st
4th
PP
P
Adults
Developmental stage

Two major components of adult behavior in *O. biroi* are nursing and foraging (Ulrich et al. 2018). In the experiments of Figure 5.4D, colonies were reared in simple nest chambers without a foraging arena and were fed by placing food directly into the brood pile. Under these conditions, the adult ants were not required to engage in foraging behavior, and the winged mutants and wild-types reared larvae with equal efficiency. These results provide no evidence for deficiencies in nursing behavior in the winged mutants, as might be expected for individuals with queen-like phenotypes (Oster & Wilson 1978; Wilson & Hölldobler 1990; Sumner et al. 2003). In contrast, foraging behavior is more typical of worker ants and is not observed in queens or workerless social parasites (Oster & Wilson 1978; Wilson & Hölldobler 1990; Sumner et al. 2003).

To test whether the winged mutants and wild-types differ in foraging behavior, I established one winged mutant and one wild-type colony composed of 16 tagged callow adult ants. Ants were placed in a plaster dish with a separated nest and foraging arena and allowed to lay eggs. Once the eggs hatched, I placed food into the foraging arena every other day and recorded the ants for ~12 hours to collect automated behavioral tracking data.

These two colonies displayed strikingly different behavior (Figure 5.5). The wild-type ants foraged outside of the nest and retrieved the food in four independent trials (as is invariably observed for wild-types in this assay; V. Chandra personal communication). In contrast, the winged mutants were virtually inactive and never retrieved the food. The wild-type larvae progressed into the final larval instar after 10 days, while the winged

mutant larvae never left the second instar and eventually all died. This initial pilot implies that the winged mutants do not exhibit foraging behavior, and that colonies composed entirely of winged mutants do not retrieve food to feed larvae. I am currently rearing ants to replicate this experiment with additional colonies.

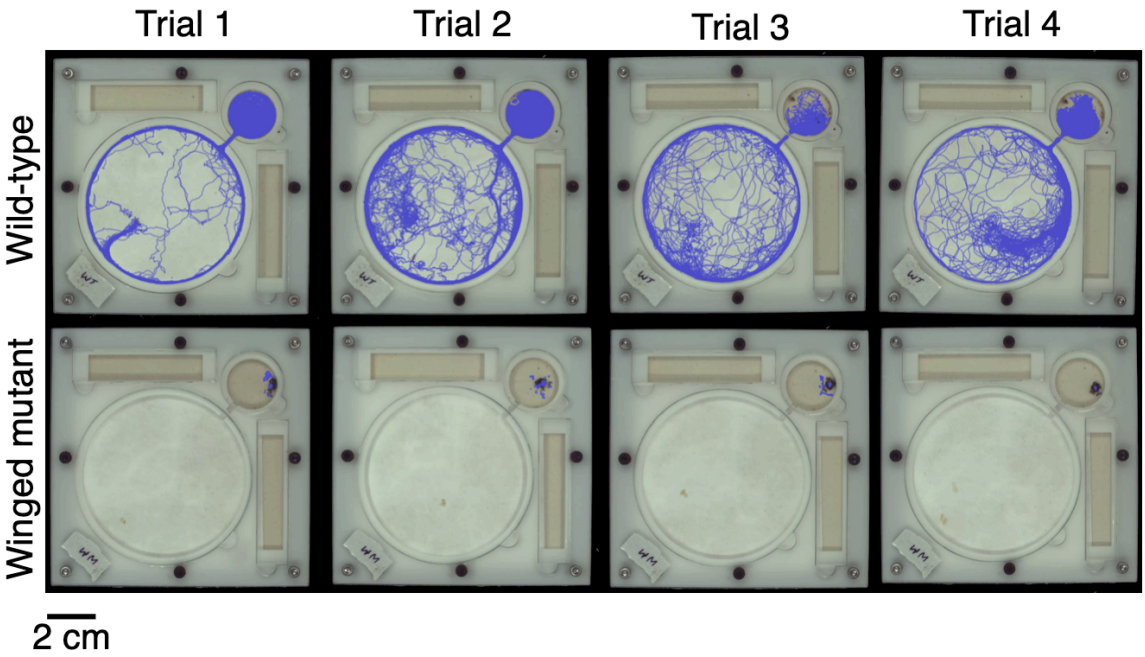

Figure 5.5: Winged mutant foraging behavior. Each image represents a foraging trial; automated behavioral tracking data are represented in blue (see Chapter 7). The ants nest in the upper right, and must leave the nest and enter the foraging arena to find the food. Across 4 independent foraging trials, the wild-type colony exhibited a high level of activity, collected the food from the foraging arena and fed it to their larvae. In contrast, the winged mutant colony exhibited very low activity overall, did not collect the food or feed it to their larvae, and consequently the larvae in this colony failed to develop and died.

The final fitness experiment I conducted was a naturalistic long-term coexistence study. I originally discovered the winged mutants in colony C1 at a low frequency (~14/10,000 adults), so I wanted to test whether the winged mutants could persist at low frequencies for multiple generations within wild-type colonies. I established four colonies, each with one winged mutant and 49 wild-type adults. These colonies were allowed to lay eggs and undergo species-typical reproductive cycles. I counted the number of winged mutant and wild-type adults in each colony for the first 10 cycles (one year).

Over one year, these colonies experienced exponential growth in size, growing from 50 to 706-2101 ants after 10 reproductive cycles. In all four colonies, the winged mutants persisted and increased in numbers, with 2-23 winged mutants per colony (Figure 5.6A). The percent of winged mutants, which was initially set at 2%, ranged from 0.1% to 2% after 10 reproductive cycles (Figure 5.6B). The changes in percent winged mutants were modest and largely centered on zero (Figure 5.6C).

This result demonstrates that the winged mutants do not deterministically go extinct or overtake wild-type colonies (which would then lead to extinction, due to their lack of foraging activity) in a one year period. Since the 10^{th} cycle, I have allowed these colonies to continue growing, but stopped counting the numbers of ants after every cycle due to the time required to phenotype such large numbers of ants. At the time of writing, the four colonies are now entering their 15^{th} reproductive cycle, and after the 20^{th} cycle I will collect another count of the numbers of winged mutants and wild-types in these colonies.

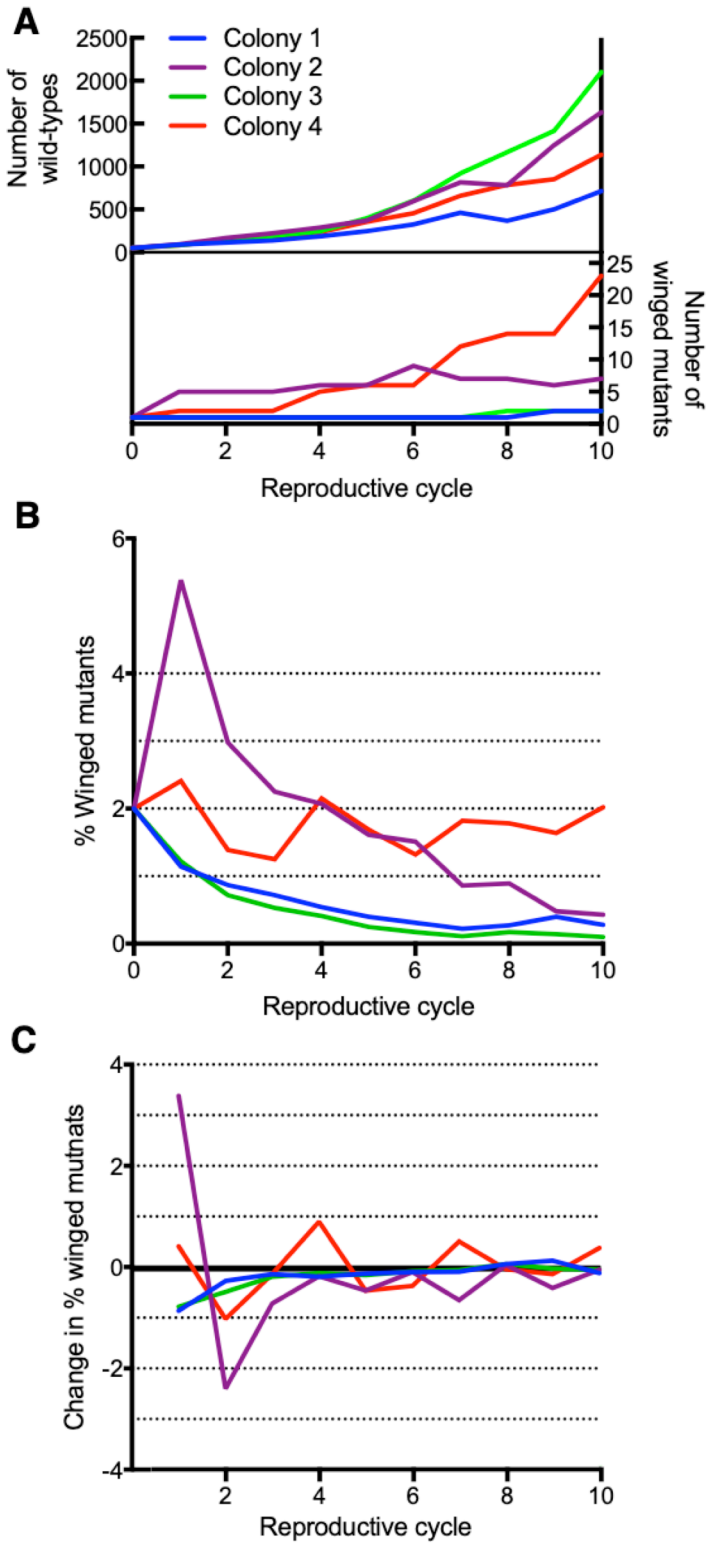

Figure 5.6: Long-term coexistence study. (A) Number of winged mutants and wild-types in the four experimental colonies over 10 reproductive cycles. (B) Percent of winged mutants. (C) Change in % winged mutants across cycles.

Discussion

In this study, I have characterized a unique winged mutant lineage of the clonal raider ant. Winged mutants differ from wild-types in a wide range of traits including caste morphology and multiple dimensions of social behavior and fitness. These mutants have a close resemblance to workerless social parasites that have been described previously in ants, and provide new insights into the way these parasites may evolve.

The winged mutant phenotype almost certainly arose from a single, highly pleiotropic genetic event, rather than a stepwise series of adaptive mutations. The winged mutants are very closely related to wild-types genome-wide, differing significantly less from their wild-type nestmates than from other closely related wild-type colonies (Figure 5.2B). Despite this genetic similarity, the winged mutants possess a suite of queen-like phenotypic traits, including wing development, ovariole number, reduced head and petiole size, and a lack of foraging behavior. This phenotypic syndrome can be viewed as an atavism: a reversion to an ancestral, wasp-like state in which individuals of all sizes possess wings and other queen-like features (Wheeler 1905). In light of my model of caste development (Chapter 4), I proposed that ants possess some caste differentiation factor(s) that induce the formation of worker-like traits at small body sizes. The winged mutants might represent loss-of-function mutants that compromise the activity of this factor.

Population genetic considerations also imply that the winged mutants arose from a single genetic event. No spontaneous morphological mutants of any kind have been observed

previously in the field or laboratory in *O. biroi*, so it is highly improbable that multiple *de novo* phenotypic variants (e.g., independent mutations affecting the wings and the ovarioles) would have arisen sequentially in any single genetic background over a short evolutionary timescale (Figure 5.2B). Second, clonality in *O. biroi*, due to the lack of recombination, is expected to lead to a generally reduced efficiency of natural selection compared to a sexual species, and the winged mutants were discovered at very low numbers (~10-20 individuals) that would even more severely reduce the potential for rapid adaptive evolution in this genetic background. Finally, I identified the winged mutants in a colony of closely related wild-types, and the most parsimonious interpretation is that they arose as a mutant lineage within this colony. The winged mutants have multiple positive and negative fitness effects with large effect sizes (Figure 5.4); if these effects arose via independent mutational events, which would most likely arise over separate generations, the winged mutants would have rapidly fixed or gone extinct within their source colony, rather than co-existing with wild-types as we discovered them.

The winged mutants are not the first observation of genetic variation affecting caste development. Previous reports of genetic variation in caste morphology stem from lineages that differ widely in genome-wide marker panels or even represent distinct species or genera (Anderson et al. 2008; Dobata et al. 2009; Schwander et al. 2010). Unlike these previous reports, however, the winged mutants most likely arose from wild-types via a single mutational step. These mutants thus provide the first evidence that

highly pleiotropic caste differentiation mutations can induce a wide range of queen-like traits at worker-like body size.

The evolutionary pathway that gives rise to workerless social parasites is a persistent mystery in ant biology and has attracted considerable controversy. It has been proposed that workerless social parasites evolve via sympatric speciation of intraspecific hyper-reproductive cheaters (Buschinger 1990; Savolainen & Vepsalainen 2003; Rabeling et al. 2014; Leppänen et al. 2016). Some researchers have questioned the plausibility of this mode of evolution, in particular because sympatric speciation requires strong disruptive selection, and because linked loci producing parasitic phenotypes could become unlinked by gene flow between an incipient parasite and its host (Ward 1996).

I found that the winged mutants have multiple negative fitness effects, including high eclosion mortality and a lack of foraging, indicating that they would not be viable in pure colonies. This is consistent with observations from ant natural history: there are no known cases of free-living all-queen species. Instead, ants that possess constitutively queen-like morphology are universally parasitic (Buschinger 2009). Queen-like differentiation mutants, like the winged mutants, have only two potential evolutionary outcomes: they can evolve into viable parasitic lineages or go extinct. Mutants such as the winged mutants thus must immediately face strong selection pressure to evolve into parasites (although this selection pressure is not necessarily realized).

Importantly, even in an outbred sexual species, a highly pleiotropic locus producing constitutively queen-like morphology would be under the same selection pressure as the winged mutants. Such a locus could act as a selfish genetic element and attract additional, linked mutations that induce other parasitic phenotypes, including reproductive isolation from the parental host species (i.e., a selfish differentiation mutation could nucleate a supergene, see *Winged mutant outlook*). In this sense, my winged mutant results indicate that the barriers to the sympatric speciation of workerless social parasites are not as severe as was previously expected. Many parasite-like features of morphology, behavior, and fitness can arise via just one or a few mutations affecting caste differentiation, and these mutations immediately produce strong selection that could promote further changes.

Regardless of a sympatric or allopatric origin, another barrier that a nascent parasite must overcome is stable long-term coexistence with its host population. If the winged mutants have negative fitness, they will go extinct, and if they have positive fitness, they will overtake their host and then go extinct. I found that multiple deleterious fitness effects of the winged mutants manifested at high frequencies (lack of foraging and eclosion mortality), and that they also have an elevated egg-laying rate (Figures 5.4, 5.5). This combination could in principle lead to negative frequency-dependent selection and long-term coexistence. Indeed, I found that the winged mutants could persist at low frequencies in wild-type colonies for at least ten reproductive cycles (one year: figure 5.6). Four years before I isolated the winged mutants from colony C1, Daniel Kronauer photographed an individual with a similar phenotype from the same colony, implying that

the winged mutants persisted for at least 4 years. Finally, anecdotal reports from colleagues imply that winged mutants may also occur in a wild *O. biroi* population in Taiwan (S. Teseo pers. comm.).

On average, most alleles of any kind rapidly go extinct, and this is likely also true for most mutations that affect caste development. However, queen-like differentiation mutants generally seem poised for long-term coexistence, given that a) queens have a higher reproductive capacity than workers, and b) all-queen colonies are not viable. My winged mutant data thus illustrate that coexistence could actually be a common outcome of caste differentiation mutations. It is important to note that, even if any particular queen-like mutant is not immediately a viable parasite, it would be expected to eventually evolve into a parasite if it can survive long enough to acquire additional mutations. In this sense, the winged mutants reveal a developmental bias that may have promoted the parallel evolution of workerless social parasites in ants: atavistic queen-like differentiation mutants display features that give them a relatively high probability of evolutionary success.

In conclusion, I have described a unique winged mutant lineage of the clonal raider ant. These winged mutants arose recently within the clonal Line A genetic background (Figure 5.2B), and resemble workerless social parasites in their morphology, behavior, and fitness (Figures 5.3-5.6). Some workerless social parasites have evolved in sympatry via caste differentiation mutations that induce queen-like traits at worker-like size. Here I have demonstrated a single-step origin of a queen-like differentiation mutant. These

mutants have a highly pleiotropic phenotypic syndrome that immediately selects for parasitic behavior, and they have an inherent potential for long-term coexistence with wild-types. This research provides a window into caste differentiation and workerless social parasites and will facilitate future mechanistic studies of caste development and evolution in ants.

Winged mutant outlook

In the previous section, I described my discovery and characterization of a parasite-like winged mutant lineage of *O. biroi*. As an outlook, I would like to present my ongoing efforts to identify the causal mutation that produces the winged mutant phenotype. Identifying a causal mutation in *O. biroi* is relatively challenging because it is a parthenogenetic species and I am not able to make crosses to conduct any kind of QTL or GWAS analysis. A further difficulty results from the haploid genome reference assembly with which I conducted my first analyses, as will be discussed below. These results should be viewed as a preliminary outlook on an ongoing project.

In Part 1, I used whole-genome resequencing of multiple winged mutant and wild-type libraries to demonstrate that the winged mutants are most closely related to Line A C1 wild-types. I exploited this dataset to identify putatively causal loci at which the winged mutants have distinct genotypes from wild-types. I aligned these data to a chromosome-length Line A reference assembly derived from C1 wild-types (McKenzie & Kronauer 2018). I used a custom Python script to identify loci where both winged mutant libraries have the same genotype, and the genotype differs from both of the two wild-type genomes (Figure 5.7).

Figure 5.7: Unique loci in winged mutants mapped across the 14 chromosomes. Data were generated by aligning short-read sequencing data to a haploid reference genome. The inferred diploid genotype at each locus is the same in both winged mutant libraries, and different from both wild-type libraries. Loci in green are homozygous in winged mutants and primarily represent losses-of-heterozygosity. Loci in red are heterozygous in winged mutants and may represent *de-novo* mutations (most commonly length variants of repetitive sequences), or ancestrally heterozygous regions that experienced independent losses-of-heterozygosity in both wild-type genomes. All four genomes are highly similar in this genome-wide dataset; 26,425 loci total were variable (0.01% of the 212Mb genome). 2,366 loci were identical in both winged mutant libraries and different from both wild-type libraries (0.001% of the genome). 62% of unique loci are found on Chromosome 13 (this is an under-estimate, see below).

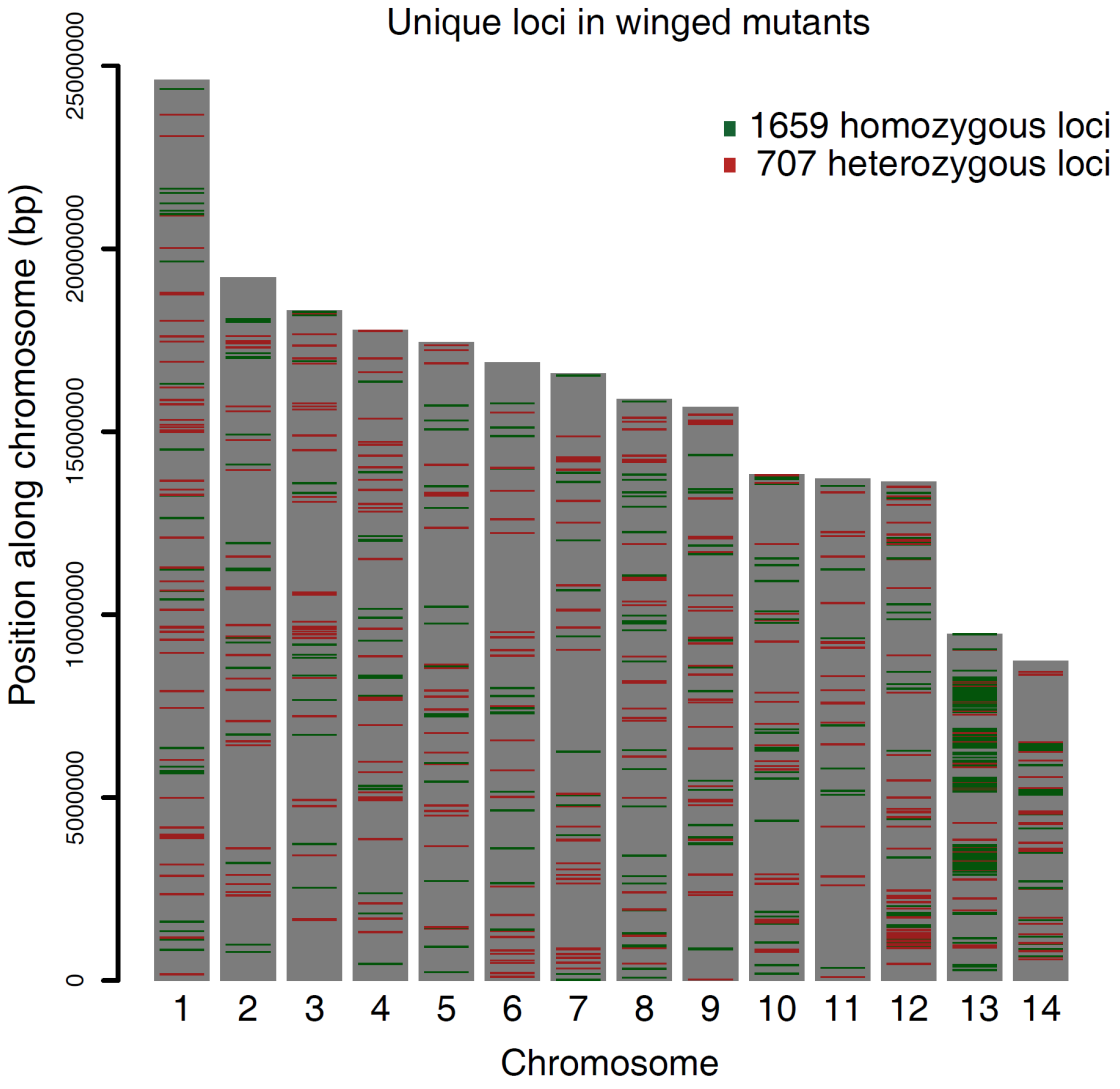
Unique loci in winged mutants
1659 homozygous loci
707 heterozygous loci
Position along chromosome (bp)
0
5000000
10000000
15000000
20000000
25000000
1
2
3
4
5
6
7
8
9
10
11
12
13
14
Chromosome

As expected from previous studies, the majority of sequence differences between winged mutants and wild-types are losses-of-heterozygosity (Kronauer et al. 2012; Kronauer et al. 2013; Oxley et al. 2014). These are mostly found on Chromosome 13, which seems to have lost heterozygosity along about one third of its length.

Several ant species possess non-recombining supergenes or 'social chromosomes' that regulate large-scale phenotypic variation (Wang et al. 2013; Purcell et al. 2014; Linksvayer et al. 2013; Schwander et al. 2014). For example, fire ants possess a non-recombining supergene, the *Sb* element, that produces variation in colony queen number and many other social traits, including queen morphology and behavior (Ross & Keller 1998; Wang et al. 2013; Stolle et al. 2019). While the specific mechanistic details of these interesting genetic elements remain an area of active investigation, the general evolutionary theory is that these chromosomal segments have undergone inversions or other structural rearrangements that suppress recombination between homologous chromosomes. This would then allow a large segment of chromosome to maintain linkage over long evolutionary timescales and evolve and be inherited as a single Mendelian element (even if it is actually millions of bases in length). A consequence of this suppression of recombination (and also of the fact that many supergenes are recessive lethal) is that one or both supergene variants may deteriorate genetically in a manner similar to a sex chromosome. Like sex chromosomes, social supergenes often possess an elevated number of transposable elements and are heteromorphic in karyotype analysis (e.g., due to a difference in overall length or centromere position) (Wang et al. 2013; Purcell et al. 2014).

Intriguingly, Chromosome 13 in the genome of *O. biroi* seems to resemble one of these social supergenes. This chromosome has a heteromorphic karyotype (Imai et al. 1984). Chromosome 13 also has a lower interaction density than the other chromosomes in Hi-C DNA crosslinking data (McKenzie and Kronauer, 2018), implying that its sequence is more heterozygous and/or repetitive than the other chromosomes in the *O. biroi* genome. Finally, Chromosome 13 has an elevated number of transposons compared to the rest of the genome (Sean McKenzie, personal communication).

An attractive hypothesis is that some aspect of social behavior in *O. biroi* is regulated by Chromosome 13, which could have acted as a social supergene in the sexual ancestor of *O. biroi*. A loss-of-heterozygosity in such a supergene could have produced the winged mutant phenotype. Two plausible hypothesis are: A) Chromosome 13 could bear a recessive element that induces a parasite-like phenotype that has become homozygous in the winged mutants, or B) Chromosome 13 could bear a dominant element that caused the loss of the morphological queen caste in wild-type *O. biroi* that has been partially or completely lost in the winged mutants, leading to an aberrant queen-like phenotype. Of course, many other possibilities exist, including that Chromosome 13 is not a supergene and/or does not cause the winged mutant phenotype. These hypotheses are difficult to test directly because *O. biroi* is clonal and wild-types within a clonal lineage possess the same diploid set of chromosomes, including both heteromorphic sister chromosomes of Chromosome 13. It is nevertheless highly suggestive that the most salient difference

between the winged mutants and wild-types is a loss-of-heterozygosity on this supergene-like chromosome.

The heteromorphy of Chromosome 13 poses a particular challenge for identifying putatively causal genetic variants in the winged mutants. Traditional reference genome sequences, even 3rd generation long-read genomes, are haploid: they consist of a single consensus sequence for every genomic contig. Heterozygosity is then assessed by aligning short-read data (e.g., Illumina or RNASeq data) back to the haploid reference. This method is successful when both chromosomal sequences are highly similar, such as when a genetic variant of interest is a single nucleotide polymorphism or short indel. In contrast, long stretches of highly heterozygous sequence, or structural variants, differ in sequence to such an extent that short reads cannot be aligned to both variants.

I have collected multiple short read datasets comparing winged mutants to wild-types, including the Illumina DNA sequencing data (Figure 5.7) and a developmental time course of RNASeq data comparing winged mutants and wild-types (Figure 5.8; see figure legend and Chapter 7 for details). Unfortunately, because Chromosome 13 is heteromorphic, the issues that I mentioned above limit my ability to interpret these data using a haploid reference genome. Table 5.3 and Figure 5.9 illustrate the kinds of bioinformatic errors that I have observed when aligning short read data to a structural variant in Chromosome 13.

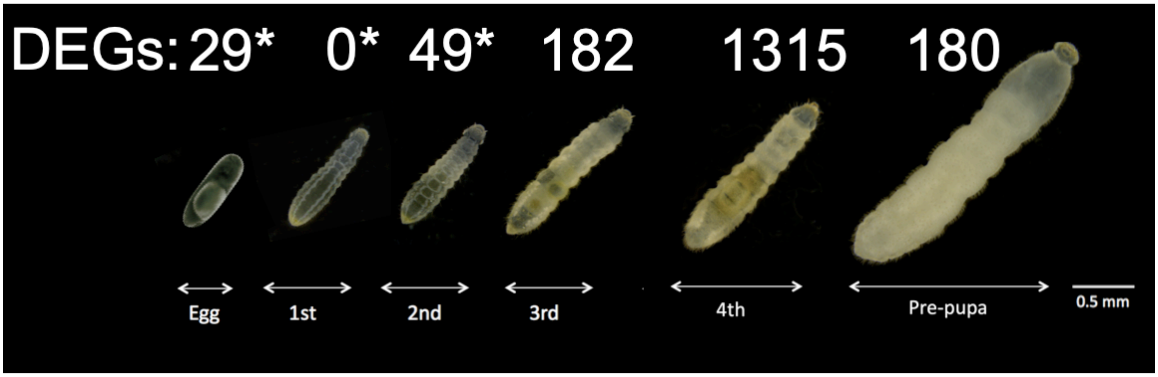

Figure 5.8: Number of differentially expressed genes between winged mutants and wild-types across six developmental time-points using a haploid reference assembly. Asterisks denote numbers of differentially expressed genes (DEGs) that are small enough to potentially result entirely from false positives (see Chapter 7). These numbers of differentially expressed genes are consistent with worker/queen RNASeq comparisons from other social insect species, where the highest levels of differential expression are found in the final larval instar, corresponding to approximately 10% of genes in the genome (Warner et al. 2016; Warner et al. 2018). This RNASeq dataset illustrates that the winged mutants are enacting a distinct developmental program compared to wild-types. The first measurable wave of differential expression occurs in the 3rd larval instar, with a large number of differentially expressed genes in the 4th larval instar. I have not identified any highly compelling candidate causal genes using this dataset, however, and I am restraining from conducting further analyses until I can do so using a diploid genome assembly. See Chapter 7 for additional details regarding RNASeq data collection and false positive analysis. Images: Qi'an Sun.

Table 5.3: DESeq adjusted read counts for a gene in a heteromorphic region of Chromosome 13. Read counts indicated that the winged mutants lack transcription at this locus, but manually inspecting the raw read alignments revealed that this result is probably spurious. An equal number of reads mapped to the body of this gene in winged mutants and wild-types, but the winged mutant genome was homozygous for a structural variant that caused the coverage to drop to zero over an intronic region in the winged mutants. I believe that this caused my read counting software (HTSeq) to incorrectly score the read count for this gene as zero.

Type	C1						WM					
Time	1	2	3	4	5	6	1	2	3	4	5	6
6d	0	0	0	0	124.8	58.5	0	0	0	0	0	0
1st	0	9.0	0	40.4	7.6	9.0	0	0	0	0	0	0
2nd	0	7.9	0	12.4	0	13.8	0	0	0	0	0	0
3rd	15.7	2.1	13.6	20.3	52.6	3.7	0	0	0	0	0	0
4th	46.4	33.4	136.1	30.2	57.7	44.5	0	0	0	0	0	0
PP	90.8	106.5	77.6	98.0	92.4	82.2	0	0	0	0	0	0

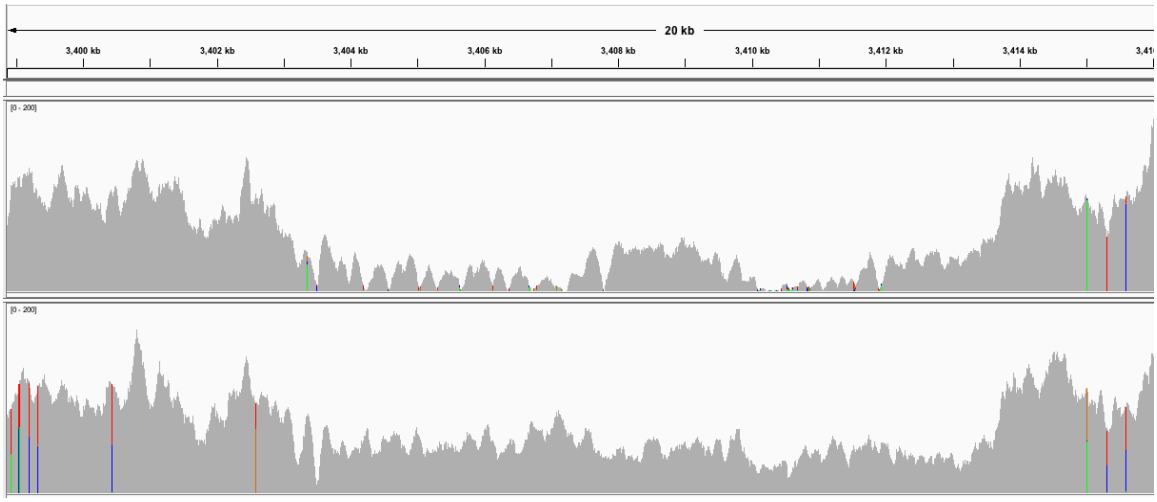

Figure 5.9: Representative example of a structural variant on Chromosome 13. Raw coverage data for a winged mutant (top) and wild-type (bottom) genome library are visualized with Integrated Genome Viewer. In the wild-type, higher coverage is seen at the beginning and end, and in these high coverage regions multiple heterozygous loci are observed (visualized as two-colored bars). The central region is homozygous and has approximately ½ coverage. The winged mutant is homozygous across the entire locus, and the central region has coverage that frequently drops to zero. I interpret this as evidence for a loss-of-heterozygosity in the winged mutant that led to homozygosity of a ~10kb structural variant that is not represented in the haploid reference genome assembly. These structural variants limit my ability to interpret short read data aligned to regions with losses-of-heterozygosity, which are especially prevalent on Chromosome 13.

Once I identified this alignment issue, I decided it was more important to resolve it than to continue to analyze my Illumina and RNASeq data using the currently available haploid reference genome. Using published PacBio and Hi-C sequencing data, I created a phased, diploid genome assembly using the Falcon-phase pipeline (Kronenberg et al. 2018). This phased assembly recovered 212Mb of primary contigs, with 322 contigs and a contig N50 of 2.017Mb (an improvement over the 530 contigs in the haploid assembly of McKenzie & Kronauer 2018). This pipeline also resolved alternative sequences for a portion of the genome, with 61.77Mb of secondary contigs (2685 contigs, N50 of 27.37kb). These results are comparable to previous assemblies created using Falcon-phase (Kronenberg et al. 2018).

I used RaGoo to independently scaffold the primary and secondary contigs using chromosomes from the haploid assembly, allowing me to check for structural rearrangements and structural variants on Chromosome 13 (Alonge et al. 2019). I found that Chromosome 13, and no other chromosome, has many contigs that differ in position and orientation between the primary and secondary assembly. Chromosome 13 also had a 6-fold enrichment in structural variants compared to the rest of the genome. Based on the size of the loss-of-heterozygosity in winged mutants, I estimate that approximately 80kb of structural variants have losses-of-heterozygosity in the winged mutants on Chromosome 13. This estimate differs dramatically from my VariantCaller results obtained by aligning short read data to a haploid reference genome (Figure 5.7), which identified only 1.5kb of sequence differences. This discrepancy likely resulted because

short reads could not be aligned or scored within structural variants, leading to an under-estimate of the number of sequence differences (Figure 5.9).

If this diploid assembly has accurately resolved both alternative sequences of all or most structural variants, it should be possible to align my short read Illumina and RNASeq data back to the diploid assembly and generate a much more accurate estimate of the losses of heterozygosity and transcriptional differences between winged mutants and wild-types on Chromosome 13. However, this assembly arose as an output from the Falcon-phase pipeline and I wish to be cautious about its interpretation. Before aligning the short read data, I will assess whether or not this diploid assembly is accurately capturing the genome sequence and its structural variants. Once I have obtained a high-quality assembly, I will annotate it and align my short-read Illumina and RNASeq data to the primary and secondary contigs. This will allow me to conduct improved analyses to seek a causal mutation in the winged mutants.

CHAPTER 6: DISCUSSION

"The understanding of wild-type behavior comes best after the discovery and analysis of mutations that alter it." – Sydney Brenner, *Genetics*, 2009.

In Chapter 1, I introduced the unique social biology of ants, and outlined my specific focus on using functional genetic methods to study chemical communication and caste development and evolution. The *orco* mutants and the winged mutants represent the first two mutant ant lines to be studied in any detail.

Developing a CRISPR protocol in *O. biroi* was a challenge; I injected over 10,000 eggs to make the *orco* mutants, and then another 20,000 eggs to get this protocol to its current, readily applied state. The winged mutants also posed their own unique difficulties; mapping this spontaneous mutation already seemed challenging due to the clonality of *O. biroi*. I now believe that the causal mutation(s) most likely resides in a large loss-of-heterozygosity on a chromosome that is so highly heteromorphic that I can't accurately describe it using traditional short-read sequencing and haploid reference genomes. If studying mutant ants is so challenging, why bother?

These studies of wild-types and mutants are controlled comparisons that differ in one variable (the locus that has been mutated). These experiments could thus be viewed as analogous to other experimental perturbations, such as nutritional manipulations, pharmacology, and RNAi. I would argue that these studies of mutants are substantially

more robust than these other methods, however, and can lead to general conclusions that would not have been possible from other methods.

For example, I observed a completely unexpected, discrete morphological phenotype in the brain of the *orco* mutants. This phenotype was strikingly different between wild-types and mutants, and was almost completely invariant, even across independently generated *orco*$^{-/-}$ lines. This discrete morphological effect was not actually a complete loss of antennal lobe glomeruli, but instead a reduction from ~500 to ~90. I interpret this result as indicating that *orco*, most likely via OR function, is required for most antennal lobe glomeruli, but not all. If I had used some kind of transient perturbation, it would have been very difficult to know whether these remaining glomeruli were biologically meaningful, or if they represented an incomplete effect of our manipulation. Instead, because this phenotype was so stereotyped, these mutants raise the possibility of conducting follow-up experiments, such as identifying the specific input tracts from the antenna that correspond to absent vs. present odorant receptor glomeruli.

I also came across a number of surprises in my behavioral observations of the *orco* mutants. Here are a few: A) The wandering phenotype implies that ants possess some kind of chemical aggregation cue that has not been previously proposed. B) *orco* mutants still groom and carry eggs, but did not pick up larvae (personal observations), implying distinct OR and non-OR cues for the recognition of these brood types. C) *orco* mutants aberrantly elicited a raiding response inside the nest that wild-type only ever elicit outside

of the nest. This implies that wild-type ants use some OR-mediated cues (possibly, but not necessarily, the same as A) to differentiate inside-nest versus outside-nest behaviors.

The *orco* mutants did not just provide a clean test of the growing consensus that ants employ ORs for pheromone perception, they implicated new developmental mechanisms and new chemical cues that had been previously overlooked. Extraordinary claims require extraordinary evidence: these kinds of surprises would have been hard to believe if they resulted from a less clean and unambiguous experimental perturbation, and were not discovered previously despite decades of observations of wild-type behavior and neuro-anatomy.

The winged mutants similarly surprised me routinely. When I first identified the winged mutants I did not interpret them as similar to workerless social parasites, but rather as winged workers. It was only after I discovered their increase in ovariole number (motivated by the observation that they lay eggs at an elevated rate) that I started to consider this hypothesis, which gave new context to my previously-idiosyncratic observation that winged mutants exhibited high eclosion mortality. I was even more surprised to find that the winged mutants had a reduction in head and petiole size, just like some social parasites that I knew from the literature.

I was able to make these discoveries because the winged mutants are a 100% penetrant mutant line that I was rearing and watching for four years. I would not have had the time or available ants to conduct the same types of exploratory studies if I had perturbed caste

development through a transient manipulation (such as juvenile hormone treatment, which can increase size and induce queen-like development in ants). Indeed, the results that I reported on the winged mutants are just the most well-controlled and interpretable set of a many more experiments I conducted with the winged mutants. Finally, unlike a transient perturbation, the winged mutants are mutants: they arose spontaneously through a natural process, and thus have the clear potential to be relevant to evolution.

Because I have the winged mutants as a stable line, I can continue to study them for years to come and, as long as I maintain the same highly controlled rearing standards, trust that my future data are comparable to data from years before. It is hard to overstate this practical advantage. For example, I am currently rearing larvae under precisely standardized conditions to collect ATACSeq data that are exactly comparable to my existing RNASeq data. In the future I hope to continue this, collecting single cell data, for example, or adding additional types of measurements to my morphological dataset (such as brain morphology or a precise description of thoracic architecture) and much richer behavioral studies. I do not yet know what is the causal mutation, but using a plurality of approaches I am confident that I will find it eventually, and knowing what it is will just give greater context to my prior data. The cumulative nature of these studies would be greatly undermined if, for example, I were studying caste using variable stocks of field-collected ants and manipulating them using variable batches of some pharmacological reagents.

The caste theory that I presented in Chapter 4 provides a glimpse toward where this kind of functional genetic approach can take us. I widely surveyed the literature of caste in ants and tried to isolate specific aspects of caste that appear to have a coherent genetic basis and thus could be amenable to future study using functional genetic manipulations. I hope to eventually identify the caste determination and differentiation mechanisms and begin to infer the pathway that leads to worker versus queen development. This includes studies of morphology, physiology, and behavior, and additional precise experiments using mutant lines. Just as one type of mutation produced a workerless social parasite-like phenotype in *O. biroi*, I will try to create mutants that recapitulate other kinds of caste evolution: to restore the ancestral large-bodied queen caste, for example, or to induce a soldier or a wingless queen. I will then describe these lines using equally (if not more) thorough methods as the *orco* and winged mutant projects I presented here.

The major frontier I see for ant functional genetics is to shift our understanding from a single model species (the clonal raider ant) to the entire phylogeny of the ants, or even to other organisms. In the case of *orco*, we were fortunate enough to have another group also make *orco* mutants in a distantly related ant species, and they replicated and strengthened our major conclusions (Yan et al. 2017). With the winged mutants, it would be ideal to complement my studies with comparable data from naturally-occurring workerless social parasite species in other types of ants. Once I find the causal mutation, I would also like to induce it in another ant species. As I start to identify mechanisms involved in caste development, I will be very interested in characterizing these

mechanisms across a range of species to see how they originated and how they are modified to produce a range of caste morphology and behavior.

In summary, working with mutant ants can be slow and challenging, but it has allowed me to make robust and general conclusions that would not have been possible with other methods. These projects only represent our first steps into this field, and we will continue to advance our ability to make informative molecular manipulations and draw robust conclusions from them. This starts at the level of one species, but is quickly going to expand to the entirety of the ants and beyond.

CHAPTER 7: METHODS

orco methods

Experimental model

Ooceraea biroi colonies were maintained at 25 °C in circular Petri dishes (50 mm diameter, 9 mm height) with a plaster of Paris floor ca. 4 mm thick. Colonies were fed 3 times weekly with fire ant (*Solenopsis invicta*) brood and cleaned and watered at least once per week. Two *O. biroi* clonal lines, which are genetically distinguishable at the *mitochondrial cytochrome oxidase subunit 1* (*CO1*) gene (Kronauer et al., 2012), were used in this study. All experimental ants belonged to Line B, while Line A ants were only used as chaperones to raise experimental Line B individuals. Experimental ants were reared by placing Line B larvae (G0s) or eggs (G1s and subsequent generations) in colonies of 20 Line A chaperones, and chaperones were removed once the callows had eclosed. This rearing method results in a small fraction of Line A offspring of chaperones in colonies with the G0s and subsequent generations. For this reason, all individuals were genotyped following experiments, and Line A individuals were removed from all analyses. All experimental colonies in this study had eggs removed twice weekly so that adults were maintained without larvae or pupae. All individuals, including those that died during experiments, were genotyped (see below) to determine their clonal line, and *orco* amplicons from Line B individuals were sequenced to determine *orco* genotype.

Potential off-target effects

It has been shown that in some cases CRISPR/Cas9 injections can lead to off-target mutagenesis that in turn can give rise to non-specific phenotypes (Fu et al. 2013). In my

experiments with *orco* I used multiple measures of precautions, making it highly unlikely that the phenotypes I report arise due to off-target effects. First, I used a high-quality reference genome to design the gRNA in this study to have no additional target sites in the genome that are likely to lead to off-target cutting (Fu et al. 2013; Oxley et al. 2014). Second, mutations induced by Cas9 are stochastically generated (Fu et al. 2013), such that any off-target effects would likely be present in some G1 lines but not others. The phenotypes I report are consistent across five independently generated $orco^{-/-}$ lines, and I do not observe the same phenotypes across two independently generated $orco^{wt/-}$ lines. Third, the striking reduction of OSNs and antennal lobes in *orco* mutant ants are phenotypes specific to the ant chemosensory system that are unlikely to arise from random off-target effects. These phenotypes provide a direct functional link between the $orco^{-/-}$ genotype and the chemosensory deficiencies described in this study. Importantly, the antennal lobe phenotype was entirely discrete: every $orco^{-/-}$ brain had substantially smaller antennal lobes than any $orco^{wt/-}$ or wild-type brain, even though this phenotype was measured across multiple independently derived $orco^{-/-}$ and $orco^{wt/-}$ lines. Therefore, while I cannot exclude the possibility that my injections gave rise to some level of off-target mutations, it is unlikely that the specific phenotypes reported in this study arise from off-target effects.

Tagging

All ants in behavioral and fitness experiments (Figures 4,5) were tagged with two color dots, one on the thorax and one on the gaster, using uni-Paint markers (models PX-20 or PX-21) such that each individual could be identified within the colony (Figure 3.4D,G).

For automated behavioral tracking, four colors were used (blue, green, orange and pink) for a total of 16 unique combinations. Ants were tagged with a randomly assigned color pair at least 10 days prior to any behavioral experiments. Tagged ants had a leg removed for genotyping and sequencing either before (Figure 3.3A,B; Figure 3.4A-C) or after (Figure 3.4D-I; Figure 3.5) experiments.

Genotyping

To distinguish Line A and Line B, eggs and adults were genotyped using PCR of mitochondrial *CO1* with standard DNA barcode primers (HCO and LCO, Folmer et al. 1994) followed by a restriction digest with MwoI from New England Biolabs. This enzyme cuts the PCR product derived from Line B, but not from Line A.

orco *sequencing*

To screen for *orco* mutations, I designed PCR primers that flanked the *orco* cut site and sequenced the resulting PCR products using Sanger and Illumina sequencing. Primer sequences were:

F: 5’

TCGTCGGCAGCGTCAGATGTGTATAAGAGACAGTCCAACTTGCTGTAAATTT
GGAT 3’

R: 5’

GTCTCGTGGGCTCGGAGATGTGTATAAGAGACAGCTCTTCTTGGTCGGCGGT

A 3’

Illumina methods followed a previously described protocol (Kistler et al., 2015). Primers included tails at the 5’ end that were used as adapters to add indices to individual samples for Illumina sequencing (Kistler et al. 2015). Sequences were aligned to the *orco* genomic sequence and reads at each base pair that aligned with an insertion or deletion were counted with the script crispralign.py from the genomepy package, available at https://github.com/oxpeter/genomepy. *orco* amplicons from 25 of 42 recovered G0s were subjected to Illumina sequencing (Figure 3.1C). Three of these individuals, all of which were found to have nearly 100% mutation rates, displayed a wandering phenotype similar to the wandering phenotype observed in G1s, indicating that somatic CRISPR in G0s may be useful for functional genetic studies even in the many social insect species where it is not logistically possible to generate or maintain stable mutant lines (Schulte et al. 2014; Yan et al. 2014; Roth et al. 2019).

Identification of mutant sequences

Mutant lines were identified via Sanger sequencing of eggs and adults of G1s and subsequent generations. All Sanger sequencing traces were scored manually. For the G1 dataset (below), manual identifications were verified by checking for misalignment against a reference sequence using MEGA7 (Kumar et al. 2016) and by using the program Mutation Surveyor (Softgenetics) for automated allele identification. Mutant lines were defined as groups of ants that possess identical *orco* genotypes, and *orco*

amplicons from representatives of each mutant line were Illumina sequenced and individual reads were manually inspected to ensure both alleles were properly identified.

Neuro-anatomy: immunohistochemistry

Immunofluorescence was performed as described previously (Dobritsa et al. 2003; Pitts et al. 2004). Antennae were removed and prefixed in a solution of 4% paraformaldehyde in PBS with 0.1% Triton (PBSTx) for 30-60 minutes at room temperature then rinsed three times with PBST. Due to the scarcity of material, antennae were collected from wild-type and *orco*$^{-/-}$ ants that had died less than 24 hr previously. Antennae were stored overnight in a solution of 25% sucrose in PBST at 4°C, then embedded in Tissue-Tek OCT (Sakura Finetek, Torrance, CA) and frozen. Antennae were sectioned at 12 µm at -20°C and allowed to dry at room temperature for 3 hr. Slides were then fixed in 4% paraformaldehyde in PBSTx at room temperature for 30 min, rinsed, then blocked with PBSTx plus 5% normal goat serum (NGS, Vector Laboratories) at room temperature for 60 min. An anti-Orco polyclonal mouse antibody (gift from Vanessa Ruta) was diluted 1:1000 in PBSTx plus 5% NGS and incubated on slides at room temperature overnight. Slides were rinsed and incubated with secondary Alexa594 donkey anti-mouse (Invitrogen) at a 1:500 dilution in PBSTx plus 5% NGS at room temperature for 2 hr then rinsed. Nuclei were labeled using DAPI diluted to 1µg/mL in PBS at room temperature for 20 min followed by a brief wash in water. Slides were mounted with Dako Fluorescent mounting medium. Images were captured using a confocal microscope (Zeiss LSM 780).

Glomerulus counts and antennal lobe volumes

One of the wild-type *O. biroi* antennal lobe reconstructions was based on published data (McKenzie et al. 2016). For the remaining data, *D. melanogaster* and *O. biroi* brains were dissected in PBS and immediately transferred to a fixative solution of either 1% glutaraldehyde or 2% PFA and 2.5% glutaraldehyde in PBS, and fixed at room temperature on a shaker for 1-30 days. To dehydrate, brains were rinsed in PBS and then suspended for 5 minutes each in an ascending series of 50%, 70%, 90%, 95%, 100%, 100%, and 100% ethanol. Brains were cleared and mounted in methyl salicylate. Glutaraldehyde-enhanced autofluorescence was imaged using a confocal laser scanning microscope (Zeiss LSM 8800) with excitation by a 488 nm laser. Three-dimensional projections were created from confocal image stacks using Fluorender (Wan et al. 2012). Three-dimensional reconstructions of glomeruli and antennal lobes were produced by manually segmenting confocal image stacks using the Segmentation Editor plugin in the Fiji distribution of ImageJ (Schindelin et al. 2012). Antennal lobe volumes were calculated using the Object Counter3D ImageJ plugin (Bolte & Cordelieres 2006), blindly with respect to genotype.

Fly and ant brains depicted in Figure 3.3 were immunostained with NC82 and SYNORF1, respectively (both deposited to the Developmental Studies Hybridoma Bank by Buchner, E. (DSHB Hybridoma Products 3C11 (anti SYNORF1) and NC82)). For these stains, brains were fixed at room temperature in 4% paraformaldehyde (with 0.5% triton-x for NC82) for 30min (NC82) or 4hrs (SYNORF1), washed 6x10min in PBS (with 0.5% triton-x for NC82), blocked for 1-2hrs in PBS with 0.5% triton-x and 5%

normal goat serum, and incubated in the blocking solution with 1% sodium azide and primary antibody (1:20 in both cases) for three days at room temperature. Brains were then washed 6x10min in PBS and then incubated in blocking solution with 1% sodium azide and secondary antibody (goat anti-mouse Alexafluor647, 1:100) for two days at room temperature. Brains were then washed 3x10min in PBS. Ant brains were subsequently dehydrated in an ascending series of 50%, 70%, 90%, 95%, 100%, 100%, and 100% isopropanol (30 seconds per solution) and cleared and mounted in methyl salicylate. Fly brains were mounted in Dako fluorescent mounting medium (Agilent Technologies). Brains were imaged as above. Three-dimensional projections were created from confocal image stacks using ZEN software (Zeiss). Flies in this experiment were aged for one month to test whether glomeruli become visibly reduced in old flies.

D. melanogaster *glomerulus counts*

My reconstructions of *D. melanogaster* antennal lobe glomeruli yielded different glomerulus numbers than what has been published previously (Table 3.1). my reconstructions also showed small differences in glomerulus numbers between wild-type and $orco^{-/-}$ flies (Figure 3.3). To address this possibility, I imaged and reconstructed two additional *D. melanogaster* antennal lobes, one from an $orco^{-/-}$ ant and one from a wild-type individual. These reconstructions were not performed strictly *de novo*, as the *O. biroi* and *D. melanogaster* reconstructions reported in the main text, but by referring to the published map of the *D. melanogaster* antennal lobe (Laissue et al. 1999; Laissue & Vosshall 2008). Due to differences in sample preparation and imaging methods, it was not possible to unambiguously match each glomerulus to the published map. However, I

identified structures in my newly reconstructed wild-type and *orco*$^{-/-}$ antennal lobes that corresponded to all published wild-type glomeruli. These results suggest that *orco*$^{-/-}$ flies have no systematic reduction in the number of antennal lobe glomeruli compared to wild-type flies, although it is possible that some neighboring glomeruli in *orco*$^{-/-}$ flies have divisions that appear less distinct or may even be fused relative to wild-types (Figure 3.3).

Behavior and fitness: sharpie assay

Sharpie assays were conducted with tagged ants (Figure 3.4A-C) on printer paper in a 5.25x5.25 in open-air arena bounded by a clear acrylic barrier. Six horizontal and 6 vertical black lines were printed on the paper using an HP LaserJet printer (Figure 3.4A,B). Immediately before each assay, 3 alternating horizontal and vertical black lines were traced with red Fine Point Sharpie Permanent Marker (item 30002). Then the ant was placed in the center of the grid. A 2 min video was recorded and the number of times the ant crossed black and Sharpie lines was manually counted (Movie S2). A Sharpie repulsion index was calculated as the ratio of black line crosses to total line crosses. Once the experiment had concluded, I determined that low numbers of line crosses caused the repulsion indices to be unreliable, and I therefore excluded four assays that had less than 10 line crosses total. As a positive control, a wild-type worker was assayed after each assay with a low repulsion index to ensure the Sharpie lines retained a repulsive effect. All positive controls had high repulsion indices and as a population were statistically indistinguishable from the other wild-type workers assayed ($p = 0.42$, t-test).

G1 preparation for behavior and fitness experiments

G1 rearing resulted in a set of 34 colonies containing a mixture of G1 ants and Line A progeny of chaperones. These colonies were used to identify mutants for egg-laying, automated behavioral tracking, and survival experiments (Figure 3.4D-I, Figure 3.5). Once each colony started producing eggs, I collected all eggs 5 times over a 14-16 day period. *CO1* amplicons from all eggs were genotyped to identify Line A and Line B eggs, and *orco* amplicons from Line B eggs were Sanger sequenced to identify *orco* mutants. I sequenced 2,184 eggs from the 533 Line B ants in these colonies, corresponding to ca. 4 eggs per ant. During the period of egg collection and one week after egg collection had concluded, I subjectively determined whether any individuals in any given colony displayed a wandering phenotype. Colonies in which *orco* mutant eggs were detected or in which wandering phenotypes were observed were selected for the egg-laying dataset.

Egg-laying dataset

I included 16 colonies in the egg-laying dataset. A subset of ants in these colonies were later also used for behavioral and survival experiments. After the experiments had been concluded, all ants had a leg removed, from which *orco* amplicons were sequenced. For each $orco^{wt/-}$ and $orco^{-/-}$ adult I identified, I counted the number of eggs of its genotype in its colony. If several adults of the same genotype were identified in a colony, for each individual I calculated the number of eggs of that genotype divided by the number of adults of that genotype. I used a two-tailed Wilcoxon test to test whether $orco^{wt/-}$ or $orco^{-}$

$^{/-}$ G1s produced different numbers of eggs than the average of wild-type G1s in this experiment (Figure 3.5A).

Behavioral and survival dataset

Before removing legs from ants for genotyping, workers from colonies that produced a high frequency of *orco* mutant eggs or contained individuals with wandering phenotypes were pooled to create 5 experimental colonies with a mixture of 12-14 G1 wild-type and *orco* mutant ants. Before pooling, all workers in these colonies were individually tagged with two color dots. These 5 colonies were recorded in 24 hr videos.

Experimental *O. biroi* colonies initially contained a total of 68 G1 ants, with 42 wild-type, 8 *orco*$^{wt/-}$, and 14 *orco*$^{-/-}$ individuals (Figure 3.1D). These colonies also contained 4 *orco* mutant individuals with in-frame mutations, which were not included in the current analyses because sample sizes were too small. G1s in experimental colonies varied in *orco* genotype but were otherwise identical in rearing methods, genetic background, and did not differ systematically in age. Before the start of each 24 hr video, plaster nest boxes were cleaned and the plaster was moistened. For four weeks after the video was recorded, I also recorded survival of all ants in the 5 experimental colonies.

Video recording and automated behavioral tracking

Automated behavioral tracking was performed in custom-made tracking setups under constant illumination. Temperature was maintained at 25°C. Videos were acquired using C910 Logitech USB webcams controlled with custom MATLAB (version R2016a, The

MathWorks, Inc.) software at 10 fps at 960x720 pixel resolution (13 pixels/mm).

Tracking was performed blind with respect to genotype. Videos were processed and analyzed using custom MATLAB software. In each frame, ants were segmented from the background of the dish using a fixed threshold. Resulting components, or blobs, were linked into trajectories using the optical flow computed between consecutive frames (Horn–Schunck method (Barron et al. 1994)). Trajectories ended and new ones were initiated whenever blobs split or merged between two consecutive frames. Trajectories stored the following data, collected from the respective blob in each frame: centroid (position of center of mass), orientation (angle between the major axis of the best-fitting ellipse and the horizontal axis) and area (in mm^2).

We used a threshold size to select trajectories that corresponded to a single ant and lasted longer than two seconds. Each trajectory was then assigned a combination of color tags using a custom classification algorithm. For each experiment, at least 500 frames per ant were manually identified to create a training set, 70% of which was used to train, and 30% of which was used to validate an automated identity classifier.

For each trajectory, a naive Bayes color classifier (Fletcher et al. 2011) was used to compute the pixel color probabilities for each pixel in the blob of each frame for six color classes: the four tag colors, the ant cuticle color and the color of the plaster of Paris (Figure 7.1). Predicted probabilities for all four tag colors were used to determine whether both tags were visible and, if so, the orientation of the ant in the frame was

deduced from the relative position of the tags with respect with the cuticle color. If both procedures were successful, the pixel color probabilities were fed into another naive Bayes classifier to assign an identity to the ant.

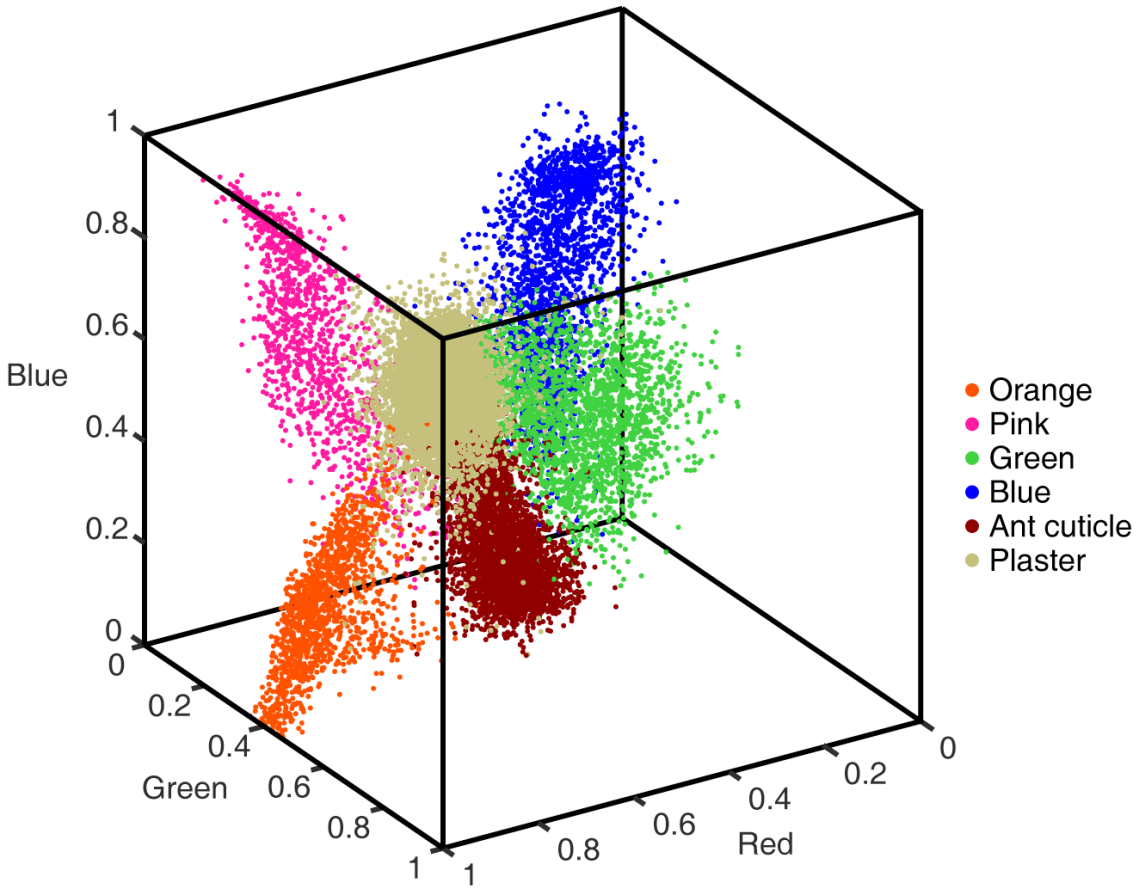

Figure 7.1: Color definition for automated behavioral tracking in RGB space. Measurements were collected manually from the four different tag colors (orange, pink, green and blue), the plaster (background) and the ant cuticle. These colors are clearly distinguishable in RGB space, allowing automated behavioral tracking based on identifying the color tags of each ant.

For each trajectory, frames were tested in a random order until 20 frames were successfully identified or no more frames were available. If at least one frame was identified, the trajectory, and thus all its underlying positions, was assigned the most frequently predicted identity. The identity classifier had an empirical error rate of 20% on single frames. However, the error rate decreased with the number of frames tested within a trajectory. Overall, I estimated that less than 10% of the total identified positions were misclassified, a performance equivalent to that reported previously for a functionally similar tracking setup for ants (Mersch et al. 2013).

Analysis of automated behavioral tracking data

Cleaning and watering the nests at the beginning of each experiment caused the ants to establish pheromone trails and actively move around the dish. I used this initial period of high activity to measure trail following behavior, reasoning that trail pheromones may cause two or more ants to move along the same path within the dish. *O. biroi* is a blind species and experiments from my laboratory indicate that their behavior is not influenced even by very bright light (Asaf Gal, personal communication), so it is unlikely that light or landscape cues cause correlation in the movement of the ants. Kronauer lab members have developed assays causing *O. biroi* to develop trails both in response to food and disturbance (Asaf Gal, personal communication), but I chose to use the disturbance-induced trails for this particular analysis because they are more robust.

For each ant, I measured the correlation between its own movement and the movement of the remaining ants in the colony during the first hour of the tracking experiment. As *O. biroi* have a tendency to walk along the edges of the dish, I discarded segments of trajectories close to the edge of the dish and included only segments where the ants moved faster than 1 mm/s continuously for at least 1 second and without contact with any other ant. I then computed a 2-D histogram, or density map, for each ant by counting the number of times one of the remaining positions in the 970x720 pixel original image fell into each bin of a 120x90 bin grid. I then computed the Pearson correlation coefficient between the density map of each ant and a density map constructed from the trajectories of all ants in the colony but the focal ant (Figure 3.4E). For each ant, the actual correlation coefficient provided an estimate of the correlation of movement of that ant with the actual movement of other ants in the colony, which presumably results from following pheromone trails.

As a baseline comparison, the density map of each ant was correlated with a randomized density map constructed by rotating the trajectories of all ants but the focal ant in the colony by a random angle around the center of the dish (Figure 3.4E). This randomized correlation coefficient provided an estimate of the correlation of the movement of that ant with the randomized movement of other ants in the colony. This residual correlation reflects the portion of the correlation that is due to non-local effects such as turning frequencies, linear and angular velocity dynamics, and radial preference for certain regions of the petri dish. After examining the data, two experimental colonies were excluded from the trail following analysis because they did not form clear trails during

the videos, resulting in Pearson correlation coefficients of approximately zero for all ants in the colony.

To measure wandering phenotypes, in each experiment I calculated the total distance traveled by each ant over the 24 hr video by computing the distances between all pairs of successive positions in meters in all identified trajectories. Time without contact was calculated as the total time each ant was identified in each experiment (since ants were only identifiable when they were separated from other ants). This provides a minimum estimate of the time without contact for each ant, given that it was also possible for ants to be spatially separated from other ants, yet unidentifiable, for example if their posture did not allow the detection of both tags.

Quantification and statistical analysis

Statistical details of all experiments can be found in the figure legends. Behavioral tracking and antennal lobe volume measurements were performed blindly with respect to genotype. Other analyses were not performed blindly with respect to genotype. Mixed model statistics were performed in R v 3.3.1 using the lmer function in the lme4 library as described previously (Bates et al. 2014, Ulrich & Schmid-Hempel 2012; Ulrich & Schmid-Hempel 2015). All other statistics were performed using GraphPad Prism 7. Normality was determined by D'Agostino-Pearson normality tests. Datasets used for ANOVA analyses had equal variance across treatments. Single groups were compared against a predicted mean using two-tailed Wilcoxon tests. Proportional data were compared between treatments using a Fisher exact test. Unpaired two-tailed Student's t-

tests or paired Wilcoxon tests were used to compare two groups, when appropriate, and two-way ANOVAs followed by Tukey's multiple comparisons test were used to compare more than two groups.

Data and software availability

Raw data and descriptions of the ants were used in each experiment is available in Table S3 in Trible et al. 2017. Raw Illumina sequencing reads are available through the National Center for Biotechnology Information Short Reads Archive. gRNA design and sequencing analyses were performed using the script crispralign.py from the genomepy package, available at https://github.com/oxpeter/genomepy.

Winged mutant methods

Whole genome resequencing

Four DNA libraries were used for whole-genome Illumina sequencing, C16, C1, WM #1, and WM #2. Adult ant tissues (pools of 5 individuals) were disrupted in a tissue lyser and genomic DNA was extracted using Qiagen's QIAmp DNA Micro Kit following manufacturer's recommendations. Sequencing coverage was approximately 80x, to ensure sufficient coverage to accurately detect heterozygosity genome-wide.

Microsatellite and CO1 sequencing

PCR amplification of *cytochrome oxidase I* (*COI*) was performed using primers as in Kronauer et al. (2012). Amplification was performed in a final volume of 12 µL using Applied Biosystems' AmpliTaq Gold Kit following manufacturers' recommendations.

Cycling profiles started with a denaturation at 94°C for 10 min, and then proceeded with 40 cycles of 94°C for 30 s, 55°C annealing for 30 s, 72°C extension for 30 s, finally followed by an extension of 72°C for 10 min.

Microsatellite reagents and cycling profiles followed Kronauer *et al.* 2012. Fragment analysis was performed by GeneWiz (Frederick, MD). Microsatellite analysis was performed using Peak Scanner (Applied Biosystems).

Morphometrics measurements

Individual ants were dissected to count their ovarioles, and then were pinned and imaged. Linear measurements were taken using the Fiji distribution of ImageJ (Figure 7.2) (Schindelin et al. 2012). Principle components analysis was conducted using Python and statistical analyses were conducted using Prism 7. For head length and petiole width, statistics were performed using the residuals from a linear regression with body length. This method was chosen to remove the effect of overall size and test whether size-matched winged mutants and wild-types differ in head length or petiole width.

Figure 7.2: Morphometric measurements. Wild-type (A), (B) and winged mutant (C), (D) ants. Note that wings have been removed in the winged mutants. Thirteen linear measures were used for morphometric analysis, extracted from images in side view (A), (C), top view (B), (D), and head view (not shown). Side view: head length, head height, Weber's length, thorax height, and length of 1st abdominal segment. Top view: thorax length, thorax width, petiole length, petiole width, post-petiole length, and post-petiole width. Head view: head length, head width.

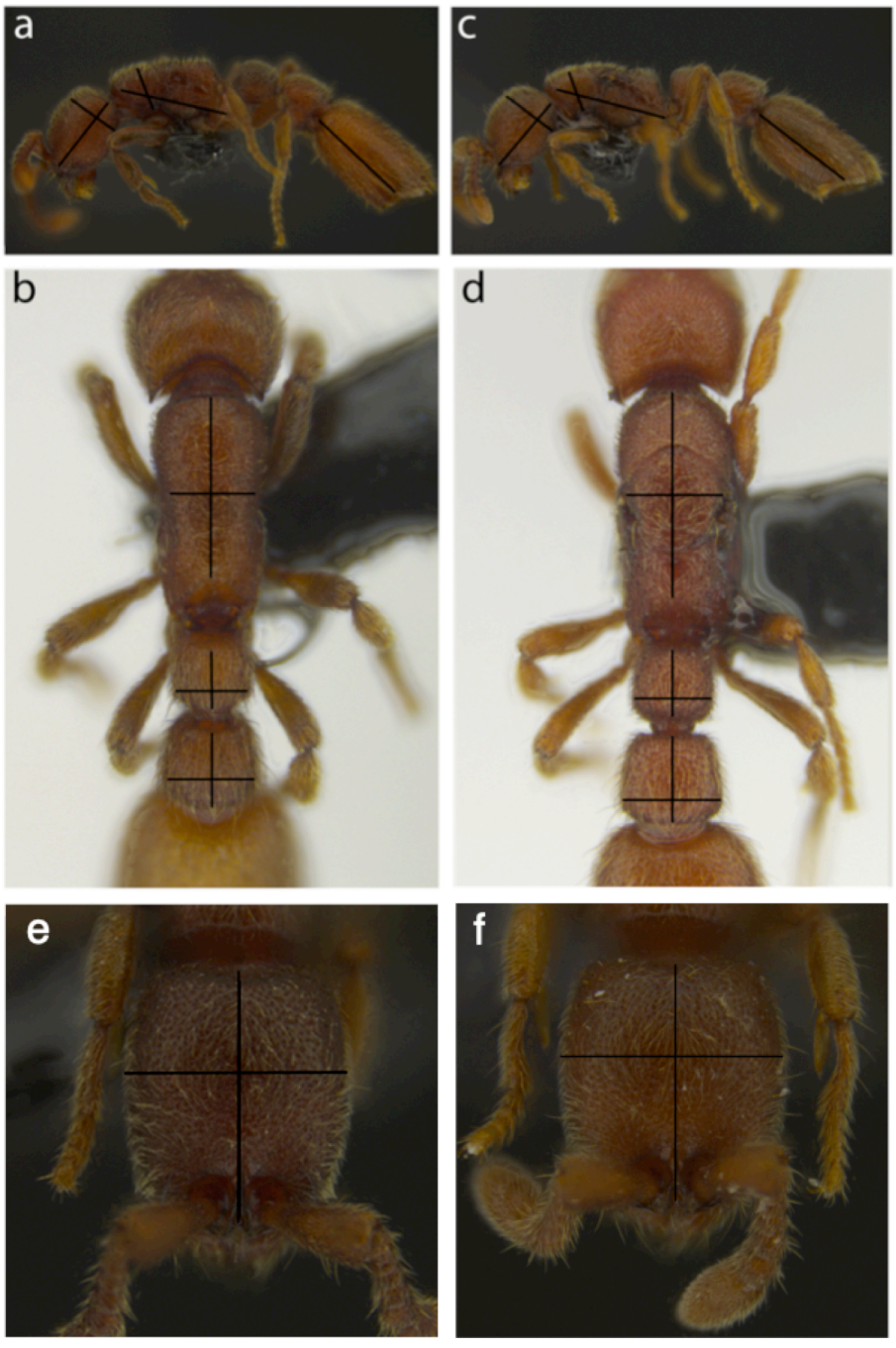
a
c
b
d
e
f

Fitness components

For all fitness datasets (Figure 5.4), extreme care was taken to specifically measure the effect of genotype (winged mutant versus wild-type) while controlling for age and rearing environment. Ants used in fitness experiments were produced in rearing units of 20 wild-type Line A chaperones established with approximately 20-40 experimental eggs. Eggs were zero to four days old at the time colonies were established. Experimental treatments were matched to control for cohort variation among the chaperone ants. Egg-laying rates were measured from five replicate winged mutant and wild-type colonies that were matched for age, colony size, and rearing environment (Figure 5.4A). Egg to pupa (Figure 5.4B) and eclosion (Figure 5.4C) survival was measured by establishing colonies with wild-type chaperones and varying frequencies of winged mutant and wild-type brood. Larval nursing efficiency (Figure 5.4D) was measured using colonies with 20 wild-type or winged mutant chaperones established with >24h old eggs. When these eggs hatched into larvae, colonies were reduced to 16 first-instar larvae. Developmental transitions were scored as the date that the majority of individuals had entered the respective developmental stage (1^{st} instar, 2^{nd} instar, 3^{rd} instar, 4^{th} instar, pre-pupal stage, pupal stage, and eclosion).

Foraging behavior

The foraging behavior pilot study was conducted comparing colonies of 16 callow ants (winged mutants and wild-types) that were obtained from the same cohort in a mixed stock colony. This assay was developed by Vikram Chandra. Briefly, ants are reared in a two-part dish with a 2cm diameter nest connected by a narrow opening to a 6.5cm

diameter foraging arena. Ants are placed in the nest (with the opening to the foraging arena sealed) and allowed to lay eggs. Once these eggs hatch into larvae, the seal is removed to allow foragers to leave the nest, and food is placed in the foraging arena. Videos of this foraging behavior and subsequent food retrieval were recorded and tracked as in *orco* Methods (above).

Long term coexistence study

All ants in the long-term coexistence study were reared under standard conditions, as in *Fitness components*. The number of winged mutants and wild-type ants was recorded once during the foraging phase of every colony cycle. I scored phenotypes by isolating all ants in the colony into groups of 10 individuals, then checking each ant under an Olympus stereoscope. By counting the same colony multiple times, I determined that I was able to score these phenotypes with 100% consistency.

RNASeq time course

For the RNASeq dataset, I selected six developmental time points: 6 day eggs (this approximately corresponds to gastrulation in *O. biroi*), 1st, 2nd, 3rd, and 4th instar larvae, and pre-pupae. Samples were reared as in the nursing behavior fitness experiment in Part 1, and were collected for RNA extraction within the first 24h of their respective developmental stage. In order to obtain enough RNA, I pooled four individuals for 6 day eggs and 1st instar larvae, and two individuals for the remaining time-points. To reduce the potential for false-positives in this dataset, I collected six winged mutant and six wild-type libraries for each time point. RNA extraction, sequencing methods, and differential

expression analyses were conducted as in Chandra et al. 2018. In brief, I aligned RNASeq reads to the genome assembly, used HTSeq to count the number of reads that mapped to each predicted gene in the current annotation, then used DESeq to identify the number of genes that were differentially expressed between winged mutants and wild-types at each developmental stage (Figure 5.8).

To distinguish true positives from false positives in this dataset, I conducted a combination test in which I measured the number of differentially expressed genes for every combination of 3 winged mutant and 3 wild-type versus 3 winged mutant and 3 wild-type libraries. This analysis indicated that up to 100 differentially-expressed genes can originate even in comparisons of randomized libraries, so I thus interpret numbers of DEGs less than 100 to be potential false positives.

REFERENCES

Abouheif E & Wray GA (2002) Evolution of the gene network underlying wing polyphenism in ants. Science 297:249–52.

Akhshabi S & Dovrolis C (2011) The evolution of layered protocol stacks leads to an hourglass-shaped architecture. ACM SIGCOMM Comput Commun Rev 41:206.

Alonge M, Soyk S, Ramakrishnan S, Wang X, Goodwin S, Sedlazeck FJ, Lippman ZB & Schatz MC (2019) Fast and accurate reference-guided scaffolding of draft genomes. bioRxiv:519637.

Altschul SF, Gish W, Miller W, Myers EW & Lipman DJ (1990) Basic local alignment search tool. J Mol Biol 215:403–410.

Anderson KE, Linksvayer T & Smith CR (2008) The causes and consequences of genetic caste determination in ants (Hymenoptera: Formicidae). Myrmecological News 11:119–132.

Aron S, Passera L & Keller L (1999) Evolution of social parasitism in ants: size of sexuals, sex ratio and mechanisms of caste determination. Proc R Soc B Biol Sci 266:173–177.

Aron S, Timmermans I & Pearcy M (2011) Ant queens adjust egg fertilization to benefit from both sexual and asexual reproduction. Biol Lett 7:571–3.

Asahina K, Pavlenkovich V & Vosshall LB (2008) The survival advantage of olfaction in a competitive environment. Curr Biol 18:1153–1155.

Barden P & Grimaldi DA (2016) Adaptive radiation in socially advanced stem-group ants from the Cretaceous. Curr Biol 26:515–521.

Barron J, Fleet D & Beauchemin S (1994) Performance of optical flow techniques. Int J

Comput Vis 12:43–77.

Bell WJ, Parsons C & Martinko EA (1972) Cockroach aggregation pheromones: analysis of aggregation tendency and species specificity (Orthoptera: Blattidae). J Kansas Entomol Soc 45:414–421.

Berdnik D, Chihara T, Couto A & Luo L (2006) Wiring stability of the adult *Drosophila* olfactory circuit after lesion. J Neurosci 26:3367–3376.

Bolte S & Cordelieres FP (2006) A guided tour into subcellular colocalisation analysis in light microscopy. J Microsc 224:13–232.

Bolton B (1986) Apterous females and shift of dispersal strategy in the *Monomorium salomonis*-group (Hymenoptera: Formicidae). J Nat Hist 20:267–272.

Bolton B & Ficken L (1994) *Identification guide to the ant genera of the world*, Cambridge, Massachusetts: Harvard University Press.

Bonasio R (2012) Emerging topics in epigenetics: ants, brains, and noncoding RNAs. Ann N Y Acad Sci 1260:14–23.

Bopp D, Saccone G & Beye M (2014) Sex determination in insects: variations on a common theme. Sex Dev 8:20–28.

Bourke AFG & Franks NR (1991) Alternative adaptations, sympatric speciation and the evolution of parasitic, inquiline ants. Biol J Linn Soc 43:157–178.

Boven J (1970) Le polymorphisme des ouvrières de *Megaponera foetens* Mayr (Hymenoptera: Formicidae). Publ van het Natuurhistorisch Genoot Limbg 20:5–9.

Brenner S (2009) In the beginning was the worm... Genetics 182:413–415.

Brian M V. (1953) Brood-rearing in relation to worker number in the ant *Myrmica*. Physiol Zool 26:355–366.

Brian M V. (1973) Caste control through worker attack in the ant *Myrmica*. Insectes Soc 20:87–102.

Brian M V. (1979) Caste differentiation and division of labor. In *Social Insects: Volume 1*. pp. 121–222.

Brian M V. (1974) Caste differentiation in *Myrmica rubra*: the role of hormones. J Insect Physiol 20:1351–1365.

Brian M V. (1955) Studies of caste differentiation in *Myrmica rubra* L.: 2. The growth of workers and intercastes. Insectes Soc 2:1–34.

Brian M V. (1956) Studies of caste differentiation in *Myrmica rubra* L.: 4. Controlled larval nutrition. Insectes Soc 3:369–394.

Brian M V. (1973b) Temperature choice and its relevance to brood survial and caste determination in the ant *Myrmica rubra* L. Physiol Zool 46:245–252.

Buschinger A (2009) Social parasitism among ants: a review (Hymenoptera: Formicidae). Myrmecological News 12:219–235.

Buschinger A (1990) Sympatric speciation and radiative evolution of socially parasitic ants - heretic hypotheses and their factual background. Z. Zool. Syst. Evolut. 20:241-260.

Buschinger A & Winter U (1978) Echte Arbeiterinnen, fertile Arbeiterinnen und sterile Wirtsweibchen in Volkern der dulotischen Ameise *Harpagoxenus sublaevis* (Nyl.) Hym., Form. Insectes Soc 25:63–78.

Butterwick JA, del Mármol J, Kim KH, Kahlson MA, Rogow JA, Walz T & Ruta V (2018) Cryo-EM structure of the insect olfactory receptor Orco. Nature 560:447–452.

Carroll SB, Grenier JK & Weatherbee SD (2001) *From DNA to diversity*, Oxford, United Kingdom: Blackwell Publishing Ltd.

Chandra V, Fetter-Pruneda I, Oxley PR, Ritger AL, McKenzie SK, Libbrecht R & Kronauer DJC (2018) Social regulation of insulin signaling and the evolution of eusociality in ants. Science 2:398–402.

Chiang A, Priya R, Ramaswami M, Vijayraghavan K & Rodrigues V (2009) Neuronal activity and Wnt signaling act through Gsk3-beta to regulate axonal integrity in mature *Drosophila* olfactory sensory neurons. Development 136:1273–1282.

Cressler CE, McLeod D V., Rozins C, Van Den Hoogen J & Day T (2016) The adaptive evolution of virulence: A review of theoretical predictions and empirical tests. Parasitology 143:915–930.

DeGennaro M, McBride CS, Seeholzer L, Nakagawa T, Dennis EJ, Goldman C, Jasinskiene N, James AA & Vosshall LB (2013) *orco* mutant mosquitoes lose strong preference for humans and are not repelled by volatile DEET. Nature 498:487–491.

Depickère S, Fresneau D & Deneubourg JL (2004) Dynamics of aggregation in *Lasius niger* (Formicidae): Influence of polyethism. Insectes Soc 51:81–90.

Dippel S (2016) *Comprehensive morphological and transcriptomic analysis of the chemosensory system in the red flour beetle (*Tribolium castaneum*)*. Georg-August-University Gottingen.

Dobata S, Sasaki T, Mori H, Hasegawa E, Shimada M & Tsuji K (2009) Cheater genotypes in the parthenogenetic ant *Pristomyrmex punctatus*. Proc R Soc B Biol Sci 276:567–574.

Dobritsa AA, Van Der Goes Van Naters W, Warr CG, Steinbrecht RA & Carlson JR

(2003) Integrating the molecular and cellular basis of odor coding in the *Drosophila* antenna. Neuron 37:827–841.

Douwes P, Jessen K & Buschinger A (1988) *Epimyrma alderzi* sp. n. (Hymenoptera: Formicidae) from Greece: morphology and life history. Entomol Scand 19:239–249.

Dyar HG & Rhinebeck NY (1890) The number of molts of lepidopterous larvae. Psyche 5:420–422.

Eddy S (1998) Profile hidden Markov models. Bioinformatics 14:755–763.

Elmes G (1976) Some observations on the microgyne form of *Myrmica rubra* L. (Hymenoptera, Formicidae). Insectes Soc 23:3–22.

Emlen DJ (1996) Artificial selection on horn length body size allometry in the horned beetle *Onthophagus acuminatus* (Coleoptera: Scarabaeidae). Evolution 50:1219–1230.

Engsontia P, Sanderson AP, Cobb M, Walden KKO, Robertson HM & Brown S (2008) The red flour beetle's large nose: An expanded odorant receptor gene family in *Tribolium castaneum*. Insect Biochem Mol Biol 38:387–397.

Favé M-J, Johnson R., Cover S, Handschuh S, Metscher BD, Müller GB, Gopalan S, Abouheif E, Muller G, Gopalan S, et al. (2015) Climate change on Sky Islands drives novelty in a core developmental gene network and its phenotype. BMC Evol Biol 15:183.

Fjerdingstad EJ & Crozier RH (2006) The evolution of worker caste diversity in social insects. Am Nat 167:390–400.

Flanagan D & Mercer AR (1989) An atlas and 3-D reconstruction of the antennal lobes in the worker honey bee, *Apis mellifera* L. (Hymenoptera: Apidae). Int J Insect

Morphol Embryol 18:145–159.

Fletcher M, Dornhaus A & Shin MC (2011) Multiple ant tracking with global foreground maximization and variable target proposal distribution. IEEE Work Appl Comput Vis:570–576.

Folmer O, Black M, Hoeh W, Lutz R & Vrijenhoek R (1994) DNA primers for amplification of *mitochondrial cytochrome c oxidase subunit I* from diverse metazoan invertebrates. Mol Mar Biol Biotechnol 3:294–299.

Friedlander T, Mayo AE, Tlusty T & Alon U (2015) Evolution of bow-tie architectures in biology. PLoS Comput Biol 11:1–19.

Fu Y, Foden J, Khayter C, Maeder ML, Reyon D, Joung JK & Sander JD (2013) High-frequency off-target mutagenesis induced by CRISPR-Cas nucleases in human cells. Nat Biotechnol 31:822–826.

Gascuel J & Masson C (1991) Developmental study of afferented and deafferented bee antennal lobes. J Neurobiol 22:795–810.

Gospocic J, Shields EJ, Glastad KM, Rgen Liebig J, Reinberg D, Correspondence RB, Lin Y, Penick CA, Yan H, Mikheyev AS, et al. (2017) The neuropeptide corazonin controls social behavior and caste identity in ants. Cell 170:748-752.e12.

Gotoh A, Sameshima S, Tsuji K, Matsumoto T & Miura T (2005) Apoptotic wing degeneration and formation of an altruism-regulating glandular appendage (gemma) in the ponerine ant *Diacamma* sp. from Japan (Hymenoptera, Formicidae, Ponerinae). Dev Genes Evol 215:69–77.

Gotoh H, Cornette R, Koshikawa S, Okada Y, Lavine LC, Emlen DJ & Miura T (2011) Juvenile hormone regulates extreme mandible growth in male stag beetles. PLoS

One 6:1–5.

Gotoh H, Miyakawa H, Ishikawa A, Ishikawa Y, Sugime Y, Emlen DJ, Lavine LC & Miura T (2014) Developmental link between sex and nutrition; *doublesex* regulates sex-specific mandible growth via juvenile hormone signaling in stag beetles. PLoS Genet 10:1–9.

Gotwald WH (1995) *Army ants: the biology of social predation*, Ithica, New York: Cornell University Press.

Green DA & Extavour CG (2014) Insulin signalling underlies both plasticity and divergence of a reproductive trait in *Drosophila*. Proc R Soc B 281:20132673.

Grüter C & Keller L (2016) Inter-caste communication in social insects. Curr Opin Neurobiol 38:6–11.

Hall ADW & Smith IC (1953) Atypical forms of the wingless worker and the winged female in *Monomorium pharaonis* (L.). (Hymenoptera: Formicidae). Evolution 7:127–135.

Hart LM & Tschinkel WR (2011) A seasonal natural history of the ant, *Odontomachus brunneus*. Insectes Soc 59:45–54.

Hartfelder K & Emlen DJ (2012) Endocrine control of insect polyphenism. In *Insect Endocrinology*. pp. 464–522.

Haskins CP & Whelden RM (1965) "Queenlessness," worker subship, and colony versus population structure in the formicid genus *Rhytidoponera*. Psyche 72:87–112.

Heinze J & Buschinger A (1989) Queen polymorphism in *Leptothorax spec.A*: its genetic and ecological background (Hymenptera: Formicidae). Insect Soc 36:139–155.

Heinze J, Buschinger A, Poettinger T & Suefuji M (2015) Multiple convergent origins of

workerlessness and inbreeding in the socially parasitic ant genus *Myrmoxenus*. PLoS One:1–10.

Heinze J & Foitzik S (2009) The evolution of queen numbers in ants: from one to many and back. In *Organization of insect societies: from genome to sociocomplexity.* pp. 26–50.

Hiruma K & Kaneko Y (2013) Hormonal regulation of insect metamorphosis with special reference to juvenile hormone biosynthesis. Curr Top Dev Biol 103:73–100.

Hölldobler B (1982) Communication, raiding behavior and prey storage in *Cerapachys* (Hymenoptera; Formicidae). Psyche 89:3–23.

Hölldobler B & Wilson EO (2009) *The superorganism: the beauty, elegance, and strangeness of insect societies.*, New York, N.Y.: WW Norton & Company.

Honegger B, Galic M, Köhler K, Wittwer F, Brogiolo W, Hafen E & Stocker H (2008) *Imp-L2*, a putative homolog of vertebrate IGF-binding protein 7, counteracts insulin signaling in *Drosophila* and is essential for starvation resistance. J Biol 7:10.

Honěk A (1993) Intraspecific variation in body size and fecundity in insects: a general relationship. Oikos 66:483.

Huang MH & Wheeler DE (2011) Colony demographics of rare soldier-polymorphic worker caste systems in *Pheidole* ants (Hymenoptera, Formicidae). Insectes Soc 58:539–549.

Imai HT, Baroni Urbani C, Kubota M, Sharma GP, Narasimhanna MH, Das BC, Sharma AK, Sharma A, Deodikar GB, Vaidya VG, et al. (1984) Karyological survey of Indian ants. Jpn J Genet 59:1–32.

Ito F, Sugiura N & Higashi S (1994) Worker polymorphism in the red-head bulldog ant

(Hymenoptera: Formicidae), with description of nest structure and colony composition. Ann Entomol Soc Am 87:337–341.

Jaffé R, Kronauer DJC, Kraus FB, Boomsma JJ & Moritz RFA (2007) Worker caste determination in the army ant *Eciton burchellii*. Biol Lett 3:513–6.

Jhaveri D & Rodrigues V (2002) Sensory neurons of the Atonal lineage pioneer the formation of glomeruli within the adult *Drosophila* olfactory lobe. Development 129:1251–1260.

Jones WD, Nguyen TAT, Kloss B, Lee KJ & Vosshall LB (2005) Functional conservation of an insect odorant receptor gene across 250 million years of evolution. Curr Biol 15:119–121.

Katoh K & Standley DM (2013) MAFFT multiple sequence alignment software version 7: Improvements in performance and usability. Mol Biol Evol 30:772–780.

Kelber C, Rössler W, Roces F & Kleineidam CJ (2009) The antennal lobes of fungus-growing ants (Attini): Neuroanatomical traits and evolutionary trends. Brain Behav Evol 73:273–284.

Keller RA, Peeters C & Beldade P (2014) Evolution of thorax architecture in ant castes highlights trade-off between flight and ground behaviors. Elife 3:e01539.

Kennedy CH & Dennis CA (1937) New ants from Ohio and Indiana, *Formica prociliata*, *F. querquetulana*, *F. postoculata* and *F. lecontei*, (Formicidae: Hymenoptera). Ann Entomol Soc Am 30:531–544.

Kijimoto T & Moczek AP (2016) Hedgehog signaling enables nutrition-responsive inhibition of an alternative morph in a polyphenic beetle. Proc Natl Acad Sci 113:5982–5987.

Kistler KE, Vosshall LB & Matthews BJ (2015) Genome engineering with CRISPR-Cas9 in the mosquito *Aedes aegypti*. Cell Rep 11:51–60.

Klein A, Schultner E, Lowak H, Schrader L, Heinze J, Holman L & Oettler J (2016) Evolution of social insect polyphenism facilitated by the sex differentiation cascade. PLoS Genet 12:1–16.

Kohno H, Suenami S, Takeuchi H, Sasaki T & Kubo T (2016) Production of knockout mutants by CRISPR/Cas9 in the European honeybee, *Apis mellifera* L. Zoolog Sci 33:505–512.

Kollmann M, Minoli S, Bonhomme J, Homberg U, Schachtner J, Tagu D & Anton S (2011) Revisiting the anatomy of the central nervous system of a hemimetabolous model insect species: The pea aphid *Acyrthosiphon pisum*. Cell Tissue Res 343:343–355.

Koto A, Mersch D, Hollis B & Keller L (2015) Social isolation causes mortality by disrupting energy homeostasis in ants. Behav Ecol Sociobiol 69:583–591.

Koutroumpa FA, Monsempes C, François M-C, de Cian A, Royer C, Concordet J-P & Jacquin-Joly E (2016) Heritable genome editing with CRISPR/Cas9 induces anosmia in a crop pest moth. Sci Rep 6:1–9.

Kramer JM, Slade JD & Staveley BE (2008) *foxo* is required for resistance to amino acid starvation in *Drosophila*. Genome 51:668–672.

Kronauer D, Pierce N & Keller L (2012) Asexual reproduction in introduced and native populations of the ant *Cerapachys biroi*. Mol Ecol 21:5221–5235.

Kronauer DJC, Tsuji K, Pierce NE & Keller L (2013) Non–nest mate discrimination and clonal colony structure in the parthenogenetic ant *Cerapachys biroi*. Behav Ecol.

Kronenberg ZN, Hall RJ, Hiendleder S, Smith TPL, Sullivan ST, Williams JL & Kingan SB (2018) FALCON-Phase: Integrating PacBio and Hi-C data for phased diploid genomes. bioRxiv:327064.

Kuhn A, Darras H & Aron S (2018) Phenotypic plasticity in an ant with strong caste – genotype association. Biol Lett 14:20170705.

Kumar S, Stecher G & Tamura K (2016) MEGA7: Molecular Evolutionary Genetics Analysis version 7.0 for bigger datasets. Mol Biol Evol 33:1870–1874.

Laissue PP, Reiter C, Hiesinger PR, Halter S, Fischbach KF & Stocker RF (1999) Three-dimensional reconstruction of the antennal lobe in *Drosophila melanogaster*. J Comp Neurol 405:543–552.

Laissue PP & Vosshall LB (2008) The olfactory sensory map in *Drosophila*. In G. M. Technau, ed. *Brain development in Drosophila melanogaster*. Landes Bioscience and Springer Science+Business Media, pp. 102–114.

Larsson MC, Domingos AI, Jones WD, Chiappe ME, Amrein H & Vosshall LB (2004) *Or83b* encodes a broadly expressed odorant receptor essential for *Drosophila* olfaction. Neuron 43:703–714.

Leimar O, Hartfelder K, Laubichler MD & Page RE (2012) Development and evolution of caste dimorphism in honeybees - a modeling approach. Ecol Evol 2:3098–3109.

Leonhardt SD, Menzel F, Nehring V & Schmitt T (2016) Ecology and evolution of communication in social insects. Cell 164:1277–1287.

Leppänen J, Seppä P, Vepsäläinen K & Savolainen R (2016) Mating isolation between the ant *Myrmica rubra* and its microgynous social parasite. Insectes Soc 63:79–86.

Li Y, Zhang J, Chen D, Yang P, Jiang F, Wang X & Kang L (2016) CRISPR/Cas9 in

locusts: Successful establishment of an olfactory deficiency line by targeting the mutagenesis of an *odorant receptor co-receptor* (*Orco*). Insect Biochem Mol Biol 79:27–35.

Libbrecht R, Corona M, Wende F, Azevedo DO, Serrão JE & Keller L (2013) Interplay between insulin signaling, juvenile hormone, and vitellogenin regulates maternal effects on polyphenism in ants. Proc Natl Acad Sci 110:11050–5.

Linksvayer T (2007) Ant species differences determined by epistasis between brood and worker genomes. PLoS One 10:e994.

Linksvayer T, Busch JW & Smith CR (2013) Social supergenes of superorganisms: Do supergenes play important roles in social evolution? BioEssays news Rev Mol Cell Dev Biol 35:683–689.

Linksvayer T, Kaftanoglu O, Akyol E, Blatch S, Amdam G V & Page RE (2011) Larval and nurse worker control of developmental plasticity and the evolution of honey bee queen-worker dimorphism. J Evol Biol 24:1939–48.

Linksvayer T & Wade MJ (2005) The evolutionary origin and elaboration of sociality in the aculeate Hymenoptera: maternal effects, sib-social effects, and heterochrony. Q Rev Biol 80:317–336.

Lobbia S, Niitsu S & Fujiwara H (2003) Female-specific wing degeneration caused by ecdysteroid in the Tussock Moth, *Orgyia recens*: hormonal and developmental regulation of sexual dimorphism. J Insect Sci 3:11.

Londe S, Monnin T, Cornette R, Debat V, Fisher BL & Molet M (2015) Phenotypic plasticity and modularity allow for the production of novel mosaic phenotypes in ants. Evodevo 6:36.

Malun D, Oland LA & Tolbert LP (1994) Uniglomerular projection neurons participate in early development of olfactory glomeruli in the moth *Manduca sexta*. J Comp Neurol 350:1–22.

Maynard Smith J & Szathmary E (1997) *The major transitions in evolution*, Oxford University Press.

McGlynn TP, Diamond SE & Dunn RR (2012) Tradeoffs in the evolution of caste and body size in the hyperdiverse ant genus *Pheidole*. PLoS One 7:e48202.

McKenzie SK, Fetter-Pruneda I, Ruta V & Kronauer DJC (2016) Transcriptomics and neuroanatomy of the clonal raider ant implicate an expanded clade of odorant receptors in chemical communication. Proc Natl Acad Sci 113:14091–14096.

McKenzie SK & Kronauer DJC (2018) The genomic architecture and molecular evolution of ant odorant receptors. Genome Res 28:1757–1765.

Mersch DP, Crespi A & Keller L (2013) Tracking individuals shows spatial fidelity is a key regulator of ant social organization. Science 360:1090–1093.

Miyazaki S, Murakami T, Azuma N, Higashi S & Miura T (2005) Morphological differences among three female castes: Worker, queen, and intermorphic queen in the ant *Myrmecina nipponica* (Formicidae: Myrmicinae). Sociobiology 46:363–374.

Miyazaki S, Murakami T, Kubo T, Azuma N, Higashi S & Miura T (2010) Ergatoid queen development in the ant *Myrmecina nipponica*: modular and heterochronic regulation of caste differentiation. Proc Biol Sci 277:1953–61.

Molet M, Maicher V & Peeters C (2014) Bigger helpers in the ant *Cataglyphis bombycina*: Increased worker polymorphism or novel soldier caste? PLoS One 9.

Molet M, Peeters C & Fisher BL (2007) Winged queens replaced by reproductives

smaller than workers in *Mystrium* ants. Naturwissenschaften 94:280–287.

Molet M, Wheeler DE & Peeters C (2012) Evolution of novel mosaic castes in ants: Modularity, phenotypic plasticity, and colonial buffering. Am Nat 180:328–341.

Morgan ED (2009) Trail pheromones of ants. Physiol Entomol 34:1–17.

Murdock TC & Tschinkel WR (2015) The life history and seasonal cycle of the ant, *Pheidole morrisi* Forel, as revealed by wax casting. Insectes Soc 62:265–280.

Nakanishi A, Nishino H, Watanabe H, Yokohari F & Nishikawa M (2010) Sex-specific antennal sensory system in the ant *Camponotus japonicus*: glomerular organizations of antennal lobes. J Comp Neurol 518:2186–2201.

Niitsu S, Toga K, Tomizuka S, Maekawa K, Machida R & Kamito T (2014) Ecdysteroid-induced programmed cell death is essential for sex-specific wing degeneration of the wingless-female winter moth. PLoS One 9:3–9.

Nijhout HF & Emlen DJ (1998) Competition among body parts in the development and evolution of insect morphology. Proc Natl Acad Sci 95:3685–3689.

Nonacs P & Tobin JE (1992) Selfish larvae: development and the evolution of parasitic behavior in the Hymenoptera. Evolution 46:1605–1620.

O'Neal J & Markin GP (1975) The larval instars of the imported fire ant, *Solenopsis invicta* Buren (Hymenoptera: Formicidae). J Kansas Entomol Soc 48:141–151.

Ohkawara K, Ito F & Higashi S (1993) Production and reproductive function of intercastes in *Myrmecina graminicola nipponica* colonies (Hymenoptera: Formicidae). Insectes Soc 40:1–10.

Okada Y, Plateaux L & Peeters C (2013) Morphological variability of intercastes in the ant *Temnothorax nylanderi*: pattern of trait expression and modularity. Insectes Soc

60:319–328.

Oster GF & Wilson EO (1978) *Caste and ecology in the social insects*, Princeton, New Jersey: Princeton University Press.

Oxley PR, Ji L, Fetter-pruneda I, McKenzie SK, Li C, Hu H, Zhang G & Kronauer DJCC (2014) The genome of the clonal raider ant *Cerapachys biroi*. Curr Biol 24:451–458.

Peeters C (2012) Convergent evolution of wingless reproductives across all subfamilies of ants, and sporadic loss of winged queens (Hymenoptera: Formicidae). Myrmecological News 16:75–91.

Peeters C & Crozier RH (1988) Caste and reproduction in ants: not all mated egg-layers are "queens." Psyche 95:283–288.

Peeters C & Ito F (2015) Wingless and dwarf workers underlie the ecological success of ants (Hymenoptera: Formicidae). Myrmecological News 21:117–130.

Peeters C, Lin CC, Quinet Y, Martins Segundo G & Billen J (2013) Evolution of a soldier caste specialized to lay unfertilized eggs in the ant genus *Crematogaster* (subgenus *Orthocrema*). Arthropod Struct Dev 42:257–264.

Peeters CP (1991) Ergatoid queens and intercastes in ants: Two distinct adult forms which look morphologically intermediate between workers and winged queens. Insectes Soc 38:1–15.

Penick CA & Liebig J (2012) Regulation of queen development through worker aggression in a predatory ant. Behav Ecol 23:992–998.

Penick CA, Prager SS & Liebig J (2012) Juvenile hormone induces queen development in late-stage larvae of the ant *Harpegnathos saltator*. J Insect Physiol 58:1643–1649.

Penick CA & Liebig J (2017) A larval 'princess pheromone' identifies future ant queens

based on their juvenile hormone content. Anim Behav 128:33–40.

Pitts RJ, Fox N & Zwiebel LJ (2004) A highly conserved candidate chemoreceptor expressed in both olfactory and gustatory tissues in the malaria vector *Anopheles gambiae*. Proc Natl Acad Sci 101:5058–5063.

Purcell J, Brelsford A, Wurm Y, Perrin N & Chapuisat M (2014) Convergent genetic architecture underlies social organization in ants. Curr Biol 24:2728–2732.

Rabeling C, Messer S, Lacau S, do Nascimento IC, Bacci M & Delabie JHC (2019) *Acromyrmex fowleri*: a new inquiline social parasite species of leaf-cutting ants from South America, with a discussion of social parasite biogeography in the Neotropical region. Insectes Soc.

Rabeling C, Schultz TR, Bacci M & Bollazzi M (2015) *Acromyrmex charruanus*: a new inquiline social parasite species of leaf-cutting ants. Insectes Soc 62:335–349.

Rabeling C, Schultz TR, Pierce NE & Bacci M (2014) A social parasite evolved reproductive isolation from its fungus-growing ant host in sympatry. Curr Biol 24:2047–2052.

Rajakumar R, Koch S, Couture M, Favé MJ, Lillico-Ouachour A, Chen T, De Blasis G, Rajakumar A, Ouellette D & Abouheif E (2018) Social regulation of a rudimentary organ generates complex worker-caste systems in ants. Nature 562:574–577.

Rajakumar R, Mauro DS & Dijkstra M (2012) Ancestral developmental potential facilitates parallel evolution in ants. Science 79.

Reid W & O'Brochta DA (2016) Applications of genome editing in insects. Curr Opin Insect Sci 13:43–54.

Richard F-J & Hunt JH (2013) Intracolony chemical communication in social insects.

Insectes Soc 60:275–291.

Robertson HM, Gadau J & Wanner KW (2010) The insect chemoreceptor superfamily of the parasitoid jewel wasp *Nasonia vitripennis*. Insect Mol Biol 19:121–136.

Robertson HM, Warr CG & Carlson JR (2003) Molecular evolution of the insect chemoreceptor gene superfamily in *Drosophila melanogaster*. Proc Natl Acad Sci 100:14537–14542.

Rosenweig ML (1978) Competitive speciation. Biol J Linn Soc 10:275–289.

Ross KG & Keller L (1998) Genetic control of social organization in an ant. Proc Natl Acad Sci 95:14232–14237.

Roth A, Vleurinck C, Netschitailo O, Bauer V, Otte M, Kaftanoglu O, Page RE & Id MB (2019) A genetic switch for worker nutrition-mediated traits in honeybees. PLoS Biol 17:e3000171.

Sato K, Pellegrino M, Nakagawa Takao, Nakagawa Tatsuro, Vosshall LB & Touhara K (2008) Insect olfactory receptors are heteromeric ligand-gated ion channels. Nature 452:1002–1006.

Savolainen R & Vepsalainen K (2003) Sympatric speciation through intraspecific social parasitism. Proc Natl Acad Sci 100:7169–7174.

Schindelin J, Arganda-Carreras I, Frise E, Kaynig V, Longair M, Pietzsch T, Preibisch S, Rueden C, Saalfeld S, Schmid B, et al. (2012) Fiji: an open-source platform for biological-image analysis. Nat Methods 9:676–682.

Schneirla T (1971) *Army ants: A study in social organization*, San Francisco, CA: W H Freeman.

Schulte C, Theilenberg E, Müller-Borg M, Gempe T & Beye M (2014) Highly efficient

integration and expression of piggyBac-derived cassettes in the honeybee (*Apis mellifera*). Proc Natl Acad Sci 111:9003–9008.

Schwander T, Humbert JY, Brent CS, Cahan SH, Chapuis L, Renai E & Keller L (2008) Maternal effect on female caste determination in a social insect. Curr Biol 18:265–269.

Schwander T, Libbrecht R & Keller L (2014) Supergenes and Complex Phenotypes. Curr Biol 24:288–294.

Schwander T, Lo N, Beekman M, Oldroyd BP & Keller L (2010) Nature versus nurture in social insect caste differentiation. Trends Ecol Evol 25:275–82.

Simpson SJ, Sword G & Lo N (2011) Polyphenism in insects. Curr Biol 21:R738–R749.

Smadja C, Shi P, Butlin RK & Robertson HM (2009) Large gene family expansions and adaptive evolution for odorant and gustatory receptors in the pea aphid, *Acyrthosiphon pisum*. Mol Biol Evol 26:2073–2086.

Smith CD, Zimin A, Holt C, Abouheif E, Benton R, Cash E, Croset V, Currie CR, Elhaik E, Elsik CG, et al. (2011) Draft genome of the globally widespread and invasive Argentine ant (*Linepithema humile*). Proc Natl Acad Sci 108:5673–5678.

Smith CR, Helms Cahan S, Kemena C, Brady SG, Yang W, Bornberg-Bauer E, Eriksson T, Gadau J, Helmkampf M, Gotzek D, et al. (2015) How do genomes create novel phenotypes? Insights from the loss of the worker caste in ant social parasites. Mol Biol Evol 32:2919–2931.

Smith CR, Smith CD, Robertson HM, Helmkampf M, Zimin A, Yandell M, Holt C, Hu H, Abouheif E, Benton R, et al. (2011) Draft genome of the red harvester ant *Pogonomyrmex barbatus*. Proc Natl Acad Sci 108:5667–5672.

Stamatakis A (2006) RAxML-VI-HPC: Maximum likelihood-based phylogenetic analyses with thousands of taxa and mixed models. Bioinformatics 22:2688–2690.

Stolle E, Pracana R, Howard P, Paris CI, Brown SJ, Castillo-Carrillo C, Rossiter SJ & Wurm Y (2019) Degenerative expansion of a young supergene. Mol Biol Evol 36:553–561.

Sumner S, Nash DR & Boomsma JJ (2003) The adaptive significance of inquiline parasite workers. Proc Biol Sci 270:1315–1322.

Suzzoni L & Passera JP (1979) Le role de la reine de *Pheidole pallidula* (Nyl.) ans la sexualisation du couvain apres traitement par l'hormone juvenile. Insectes Soc 26:343–353.

Tang HY, Smith-Caldas MSB, Driscoll M V., Salhadar S & Shingleton AW (2011) *FOXO* regulates organ-specific phenotypic plasticity in *Drosophila*. PLoS Genet 7.

Terrapon N, Li C, Robertson HM, Ji L, Meng X, Booth W, Chen Z, Childers CP, Glastad KM, Gokhale K, et al. (2014) Molecular traces of alternative social organization in a termite genome. Nat Commun 5:1–12.

Teseo S, Châline N, Jaisson P & Kronauer DJC (2014) Epistasis between adults and larvae underlies caste fate and fitness in a clonal ant. Nat Commun 5.

Trible W & Kronauer DJC (2017) Caste development and evolution in ants: it's all about size. J Exp Biol 220:53–62.

Trible W, Olivos-Cisneros L, Mckenzie SK, Saragosti J, Chang N-C, Matthews BJ, Oxley PR & Kronauer DJC (2017) *orco* mutagenesis causes loss of antennal lobe glomeruli and impaired social behavior in ants. Cell 170:727–732.

Tschinkel WR (2006) *The fire ants*, Cambridge, Massachusetts: Harvard University

Press.

Tsuji K & Dobata S (2011) Social cancer and the biology of the clonal ant *Pristomyrmex punctatus* (Hymenoptera: Formicidae). Myrmecological News 15:91–99.

Tsuji K, Furukawa T, Kinomura K, Takamine H & Yamauchi K (1991) The caste system of the dolichoderine ant *Technomyrmex albipes* (Hymenoptera: Formicidae): morphological description of queens, workers and reproductively active intercastes. Insectes Soc 38:413–422.

Tu M-P & Tatar M (2003) Juvenile diet restriction and the aging and reproduction of adult Drosophila melanogaster. Aging Cell 2:327–333.

Tulloch GS (1930) An unusual nest of *Pogonomyrmex*. Psyche (New York) 37:61–70.

Ulrich Y, Saragosti J, Tokita CK, Tarnita CE & Kronauer DJC (2018) Fitness benefits and emergent division of labour at the onset of group living. Nature 560:635-640.

Ulrich Y & Schmid-Hempel P (2012) Host modulation of parasite competition in multiple infections. Proc R Soc B Biol Sci 279:2982–2989.

Ulrich Y & Schmid-Hempel P (2015) The distribution of parasite strains among hosts affects disease spread in a social insect. Infect Genet Evol 32:348–353.

Urbani BC (1998) The number of castes in ants, where major is smaller than minor and queens wear the shield of the soldiers. Insectes Soc 45:315–333.

Urbani CB & Passera L (1996) Origin of ant soldiers. Nature 383:223–223.

Wagner GP (2014) *Homology, genes, and evolutionary innovation*, Princeton, New Jersey: Princeton University Press.

Wan Y, Otsuna H, Chien C-B & Hansen C (2012) FluoRender: An application of 2D image space methods for 3D and 4D confocal microscopy data visualization in

neurobiology research. IEEE Pacific Vis Symp:201–208.

Wang J, Wurm Y, Nipitwattanaphon M, Riba-Grognuz O, Huang Y-C, Shoemaker D & Keller L (2013) A Y-like social chromosome causes alternative colony organization in fire ants. Nature 493:664–668.

Ward PS (1996) A new workerless social parasite in the ant genus *Pseudomyrmex* (Hymenoptera: Formicidae), with a discussion of the origin of social parasitism in ants. Syst Entomol 21:253–263.

Ward PS (1997) Ant soldiers are not modified queens. Nature 385:494–495.

Warner MR, Mikheyev A & Linksvayer TA (2016) Genomic signature of kin selection in an ant with obligately sterile workers. Mol Biol Evol 34:072496.

Warner MR, Qiu L, Holmes MJ, Mikheyev AS & Timothy A (2018) The convergent evolution of caste in ants and honey bees is based on a shared core of ancient reproductive genes and many plastic genes. bioRxiv 454645.

West-Eberhard MJ (2003) *Developmental plasticity and evolution*, Oxford, United Kingdom: Oxford University Press.

Wheeler D (1990) The developmental basis of worker polymorphism in fire ants. J Insect Physiol.

Wheeler DE (1991) The developmental basis of worker caste polymorphism in ants. Am Nat 138:1218–1238.

Wheeler GC & Wheeler J (1976) Ant larvae: review and synthesis. Mem Ent Soc Washingt 7.

Wheeler WM (1905) Worker ants with vestiges of wings. Bull Am Mus Nat Hist 21:405–408.

Wilson EO (1953) The origin and evolution of polymorphism in ants. Q Rev Biol 28:136–156.

Wilson EO (1984) Tropical social parasites in the ant genus *Pheidole*, with an analysis of the anatomical parasitic syndrome (Hymenoptera: Formicidae). Insectes Soc 31:316–334.

Wilson EO & Hölldobler B (1990) *The ants*, Cambridge, Massachusetts: Harvard University Press.

Wright AV, Nuñez JK & Doudna JA (2016) Biology and applications of CRISPR systems: Harnessing nature's toolbox for genome engineering. Cell 164:29–44.

Xu H-J, Xue J, Lu B, Zhang X-C, Zhuo J, He S, Ma X-F, Jiang Y, Fan H, Xu J, et al. (2015) Two insulin receptors determine alternative wing morphs in planthoppers. Nature 519:464–467.

Yan H, Opachaloemphan C, Mancini G, Rgen Liebig J, Reinberg D, Desplan C, Yang H, Gallitto M, Mlejnek J, Leibholz A, et al. (2017) An engineered *orco* mutation produces aberrant social behavior and defective neural development in ants. Cell 170:736–747.

Yan H, Simola DF, Bonasio R, Liebig J, Berger SL & Reinberg D (2014) Eusocial insects as emerging models for behavioural epigenetics. Nat Rev Genet 15:677–688.

Yang AS, Martin CH, Nijhout HF & Carolina N (2004) Geographic variation of caste structure among ant populations. Curr Biol 14:514–519.

Yang B, Fujii T, Ishikawa Y & Matsuo T (2016) Targeted mutagenesis of an *odorant receptor co-receptor* using TALEN in *Ostrinia furnacalis*. Insect Biochem Mol Biol 70:53–59.

Yu CR, Power J, Barnea G, O'Donnell S, Brown HE V, Osborne J, Axel R & Gogos JA (2004) Spontaneous neural activity is required for the establishment and maintenance of the olfactory sensory map. Neuron 42:553–566.

Zhang H, Liu J, Li CR, Momen B, Kohanski R a & Pick L (2009) Deletion of *Drosophila* insulin-like peptides causes growth defects and metabolic abnormalities. Proc Natl Acad Sci 106:19617–19622.

Zhou X, Slone JD, Rokas A, Berger SL, Liebig J, Ray A, Reinberg D & Zwiebel LJ (2012) Phylogenetic and transcriptomic analysis of chemosensory receptors in a pair of divergent ant species reveals sex-specific signatures of odor coding. PLoS Genet 8:e1002930.

Zhu LJ, Holmes BR, Aronin N & Brodsky MH (2014) CRISPRseek: A Bioconductor package to identify target-specific guide RNAs for CRISPR-Cas9 genome-editing systems. PLoS One 9:e108424.

Zinna R, Gotoh H, Brent CS, Dolezal A, Kraus A, Niimi T, Emlen D & Lavine LC (2016) Endocrine control of exaggerated trait growth in rhinoceros beetles. Integr Comp Biol 56:247-259.

Zube C, Kleineidam CJ, Kirschner S, Neef J & Rossler W (2008) Organization of the olfactory pathway and odor processing in the antennal lobe of the ant *Camponotus floridanus*. J Comp Neurol 506:425–441.